

Selective Formation and Cleavage of Carbon–Heteroatom Bonds using Visible-Light Photocatalysis

Inaugural-Dissertation
to obtain the academic degree
Doctor rerum naturalium (Dr. rer. nat.)

Submitted to the Department of Biology, Chemistry, Pharmacy
of Freie Universität Berlin

by
Cristian Cavedon

June 2021

My doctoral degree thesis entitled “Selective Formation and Cleavage of Carbon–Heteroatom Bonds using Visible-Light Photocatalysis” has been prepared by myself and is based on my own work; the work from others has been specifically acknowledged in the text. This thesis is submitted to the Department of Biology, Chemistry, Pharmacy of Freie Universität Berlin to obtain the academic degree Doctor rerum naturalium (Dr. rer. nat.) and has not been submitted for any other degree.

1st reviewer: Prof. Dr. Peter H. Seeberger

2nd reviewer: Prof. Dr. Mathias Christmann

Date of oral defense: September 2nd, 2021

Acknowledgements

First, I want to express my deepest gratitude to Dr. Bartholomäus Pieber for his excellent support, scientific guidance and supervision throughout the last years.

I am thankful to Prof. Dr. Peter Seeberger for giving me the opportunity to perform my research in the Biomolecular Systems Department at Max Planck Institute of Colloids and Interfaces.

I thank Prof. Dr. Mathias Christmann for kindly agreeing to review this thesis.

Special thanks go to the members of the Catalysis group: Sebastian, Susanne, Amiera, Noah and Lucia, for creating a great working environment and for the fun we had over the years.

Thanks to my colleagues Agata, Antonella, Ankita, Dario, Enrico, Eric, Giulio, José, Júlia, Mara, Nieves and Pietro for scientific advice and in particular for your friendship outside the institute.

To my long-time friends Marco, Martino, Marta and Giovanni, and to those I met recently: thank you for all the adventures, the fun and the moments we are sharing.

Finally, I want to express my gratitude to my family, who unconditionally supported me and my decisions, this thesis is for you.

List of Publications

Cavedon, C.; Seeberger, P. H.; Pieber, B. Photochemical Strategies for Carbon–Heteroatom Bond Formation. *European Journal of Organic Chemistry* **2020**, 1379-1392.

Pieber, B.; Malik, J. A.; **Cavedon, C.**; Gisbertz, S.; Savateev, A.; Cruz, D.; Heil, T.; Zhang, G.; Seeberger, P. H. Semi-Heterogeneous Dual Nickel/Photocatalysis using Carbon Nitrides: Esterification of Carboxylic Acids with Aryl Halides. *Angewandte Chemie International Edition* **2019**, *58*, 9575-9580.

Cavedon, C.; Madani, A.; Seeberger, P. H.; Pieber, B. Semiheterogeneous Dual Nickel/Photocatalytic (Thio)etherification Using Carbon Nitrides. *Organic Letters* **2019**, *21*, 5331-5334.

Cavedon, C.; Gisbertz, S.; Vogl, S.; Richter, N.; Seeberger, P. H.; Thomas, A.; Pieber, B. Photocatalyst-Free, Visible-Light-Mediated Nickel Catalysis for Carbon–Heteroatom Cross-Couplings. *Manuscript in preparation*.

Cavedon, C.; Sletten, E. T.; Madani, A.; Niemeyer, O.; Seeberger, P. H.; Pieber, B. Visible-Light-Mediated Oxidative Debenzylation Enables the Use of Benzyl Ethers as Temporary Protecting Groups. *Organic Letters* **2021**, *23*, 514-518.

Table of Contents

Summary	1
Zusammenfassung	3
1 Introduction	5
<hr/>	
1.1 General principles of photocatalysis	5
1.2 Main classes of photocatalysts	9
1.3 Photocatalytic cross-coupling reactions for carbon–heteroatom bond formation	11
1.4 Photocatalytic cleavage of benzyl-type ethers	13
1.5 Aim of this Thesis	14
1.6 References	15
2 Photochemical strategies for carbon–heteroatom bond formation	19
<hr/>	
2.1 Introduction	20
2.2 Photocatalytic carbon–heteroatom bond formation	21
2.3 Carbon–heteroatom bond formation by combining photo- and transition-metal catalysis	32
2.4 Photocatalyst-free carbon–heteroatom coupling reactions	42
2.5 Summary and Outlook	48
2.6 References	50
3 Semi-heterogeneous dual nickel/photocatalysis using carbon nitrides: esterification of carboxylic acids with aryl halides	61
<hr/>	
3.1 Introduction	63
3.2 Results and discussion	64
3.3 Conclusion	71
3.4 Supporting information	72
3.5 References	123
4 Semi-heterogeneous dual nickel/photocatalytic (thio)etherification using carbon nitrides	127
<hr/>	
4.1 Introduction	128
4.2 Results and discussion	129
4.3 Conclusion	134
4.4 Supporting information	135
4.5 References	176

5	Photocatalyst-free, visible-light-mediated nickel catalysis for carbon–heteroatom cross-couplings	183
<hr/>		
5.1	Introduction	184
5.2	Ligand design and evaluation	185
5.3	Polymerization of czbpy for heterogeneous, visible-light-mediated nickel catalysis	190
5.4	Conclusion	193
5.5	Supporting information	194
5.6	Copies of NMR spectra of new isolated compounds	259
5.7	References	275
6	Visible light-mediated oxidative debenylation enables the use of benzyl ethers as temporary protecting groups	281
<hr/>		
6.1	Introduction	282
6.2	Results and discussion	283
6.3	Conclusion	287
6.4	Supporting information	288
6.5	References	347
7	Discussion of individual works	351
<hr/>		
7.1	Photochemical strategies for carbon–heteroatom bond formation	351
7.2	Semi-heterogeneous nickel/carbon nitride catalysis for cross-coupling reactions	353
7.3	Photocatalyst-free, visible-light-mediated nickel catalysis for cross coupling reactions	356
7.4	Visible-light-mediated cleavage of benzyl ethers for the selective deprotection of carbohydrates	358
7.5	References	360
	Abbreviations list	363

Summary

Since the beginning of the 21st century, a renaissance of photochemistry has led to the development of new synthetic methods that use light as a sustainable reagent to achieve organic transformations. In particular, photocatalysis allows to harvest visible light and activate reagents and intermediates by means of catalytic amounts of a suitable chromophore.

Due to the presence of heteroatoms in multiple natural products and active pharmaceutical ingredients, methodologies for the formation and cleavage of carbon-heteroatom bonds are highly valuable in synthetic organic chemistry.

Cross-couplings are among the most powerful tools available to the synthetic organic chemist, enabling strategic bond constructions. Previously dominated by transition metal catalysis, cross-coupling reactions were revolutionized by photochemical approaches (Chapter 2). Photocatalysis allows to initiate radical couplings by selective reduction or oxidation of the coupling partners under mild reaction conditions. Alternatively, a photocatalyst (PC) can be used to regulate the reactivity of a transition metal catalyst. Photochemical strategies that do not require a PC rely on photoactive starting materials or formation of electron donor-acceptor complexes or catalytic intermediates that can be activated with light.

Nickel is an appealing, sustainable alternative to palladium in transition metal-catalyzed cross-couplings, but the reaction of aryl halides and nucleophiles is hampered by the stability of nickel(II) intermediates. Visible light irradiation and a photocatalyst can enable nickel-catalyzed cross-couplings. While most dual nickel/photocatalytic methods rely on homogeneous iridium- or ruthenium-polypyridyl complexes as photocatalysts, semiconductor materials emerged as sustainable, inexpensive alternatives.

Carbon nitrides are a class of metal-free semiconductors that can be prepared from inexpensive, abundant commodity chemicals and absorb visible light. The carbon nitride CN-OA-m was combined with nickel catalysts to promote carbon-heteroatom cross-couplings. Aryl iodides and carboxylic acids are coupled using a combination of a nickel(II) salt, a bipyridyl ligand, CN-OA-m and visible light irradiation (Chapter 3). The same approach was later extended to the coupling of aryl bromides with alcohols and aryl iodides with thiols (Chapter 4). The heterogeneous CN-OA-m is straightforward to separate from the reaction mixture and was reused several times without loss in reactivity.

The ligand 5,5'-dicarbazolyl-2,2'-bipyridyl (czbpy) forms nickel complexes that absorb visible light up to 450 nm. A complex prepared in situ from NiCl₂·glyme and czbpy can promote the coupling of aryl iodides with sodium sulfinates, carboxylic acids and sulfonamides under blue light irradiation, without an additional photocatalyst (Chapter 5). Polymerization of czbpy resulted in a polymeric ligand network that enables immobilization of nickel. The heterogeneous material catalyzes carbon–heteroatom cross-coupling under visible-light irradiation and was recycled multiple times.

Benzyl ethers are convenient protective groups in carbohydrate chemistry due to their high stability. Harsh reaction conditions required for their cleavage by catalytic hydrogenation, Birch reduction or ozonolysis have poor functional-group compatibility and limit their use.

Visible-light photocatalysis using iridium-polypyridyl complexes or organic dyes as PC are suitable for the cleavage of electron-rich *para*-methoxy benzyl ethers but do not affect benzylic ones. Upon visible light irradiation, 2,3-dichloro-5,6-dicyano-1,4-benzoquinone (DDQ) forms a highly oxidizing triplet state that can cleave benzyl ethers. Combinations of DDQ and *tert*-butyl nitrite in presence of air catalyze the selective, oxidative cleavage of benzyl ethers in carbohydrate structures in presence of many other common functional groups (Chapter 6).

Zusammenfassung

Seit Beginn des 21. Jahrhunderts hat eine Renaissance der Photochemie zu einer Entwicklung von neuen synthetischen Methoden geführt, bei denen Licht als nachhaltiges Reagenz für die organische Synthese verwendet wird. Insbesondere Photokatalyse, die erlaubt den Einsatz von sichtbarem Licht zur Aktivierung von Reagenzien und Zwischenprodukten mit Hilfe von katalytischen Mengen eines geeigneten Chromophors.

Da Heteroatome in einer Vielzahl von Naturstoffen und Arzneistoffen vorkommen, sind Methoden für die Bildung und Spaltung von Kohlenstoff–Heteroatom Bindungen besonders wichtig in der synthetischen organischen Chemie.

Kreuzkupplungen gehören zu den leistungsstärksten Werkzeugen, die dem organischen Chemiker zur Verfügung stehen, um strategische Bindungskonstruktionen durchzuführen. Dieses, von der Übergangsmetallkatalyse dominierte Gebiet, wird mittels Kreuzkupplungsreaktionen durch photochemische Ansätze revolutioniert (Kapitel 2). Die Photokatalyse ermöglicht die Initiierung radikalischer Kupplungen durch selektive Reduktion oder Oxidation der Kupplungspartner unter milden Reaktionsbedingungen. Alternativ kann ein Photokatalysator (PC) dazu verwendet werden die Reaktivität eines Übergangsmetallkatalysators zu regulieren. Zusätzlich gibt es photochemische Strategien, für die kein PC erforderlich ist. Hierbei werden mit Hilfe von Licht photoaktive Ausgangsmaterialien, Elektronendonoraakzeptor-Komplexe oder katalytischen Zwischenprodukte aktiviert.

Nickel ist eine attraktive, nachhaltige Alternative zu Palladium. Kreuzkupplungsreaktionen zwischen Arylhalogeniden und Nucleophilen werden allerdings durch die Stabilität von Nickel (II) -Zwischenprodukten verhindert. Durch Bestrahlung eines Photokatalysators mit sichtbarem Licht kann dieser Nickel für die Katalyse von Kreuzkupplungen aktivieren. Während die meisten dualen Nickel / photokatalytischen Verfahren auf homogenen Iridium- oder Ruthenium-Polypyridyl-Komplexen als Photokatalysatoren beruhen, haben sich Halbleitermaterialien als nachhaltige, kostengünstige Alternativen herausgestellt.

Kohlenstoffnitride sind eine Klasse von metallfreien Halbleitern, die aus kostengünstigen, reichlich vorhandenen Grundchemikalien hergestellt werden können und sichtbares Licht absorbieren. Das Kohlenstoffnitrid CN-OA-m wurde mit Nickelkatalysatoren kombiniert, um Kohlenstoff-Heteroatom-Kreuzkupplungen zu ermöglichen. Aryliodide und Carbonsäuren werden unter der Verwendung von semi-heterogenen Kombination eines Nickel (II) -Salzes, eines Bipyridylliganden, CN-OA-m und unter Bestrahlung mit sichtbarem Licht miteinander

verknüpft (Kapitel 3). Der gleiche Ansatz wurde später auf die Kupplung von Arylbromiden mit Alkoholen, sowie Aryliodiden mit Thiolen erweitert (Kapitel 4). Das heterogene CN-OA-m lässt sich leicht vom Reaktionsgemisch abtrennen und wurde ohne Reaktivitätsverlust mehrmals wiederverwendet.

Der Ligand 5,5'-Dicarbazolyl-2,2'-bipyridyl (czbpy) bildet Nickelkomplexe, die sichtbares Licht bis zu 450 nm absorbieren können. Ein *in situ* aus $\text{NiCl}_2 \cdot \text{glyme}$ und czbpy hergestellter Komplex kann die Kupplung von Aryliodiden mit Natriumsulfonaten, Carbonsäuren oder Sulfonamiden unter Bestrahlung mit blauem Licht ermöglichen, ohne die Notwendigkeit eines zusätzlichen Photokatalysators (Kapitel 5). Durch die Polymerisation von czbpy wird ein polymeres Ligandennetzwerk gebildet, das Nickel immobilisieren kann. Dieses heterogene Material katalysiert Kohlenstoff-Heteroatom-Kreuzkupplungen unter Bestrahlung mit sichtbarem Licht und kann mehrfach recycelt werden.

Benzylether sind aufgrund ihrer hohen Stabilität geeignete Schutzgruppen in der Kohlenhydratchemie. Die extremen Reaktionsbedingungen, die für ihre Abspaltung mittels katalytischer Hydrierung, Birch-Reduktion oder Ozonolyse erforderlich sind, weisen eine schlechte Verträglichkeit mit funktionellen Gruppen auf und limitieren daher ihre Verwendung. Photokatalyse mit sichtbarem Licht, bei der Iridium-Polypyridyl-Komplexe oder organischen Farbstoffe als Photokatalysatoren eingesetzt werden, eignet sich zur Abspaltung elektronenreicher *para*-Methoxybenzylether. Diese Methoden sind aber nicht für Benzylether geeignet. Durch die Bestrahlung mit sichtbarem Licht bildet 2,3-Dichlor-5,6-dicyano-1,4-benzochinon (DDQ) einen stark oxidierenden Triplettzustand, der Benzylether abspalten kann. Auch in der Anwesenheit vieler anderer üblicher funktioneller Gruppen katalysieren Kombinationen von DDQ und *tert*-Butylnitrit in Gegenwart von Luft selektiv die oxidative Abspaltung von Benzylethern in Kohlenhydratstrukturen (Kapitel 6).

Chapter 1

Introduction

This chapter provides the scientific concepts and notions necessary to understand the following ones. Chapters 2 to 6 report the publications listed at page vii, reformatted but with unaltered content. For each publication, supporting information containing experimental details is included. Copies of the NMR spectra of new compounds are reported for the unpublished work of Chapter 5. A discussion of the individual projects and their interpretation within the overall dissertation is given in Chapter 7.

1.1 General principles of photocatalysis

Nature has developed elegant ways to use solar light as an energy source for chemical reactions. Inspired by nature, chemists explored the use of light to promote chemical reactions. The chain of events to convert photons into chemical energy starts with chromophores that absorb visible light and reach excited states, before funneling this energy to the reaction center.¹

Transitions between different energetic levels for a molecule that absorbs light can be represented in a simplified manner using a Jablonski diagram (Figure 1.1). Upon absorption of photons with appropriate energy, a molecule in its ground state (S_0) is converted to a singlet excited state (S_1). This transition is represented by the promotion of an electron from the highest occupied molecular orbital (HOMO) to an empty orbital with higher energy (lowest unoccupied molecular orbital, LUMO).

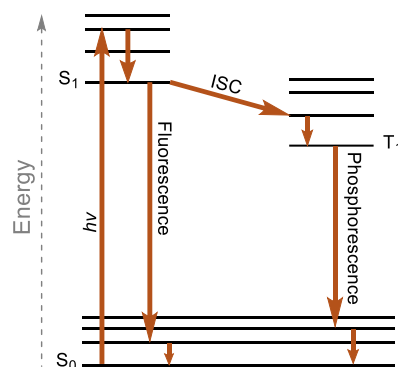


Figure 1.1. Simplified Jablonski diagram.

From S_1 the molecule can relax back to S_0 by emitting energy as radiation (fluorescence) or undergo intersystem crossing (ISC) to generate a triplet excited state (T_1). The transition $T_1 \rightarrow S_0$ (phosphorescence) is spin-forbidden. Therefore, triplet excited states have long lifetimes, ranging from 100 ns to few μs , that allow them to take part in bimolecular processes.

In a photochemical reaction, one of the reagents absorbs light and reaches an excited state. The desired reaction takes place from the excited state molecule, that would be otherwise inert. Most of organic molecules absorb only highly energetic UV radiation, that leads to unselective reactions.²

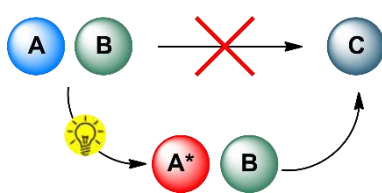


Figure 1.2. Photochemistry enables reactions of excited states of otherwise inert molecules.

Photocatalysis uses small amounts of a suitable chromophore (photocatalyst, PC) that absorbs light and initiates the desired reaction sequence. Commonly used PCs are organometallic complexes, organic dyes or semiconductors that absorb visible light (400-700 nm). As these wavelengths are not absorbed by most organic molecules, the photocatalyst is the only species to reach an excited state and the desired reaction takes place selectively from interaction of the catalyst with one of the substrates or reagents.

Two modes of action are possible in photocatalysis. In energy transfer catalysis the excited state of the photocatalyst (PC^*) is quenched by reagents via energy transfer (EnT). In photoredox catalysis, electron transfer (ET) events between the photocatalyst and reagents are responsible for quenching of PC^* and formation of reactive radical intermediates.

Energy Transfer

Quenching of molecules in their excited state (donor^{*}) by energy transfer (EnT) to an acceptor can be rationalized through two mechanisms: Förster and Dexter energy transfer.

Förster energy transfer is based on coulombic electron-electron interactions between the donor and acceptor. The energy released from the donor when an electron relaxes from LUMO to HOMO is transferred to an electron in the acceptor that undergoes a HOMO-to-LUMO

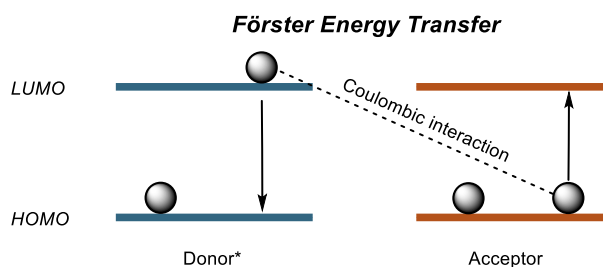


Figure 1.3. Förster energy transfer.

transition (Figure 1.3). This model is unsuitable to describe quenching of triplet excited states ($\text{donor}^* = T_1$), as it would involve two spin-forbidden transitions: donor^* would have to release energy as phosphorescence ($T_1 \rightarrow S_0$) and simultaneously the acceptor should absorb equal energy undergoing a $S_0 \rightarrow T_1$ transition.³

Dexter energy transfer relies on a double electron transfer process.³ The donor and acceptor have to get in close spatial proximity to form a collision complex. Orbital overlap enables movement of an electron from donor's LUMO to acceptor's LUMO while simultaneously one electron moves from acceptor's HOMO to donor's HOMO (Figure 1.4). The electron transfer within the collision complex is reversible and efficiency of the process depends on the diffusion rate of donor and acceptor, which affects formation and dissolution of the collision complex. Another crucial parameter is the spectral overlap, that quantifies the amount of orbitals available for electron transitions.³

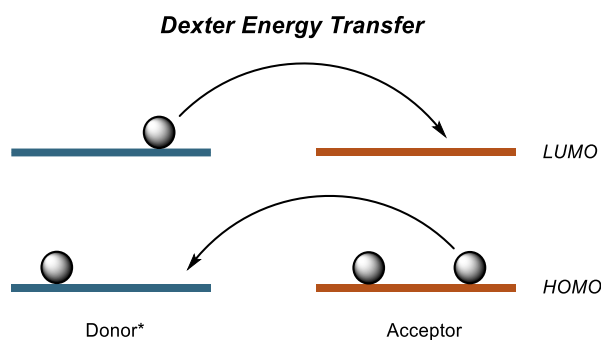


Figure 1.4. Dexter energy transfer.

Electron Transfer

After light absorption and intersystem crossing, species in their triplet excited state can engage in single electron transfer (SET) events and undergo oxidative quenching by interaction with an electron acceptor or reductive quenching by interaction with an electron donor (Figure 1.5).

Whether one or the other process takes place depends on several factors, such as redox potential of the triplet species and the quencher.^{4,5}

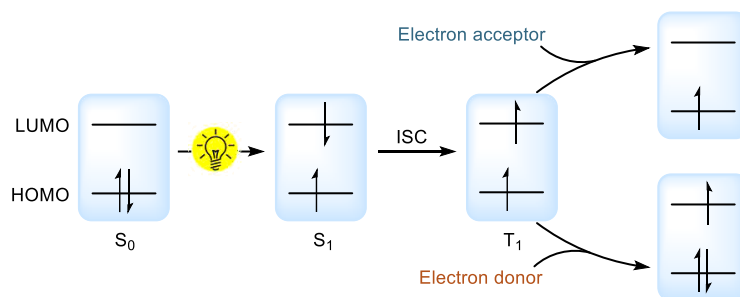


Figure 1.5. Schematic representation of electron transfer processes.

In photoredox catalysis, SET events account for quenching of the catalyst and formation of radical species that initiate the desired reaction. The photocatalyst is quenched to a reduced or oxidized form (PC^{red} or PC^{ox}) and a second electron transfer is necessary to turnover the photocatalyst (Figure 1.6).

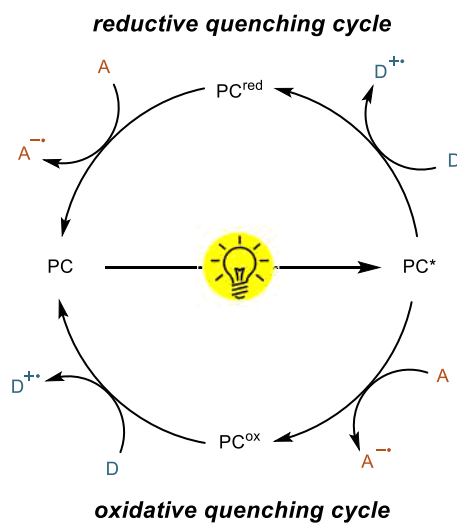


Figure 1.6. Reductive and oxidative quenching cycles in photoredox catalysis. D = electron donor, A = electron acceptor.

1.2 Main classes of photocatalysts

Photocatalysts that are used in synthetic organic chemistry can be divided into three different classes: organometallic complexes, organic dyes and heterogeneous semiconductors.

Organometallic complexes

Ruthenium- and iridium-polypyridyl complexes play a predominant role in visible-light photocatalysis as they can undergo metal-to-ligand charge transfer transitions to generate long-lived triplet excited states.⁵ For example, tris(2,2'-bipyridyl)ruthenium(II) ($\text{Ru}(\text{bpy})_3^{2+}$) absorbs visible-light up to 450 nm and has triplet lifetime longer than 1 μs , suitable to engage in bimolecular ET or EnT processes. Additionally, redox properties of the metal complex can be tuned by ligand modification.

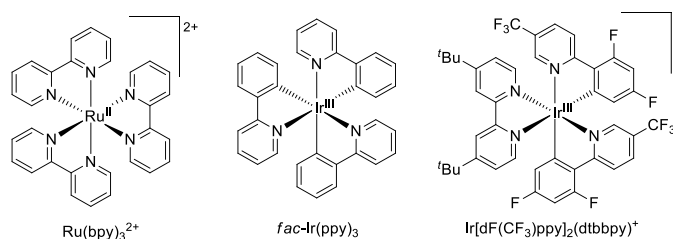


Figure 1.7. Structures of commonly used noble metal-based organometallic complexes.

The use of iridium and ruthenium complexes as photocatalyst is hampered by the high cost and the limited sustainability of these rare metals. Alternative approaches to use copper complexes as photocatalysts have been attempted, but found limited application.⁶

Organic dyes

Metal-free photocatalysts such as xanthene dyes, benzophenones, cyanoarenes, acridinium salts and boron dipyrromethenes (BODIPY) are intensively studied as alternatives to ruthenium and iridium complexes (Figure 1.8).⁷ This class of photocatalyst benefits from low cost and optical properties that can be tuned by chemical modifications. Unfortunately, only few dyes have excited state lifetimes long enough to engage in bimolecular energy or electron transfers and their use as photocatalysts remains limited. For example, 4-CzIPN and Eosin Y (Figure 1.8) undergo intersystem crossing and generate triplet states of 5.1 μs and 24 μs respectively. Rhodamine B and Fluorescein rather emit fluorescence from their singlet excited states and have short excited-state lifetimes (4.1 ns and 2.5 ns respectively).⁷

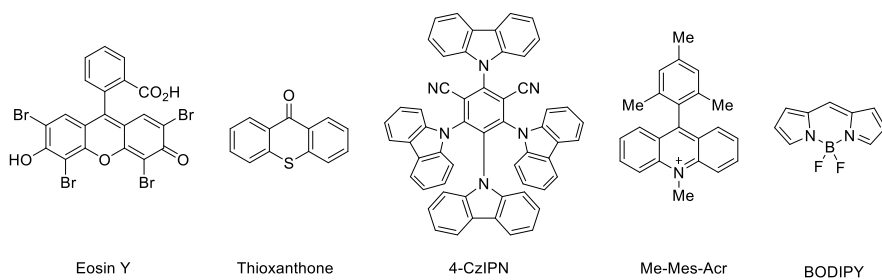


Figure 1.8. Structures of common organic dyes used as photocatalyst.

Semiconductors

Medium bandgap semiconductors have energy difference between valence band (VB) and conduction band (CB) that enables their activation with visible light. Irradiation with photonic energy higher than semiconductor's bandgap generates an electron-hole pair that can engage in electron transfers: an electron donor can add an electron to the valence band, while an electron acceptor can abstract an excited electron from the conduction band.

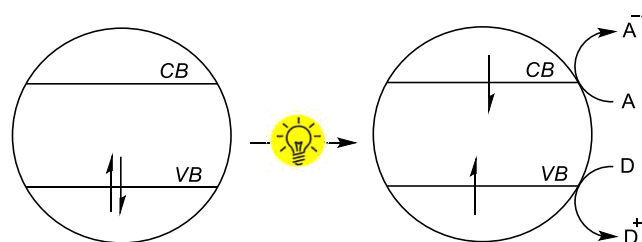


Figure 1.9. Charge separation in semiconductors upon light absorption.

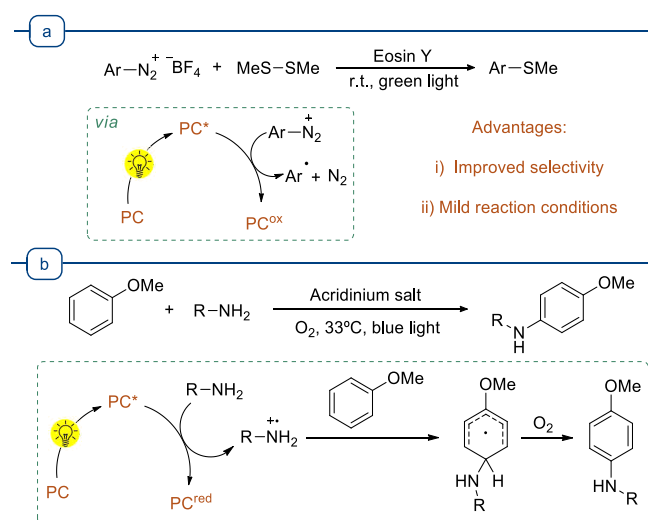
Titanium dioxide is an abundant, non-toxic mineral that can act as a photocatalyst but requires UV light irradiation to induce charge separation. Other inorganic semiconductors, such as cadmium sulphide, cadmium selenide or bismuth oxide, readily absorb visible light and were efficiently applied in heterogeneous photocatalysis.⁸ Carbon nitrides are organic, polymeric semiconductors that can act as visible-light photocatalysts to induce organic transformations, such as oxidations, alkylations and cross-couplings.⁹⁻¹⁰

1.3 Photocatalytic cross-coupling reactions for carbon–heteroatom bond formation

The molecular backbone of polymers, natural products and active pharmaceutical ingredients consists of carbon-carbon bonds, but the presence of heteroatoms accounts for chemical and biological activity. Methods for the formation of carbon–heteroatom bonds are important in synthetic organic chemistry, and photocatalytic radical reactions emerged as a promising alternative to nucleophilic substitution and transition metal catalysis.

Cross-couplings are fundamental tools in modern synthetic chemistry that enable strategic bond formations to quickly generate molecular complexity. Photocatalysis enables cross-coupling reactions through alternative mechanistic pathway (see Chapter 2). The main approach to photocatalytic cross-couplings uses visible-light excitation of a photocatalyst to form a reactive radical species from one of the coupling partners. This approach is described in details in Section 2.2.

As an example, the coupling of aryl diazonium salts with disulfides (Scheme 1.1a) can be promoted with green light irradiation using Eosin Y as photocatalyst.¹¹⁻¹² Main advantages of such strategy are superior selectivity in the formation of aryl radicals using photocatalysis rather than heat or UV light irradiation, and reduced safety concerns using the mild conditions, as diazonium salts are potentially explosive.



Scheme 1.1. Examples of cross-coupling reactions enabled by photoredox catalysis.

Synthesis of *N*-substituted anisidines (Scheme 1.1b) would traditionally require nitration of anisole, reduction to aniline and nucleophilic substitution of an alkyl halide. With a suitable

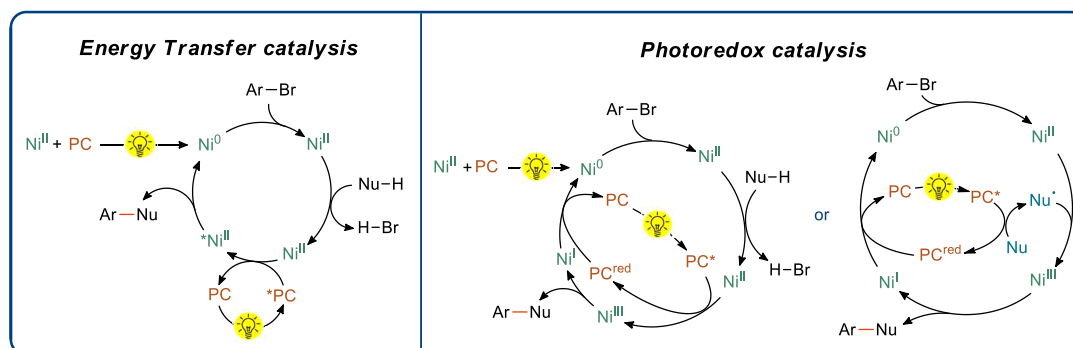
photocatalyst, such as a highly oxidizing acridinium salt, the amine can be oxidized to the corresponding radical cation to obtain the same product in one step.¹²⁻¹³

Combined nickel-/photocatalysis for cross-coupling reactions

Palladium-catalyzed cross-couplings have been thoroughly studied and the Buchwald-Hartwig reaction is the benchmark for the cross-coupling of aryl halides and nucleophiles such as amines, alcohols and thiols.

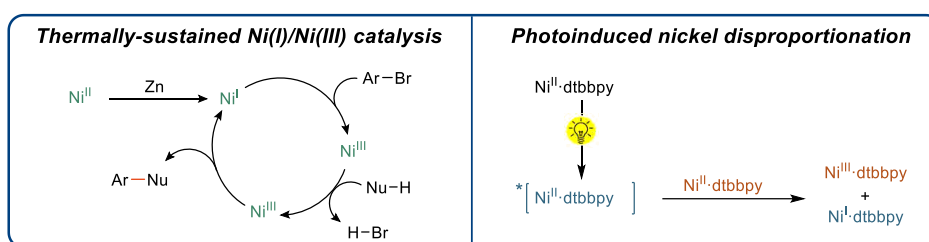
Nickel is an appealing, sustainable alternative that has lower price and higher abundance than palladium. Nevertheless, replacing palladium in Buchwald-Hartwig cross-coupling reactions is not straightforward. Oxidative addition of aryl halides on Ni(0) complexes, followed by ligand exchange of nucleophiles results in Ni(II) intermediates that are thermodynamically stable.¹⁴ To promote the reductive elimination step and form the desired carbon–heteroatom bond, such nickel intermediates need to be destabilized using tailored phosphine-ligands¹⁵ or a photocatalyst.¹⁶

Combinations of nickel/photocatalysis have been reported for the formation of numerous carbon–heteroatom bonds. Early reports on this type of reactions proposed catalytic cycles that start from Ni(0) and form the Ni(II) intermediates described before (Scheme 1.2). Using energy transfer catalysis, the photocatalyst induces reductive elimination of the product by activating this nickel complex. In photoredox catalysis the photocatalyst engages in electron transfers with the nickel complex, inducing oxidation to Ni(III) from which the reductive elimination happens. These two mechanistic scenarios are discussed thoroughly in Section 2.3, but it is noteworthy that in this hypotheses the PC accounts for the reduction of the Ni(II) precatalyst to Ni(0) and to promote the rate-limiting elimination step.



Scheme 1.2. Activation of Ni(II) intermediates with energy transfer catalysis (left) and photoredox catalysis for modulation of nickel oxidation state (right).

In light of recent evidence, the role of the photocatalyst has been reconsidered. After reduction of the nickel(II) precatalyst, carbon-heteroatom cross-couplings might proceed via Ni(I)-Ni(III) sequences. Nocera and coworkers applied this concept in the photocatalyst-free coupling of aryl halides with carboxylic acids, alcohols and amines using substoichiometric amounts of zinc powder for the initial reduction of a nickel (II) complex to Ni(I) (Scheme 1.3).¹⁷ Mechanistic studies suggest that this Ni(I)-Ni(III) reactivity could be active in the background of all dual nickel/photocatalytic carbon-heteroatom couplings.¹⁸⁻²⁰



Scheme 1.3. Thermally-sustained Ni(I)-Ni(III) catalysis initiated by reduction with zinc (left), and photodisproportionation of nickel(II) complexes (right).

Studying the photophysics of nickel-polypyridyl complexes, Doyle and coworkers observed that some Ni(II) complexes can absorb UV light through metal-to-ligand charge transfer transitions.²¹⁻²² Disproportionation between a Ni(II) complex in an excited state and a ground-state species results in formation of a Ni(I)-Ni(III) couple, suitable for thermally-sustained catalysis. In agreement with these findings, protocols for the formation of C–O²³ and C–N²⁴ bonds by direct irradiation of nickel complexes at 390 nm were reported.

1.4 Photocatalytic cleavage of benzyl-type ethers

Upon light absorption, the excited state of a photocatalyst can induce the selective cleavage of carbon–heteroatom bonds. Cleavage of the CH₂–O bond in *para*-methoxybenzyl (PMB) ethers was achieved by the group of Stephenson using a photocatalyst, in combination with a stoichiometric, sacrificial oxidant.²⁵ While the original protocol used an iridium-polypyridyl complex as photocatalyst, the reaction was later adapted to use organic dyes such as Eosin Y and a mesityl acridinium salt.²⁶⁻²⁷

The mechanistic proposal suggests initial oxidative quenching of PC* followed by oxidation of the PMB moiety (Figure 1.10). Hydrogen atom transfer (HAT) with a carbon-centered radical

affords a cationic intermediate that is hydrolyzed to free alcohol and aldehyde. The protocols are selective for the cleavage of electron-rich PMB ethers, but no reaction was observed for benzyl ethers. Benzyl ethers have higher reduction potential than *para*-methoxybenzyl ones ($E_{\text{PMB-O-Me}} = 1.60 \text{ V vs SCE}$ and $E_{\text{Bn-O-Me}} = 2.20 \text{ V vs SCE}$)²⁸ and are therefore more difficult to oxidize.

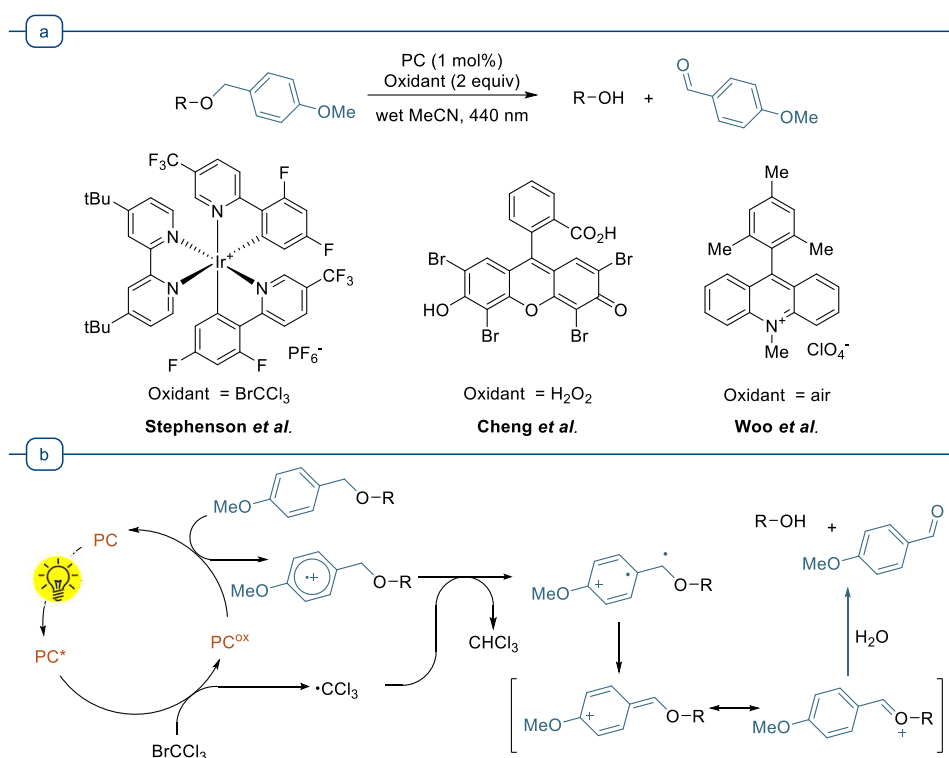


Figure 1.10. a, Photocatalytic cleavage of PMB ethers; b, Proposed reaction mechanism.²⁵

1.5 Aim of this Thesis

The aim of my doctoral research was to extend the application of photocatalysis in organic synthetic chemistry, by investigating more sustainable and efficient catalysts or new reactivities. A particular attention was dedicated to light-mediated cross-coupling reactions using nickel catalysis. In combination with a photocatalyst, nickel can be used as a sustainable alternative to palladium in the Buchwald-Hartwig reaction for the cross-coupling of aryl halides and nucleophiles. This approach still largely relies on the use of iridium- and ruthenium complexes as photocatalyst, which have low sustainability and high price.

I investigated the use of carbon nitride materials as sustainable alternatives to organometallic photocatalysts in nickel-catalyzed carbon–heteroatom cross-couplings. Semi-heterogeneous protocols for the cross-coupling of aryl halides with carboxylic acids, alcohols and thiols were developed, that use homogeneous nickel complexes in combination with the heterogeneous material CN-OA-m under visible light irradiation. The carbon nitride photocatalyst was prepared by inexpensive and abundant commodity chemicals and could be recycled multiple times.

In a second approach, the use of the ligand 5,5'-dicarbazolyl-2,2'-bipyridyl (czbpy) was investigated to promote light-mediated, photocatalyst-free nickel catalysis. Nickel-czbpy complexes absorb light and can promote the cross-coupling of aryl iodides with sodium sulfinates, carboxylic acids and sulfonamides. Optimized reaction conditions require only an air-stable nickel(II) salt, the ligand czbpy and blue light irradiation. Polymerization of czbpy afforded a ligand network that can immobilize nickel and promote the same reactions under visible light irradiation in a heterogeneous manner. This strategy not only provides a heterogeneous, recyclable catalytic system, but proves that visible light can be used to activate the nickel catalyst without the need of an exogenous photocatalyst.

The last part of this thesis evaluates the use of photocatalysis for the oxidative C–O cleavage of benzyl ethers. Current debenzylation methods require harsh reaction conditions that are poorly functional group-tolerant and limit their use as protective group. Due to their high stability benzyl ethers are strategic protective groups in carbohydrate chemistry and development of orthogonal deprotection methods would be beneficial. The use of visible-light photocatalysis was investigated for the selective cleavage of benzyl groups in carbohydrate structures and a protocol is reported that uses green light irradiation and a dual catalytic system comprising DDQ and *tert*-butyl nitrite. Mild reaction conditions and broad functional group tolerance are key features of this strategy.

1.6 References

- (1) Scholes, G. D.; Fleming, G. R.; Olaya-Castro, A.; van Grondelle, R. Lessons from nature about solar light harvesting. *Nat. Chem.* **2011**, *3*, 763-774.
- (2) Marzo, L.; Pagire, S. K.; Reiser, O.; König, B. Visible-Light Photocatalysis: Does It Make a Difference in Organic Synthesis? *Angew. Chem. Int. Ed.* **2018**, *57*, 10034-10072.

Chapter 1

- (3) Strieth-Kalthoff, F.; James, M. J.; Teders, M.; Pitzer, L.; Glorius, F. Energy transfer catalysis mediated by visible light: principles, applications, directions. *Chem. Soc. Rev.* **2018**, *47*, 7190-7202.
- (4) Shaw, M. H.; Twilton, J.; MacMillan, D. W. C. Photoredox Catalysis in Organic Chemistry. *J. Org. Chem.* **2016**, *81*, 6898-6926.
- (5) Prier, C. K.; Rankic, D. A.; MacMillan, D. W. C. Visible Light Photoredox Catalysis with Transition Metal Complexes: Applications in Organic Synthesis. *Chem. Rev.* **2013**, *113*, 5322-5363.
- (6) Hossain, A.; Bhattacharyya, A.; Reiser, O. Copper's rapid ascent in visible-light photoredox catalysis. *Science* **2019**, *364*, eaav9713.
- (7) Romero, N. A.; Nicewicz, D. A. Organic Photoredox Catalysis. *Chem. Rev.* **2016**, *116*, 10075-10166.
- (8) Gisbertz, S.; Pieber, B. Heterogeneous Photocatalysis in Organic Synthesis. *ChemPhotoChem* **2020**, *4*, 456-475.
- (9) Savateev, A.; Ghosh, I.; König, B.; Antonietti, M. Photoredox Catalytic Organic Transformations using Heterogeneous Carbon Nitrides. *Angew. Chem. Int. Ed.* **2018**, *57*, 15936-15947.
- (10) Markushyna, Y.; Smith, C. A.; Savateev, A. Organic Photocatalysis: Carbon Nitride Semiconductors vs. Molecular Catalysts. *Eur. J. Org. Chem.* **2020**, *2020*, 1294-1309.
- (11) Majek, M.; von Wangelin, A. J. Organocatalytic visible light mediated synthesis of aryl sulfides. *Chem. Commun.* **2013**, *49*, 5507-5509.
- (12) Cavedon, C.; Seeberger, P. H.; Pieber, B. Photochemical Strategies for Carbon–Heteroatom Bond Formation. *Eur. J. Org. Chem.* **2020**, *2020*, 1379-1392.
- (13) Margrey, K. A.; Levens, A.; Nicewicz, D. A. Direct Aryl C–H Amination with Primary Amines Using Organic Photoredox Catalysis. *Angew. Chem. Int. Ed.* **2017**, *56*, 15644-15648.
- (14) Han, R.; Hillhouse, G. L. Carbon–Oxygen Reductive-Elimination from Nickel(II) Oxametallacycles and Factors That Control Formation of Ether, Aldehyde, Alcohol, or Ester Products. *J. Am. Chem. Soc.* **1997**, *119*, 8135-8136.
- (15) Lavoie, C. M.; Stradiotto, M. Bisphosphines: A Prominent Ancillary Ligand Class for Application in Nickel-Catalyzed C–N Cross-Coupling. *ACS Catal.* **2018**, *8*, 7228-7250.
- (16) Twilton, J.; Le, C.; Zhang, P.; Shaw, M. H.; Evans, R. W.; MacMillan, D. W. C. The merger of transition metal and photocatalysis. *Nat. Rev. Chem.* **2017**, *1*, 0052.
- (17) Sun, R.; Qin, Y.; Nocera, D. G. General Paradigm in Photoredox Nickel-Catalyzed Cross-Coupling Allows for Light-Free Access to Reactivity. *Angew. Chem. Int. Ed.* **2020**, *59*, 9527-9533.

- (18) Qin, Y.; Sun, R.; Gianoulis, N. P.; Nocera, D. G. Photoredox Nickel-Catalyzed C–S Cross-Coupling: Mechanism, Kinetics, and Generalization. *J. Am. Chem. Soc.* **2021**, *143*, 2005-2015.
- (19) Till, N. A.; Tian, L.; Dong, Z.; Scholes, G. D.; MacMillan, D. W. C. Mechanistic Analysis of Metallaphotoredox C–N Coupling: Photocatalysis Initiates and Perpetuates Ni(I)/Ni(III) Coupling Activity. *J. Am. Chem. Soc.* **2020**, *142*, 15830-15841.
- (20) Sun, R.; Qin, Y.; Ruccolo, S.; Schnedermann, C.; Costentin, C.; Daniel, G. N. Elucidation of a Redox-Mediated Reaction Cycle for Nickel-Catalyzed Cross Coupling. *J. Am. Chem. Soc.* **2019**, *141*, 89-93.
- (21) Shields, B. J.; Kudisch, B.; Scholes, G. D.; Doyle, A. G. Long-Lived Charge-Transfer States of Nickel(II) Aryl Halide Complexes Facilitate Bimolecular Photoinduced Electron Transfer. *J. Am. Chem. Soc.* **2018**, *140*, 3035-3039.
- (22) Ting, S. I.; Garakyaraghi, S.; Taliaferro, C. M.; Shields, B. J.; Scholes, G. D.; Castellano, F. N.; Doyle, A. G. 3d-d Excited States of Ni(II) Complexes Relevant to Photoredox Catalysis: Spectroscopic Identification and Mechanistic Implications. *J. Am. Chem. Soc.* **2020**, *142*, 5800-5810.
- (23) Yang, L.; Lu, H.-H.; Lai, C.-H.; Li, G.; Zhang, W.; Cao, R.; Liu, F.; Wang, C.; Xiao, J.; Xue, D. Light-Promoted Nickel Catalysis: Etherification of Aryl Electrophiles with Alcohols Catalyzed by a NiIII-Aryl Complex. *Angew. Chem. Int. Ed.* **2020**, *59*, 12714-12719.
- (24) Li, G.; Yang, L.; Liu, J.-J.; Zhang, W.; Cao, R.; Wang, C.; Zhang, Z.; Xiao, J.; Xue, D. Light-Promoted C–N Coupling of Aryl Halides with Nitroarenes. *Angew. Chem. Int. Ed.* **2021**, *60*, 5230-5234.
- (25) Tucker, J. W.; Narayanam, J. M. R.; Shah, P. S.; Stephenson, C. R. J. Oxidative photoredox catalysis: mild and selective deprotection of PMB ethers mediated by visible light. *Chem. Commun.* **2011**, *47*, 5040-5042.
- (26) Ahn, D. K.; Kang, Y. W.; Woo, S. K. Oxidative Deprotection of p-Methoxybenzyl Ethers via Metal-Free Photoredox Catalysis. *J. Org. Chem.* **2019**, *84*, 3612-3623.
- (27) Liu, Z.; Zhang, Y.; Cai, Z.; Sun, H.; Cheng, X. Photoredox Removal of p-Methoxybenzyl Ether Protecting Group with Hydrogen Peroxide as Terminal Oxidant. *Adv. Synth. Catal.* **2015**, *357*, 589-593.
- (28) Mayeda, E. A.; Miller, L. L.; Wolf, J. F. Electrooxidation of benzylic ethers, esters, alcohols, and phenyl epoxides. *J. Am. Chem. Soc.* **1972**, *94*, 6812-6816.

Chapter 2

Photochemical strategies for carbon–heteroatom bond formation

Cavedon, C.; Seeberger, P. H.; Pieber, B. Photochemical Strategies for Carbon–Heteroatom Bond Formation. *Eur. J. Org. Chem.* **2020**, 2020 1379-1392.
<https://doi.org/10.1002/ejoc.201901173>

Specific contribution

I collected and organized the literature existing on the topic at the time (July 2019). I outlined a structure for the work, prepared figures, tables and schemes and wrote the manuscript. Dr. B. Pieber and Prof. P. H. Seeberger revised and corrected the manuscript.

Chapter 3

Semi-heterogeneous dual nickel/photocatalysis using carbon nitrides: esterification of carboxylic acids with aryl halides

Pieber, B.; Malik, J. A.; **Cavedon, C.**; Gisbertz, S.; Savateev, A.; Cruz, D.; Heil, T.; Zhang, G.; Seeberger, P. H. Semi-heterogeneous Dual Nickel/Photocatalysis using Carbon Nitrides: Esterification of Carboxylic Acids with Aryl Halides *Angew. Chem. Int. Ed.* **2019**, *58*, 9575-9580. <https://doi.org/10.1002/anie.201902785>

Specific contribution

Dr. B. Pieber conceived the project and optimized the reaction protocols. Dr. J. Malik studied the reaction with the FT-IR setup. I prepared the carbon nitride materials used as photocatalyst and characterized them before and after the reactions.

Dr. B. Pieber, S. Gisbertz and I investigated the scope and limitations of the protocol.

Dr. A. Savateev, Dr. D. Cruz, Dr. T. Heil and Dr. G. Zhang performed material characterizations. Dr. B. Pieber wrote the manuscript with contributions from all other authors.

Chapter 4

Semi-heterogeneous dual nickel/photocatalytic (thio)etherification using carbon nitrides

Cavedon, C.; Madani, A.; Seeberger, P. H.; Pieber, B. Semiheterogeneous Dual Nickel/Photocatalytic (Thio)etherification Using Carbon Nitrides *Org. Lett.* **2019**, *21*, 5331-5334.

<https://doi.org/10.1021/acs.orglett.9b01957>

Specific contribution

Together with Dr. B. Pieber, I conceived the idea behind this project. I verified its feasibility and prepared catalysts and reagents. After optimizing the reactions, I studied the recycling of the catalyst and evaluated scope and limitations of the etherification protocol. I wrote the manuscript.

A. Madani investigated the scope of the thioetherification protocol.

Dr. B. Pieber and Prof. P. H. Seeberger revised and corrected the manuscript.

Chapter 5

Photocatalyst-free, visible-light-mediated nickel catalysis for carbon–heteroatom cross-couplings

Cavedon, C.; Gisbertz, S.; Vogl, S.; Richter, N.; Seeberger, P. H.; Thomas, A.; Pieber, B.

Manuscript in preparation

Abstract

Metallaphotocatalysis typically requires a photocatalyst to harness the energy of visible-light and activate transition metal catalysts. The most prominent example is the merger of photo- and nickel catalysis that unlocked new cross-coupling strategies. We show that a bipyridyne ligand, which was modified with two carbazole moieties, forms a nickel complex that absorbs visible-light and promotes several carbon–heteroatom cross-couplings in absence of an exogenous photocatalyst. Treatment of the ligand with iron(III) chloride affords a porous organic polymer, which can be used for heterogeneous nickel catalysis. The material can be easily recovered and reused several times.

Specific contribution

Dr. B. Pieber and I conceived the idea behind the project.

N. Richter and I verified the feasibility of this approach by screening and optimizing the coupling protocols.

S. Gisbertz and I evaluated the scope and limitations of the C–S, C–N and C–O protocols.

S. Vogl synthesized the homogeneous and polymeric ligand and performed material characterizations.

S. Gisbertz studied the recycling of the heterogeneous catalytic system.

I organized the data and wrote the first draft of the manuscript.

Dr. B. Pieber, Prof. A. Thomas and Prof. P. H. Seeberger revised and corrected the manuscript.

5.1 Introduction

Palladium catalyzed cross-couplings enable strategic carbon–carbon and carbon–heteroatom bond formations and are among the most important transformations in modern synthetic chemistry.¹⁻³ Nickel catalysts are intensively studied as an abundant alternative for these transformations.⁴⁻⁵ Rational ancillary ligand design provided nickel biphosphine complexes that catalyze a range of challenging carbon–heteroatom cross-couplings.⁶⁻⁷ Simple 2,2'-bipyridyl (bpy) derivatives, on the contrary, can be used as ligands when nickel catalysis is combined with photocatalysis (Figure 5.1a).⁸⁻¹⁰ Suitable photocatalysts for dual photo/nickel catalytic carbon–heteroatom cross-couplings range from ruthenium and iridium polypyridyl complexes and organic dyes to heterogeneous semiconductors.¹⁰ Nickel complexes and photocatalysts were combined in bifunctional heterogeneous materials, such as metal-organic frameworks,¹¹⁻¹² organic polymers¹³ or functionalized semiconductors.¹⁴⁻¹⁷

The predominant mechanistic hypothesis for dual photo/nickel catalyzed carbon–heteroatom cross-couplings suggests that energy- or electron transfer between the photocatalyst and a thermodynamically stable Ni^{II} intermediate triggers reductive elimination of the desired product.¹⁰ Further, an initial photocatalytic reduction of Ni^{II} was proposed to generate a key Ni⁰ species that engages in oxidative addition with the aryl halide.¹⁸ However, there is growing evidence that these reactions might proceed through Ni^I/Ni^{III} cycles that do not involve Ni⁰ or Ni^{II} species.¹⁹⁻²¹ Doyle and colleagues showed that upon absorption of light, Ni^{II}(dtbbpy) aryl halide complexes (dtbbpy = 4,4'-di-*tert*-butyl-2,2'-bipyridyl) undergo Ni–aryl hemolysis to form a catalytically active Ni^I catalyst.²²⁻²³ This observation was expanded to a synthetic protocol for C–O and C–N cross-couplings using UV-light irradiation.²⁴⁻²⁵ More recently, Nocera and coworkers showed that sub-stoichiometric amounts of zinc can be used instead of a photocatalyst and light (Figure 5.1b).²⁶ Here, the metal reductant was proposed to generate an active Ni^I catalyst from a Ni^{II} pre-catalyst that engages in a thermally sustained Ni^I/Ni^{III} cycle. Inspired by these findings, we questioned whether a visible-light-mediated approach to nickel-catalyzed carbon–heteroatom cross-couplings using a benchstable Ni^{II} pre-catalyst that does neither require an exogenous photocatalyst, nor the addition of an artificial reductant is feasible. We hypothesized that this can be realized via the functionalization of a bipyridyl ligand with a structural motif that extends the absorption of an *in situ* formed Ni^{II} pre-catalyst to visible light. We speculated that such a complex could form the key Ni^I species upon irradiation through, for example, intramolecular charge transfer. Here we show that this can be indeed achieved by

decorating 2,2'-bipyridine with two carbazole units (Figure 5.1c). This simple ligand modification enables visible-light-mediated cross-couplings of several nucleophiles with aryl halides. Moreover, we demonstrate that the ligand can be polymerized to yield a conjugated microporous polymer that serves as a recyclable heterogeneous macroligand for light-mediated nickel-catalyzed carbon–heteroatom couplings.

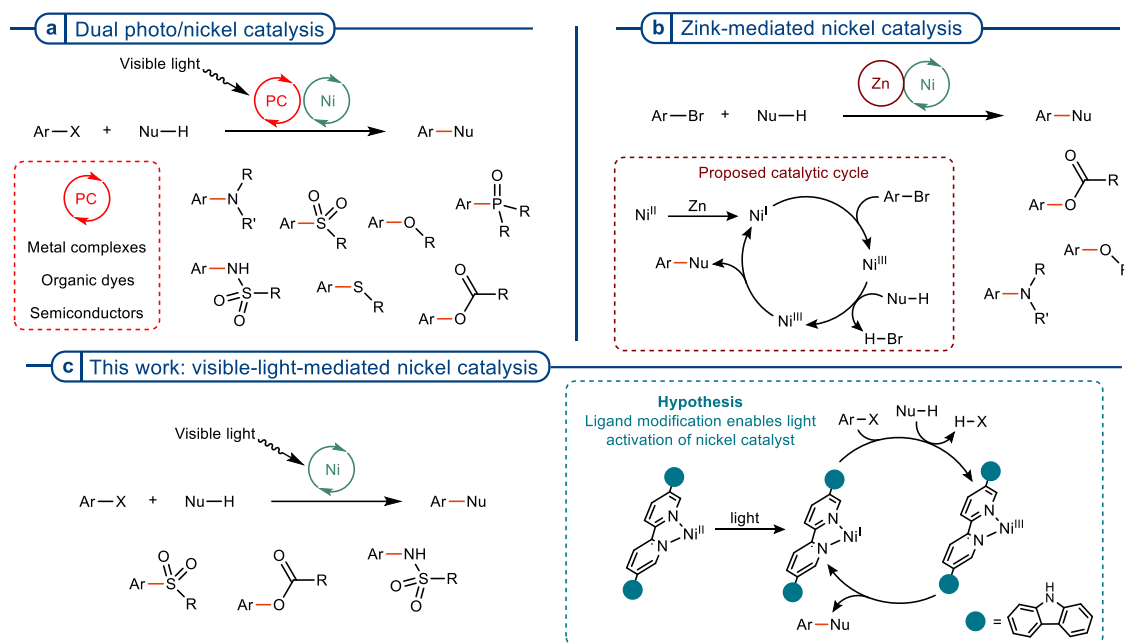


Figure 5.1. Strategies for nickel catalyzed carbon–heteroatom cross-couplings using bipyridyl ligands. a, Dual photo/nickel catalysis requires exogenous photocatalysts. b, Thermally-sustained nickel catalysis initiated by elemental zinc. c, Visible-light-mediated nickel catalysis through ligand modification (this work).

5.2 Ligand design and evaluation

Ni^{II} (dtbbpy) aryl halide complexes were previously shown to catalyze cross-couplings using 390 nm LEDs, but these catalysts have to be synthesized from $\text{Ni}(\text{COD})_2$, which requires glove-box- or Schlenk techniques, limiting the practicability of this approach.^{22–23} In dual photo/nickel catalysis, on the contrary, Ni^{II} (2,2'-bipyridyl) X_2 ($\text{X} = \text{Cl}, \text{Br}$) complexes that form *in situ* from cheap, benchstable Ni^{II} salts and the corresponding ligand can be used.^{8–10} UV-Vis absorption spectroscopy of a mixture of NiCl_2 :glyme (glyme = 1,2-dimethoxyethane) and dtbbpy in DMAc shows that the resulting complex only absorbs light below 320 nm (Figure 5.6). To shift the absorption of such a nickel complex towards the visible-light spectrum, we synthesized 5,5'-dicarbazolyl-2,2'-bipyridyl (czbpy) via a copper-catalyzed Ullmann coupling between 5,5'-dibromo-bipyridine and 9*H*-carbazole (Figure 5.2a).²⁷ The UV-visible spectrum of czbpy shows

a strong absorption until 400 nm (Figure 5.6). More importantly, dissolving NiCl₂·glyme and czbpy in DMAc resulted in a complex that absorbs up to 450 nm (Figure 5.6).

We tested czbpy as ligand for a set of visible-light-mediated, nickel catalyzed carbon–heteroatom cross-couplings without adding an exogenous photocatalyst (Figure 5.2b). To our delight, this ligand was indeed suitable for the coupling of aryl halides with sulfinates, carboxylic acids, and sulfonamides.²⁸ Attempts to form carbon–carbon bonds through coupling of aryl halides with borontrifluorides²⁹ or α -silylamines³⁰ were unsuccessful or suffered from low selectivity (Table 5.6).

The coupling of 4-iodobenzotrifluoride and a sodium sulfinate salt (C–S coupling), which was previously reported using combinations of a nickel catalyst with iridium³¹ or ruthenium³²⁻³³ polypyridyl complexes as photocatalyst, afforded sulfone **1** in excellent yield after 22 hours of irradiation with blue light (440 nm, entry 1). No conversion was detected when the reaction was carried out in the dark (entry 2). Sodium sulfinates and aryl halides can assemble in electron-donor acceptor (EDA) complexes and afford sulfones upon UV light irradiation.³⁴ Accordingly, even in absence of NiCl₂·glyme small amounts of **1** were formed (entry 3), due to partial emission in the UV region of the light source. When 2,2'-bipyridine (bpy), 9*H*-carbazole or a combination of bpy and 9*H*-carbazole were used, the desired product was also formed, although with significantly lower selectivity (entry 4-6).

The C–O coupling of 4-iodobenzotrifluoride with *N*-Boc-proline under optimized conditions resulted in 88% of the desired product (**2**). No product formation was observed in the dark, without NiCl₂·glyme, or when 9*H*-carbazole was used as ligand (entry 8-10). Only small amounts (<10 %) of **2** were formed using bpy, or bpy together with 9*H*-carbazole (entry 9, 11). This supports our hypothesis that czbpy enables activation of nickel catalysts with wavelengths above 400 nm, which are not accessible to bpy complexes.

Under optimized conditions, the light-mediated, nickel-catalyzed *N*-arylation of sulfonamides afforded **3** in 75% yield (entry 13). Light and the nickel salt were crucial for product formation (entry 14-15). Partial consumption of the starting material in absence of a nickel salt (entry 15) might be a result of a photocatalytic activation of aryl iodides.³⁵ Product formation was not detected using bpy as ligand (entry 17), but significant amounts of **3** were obtained in presence of 9*H*-carbazole (entry 16) or a combination of 9*H*-carbazole and bpy (entry 16, 18). Although such reactivity was not observed in the other coupling protocols, this effect might result from formation of photoactive Ni-carbazolyl complexes. It was recently shown that carbazole acts as

a strong σ -donating ligand that reduces the energy difference in MLCT transitions that account for light absorption of nickel complexes.³⁶⁻³⁷

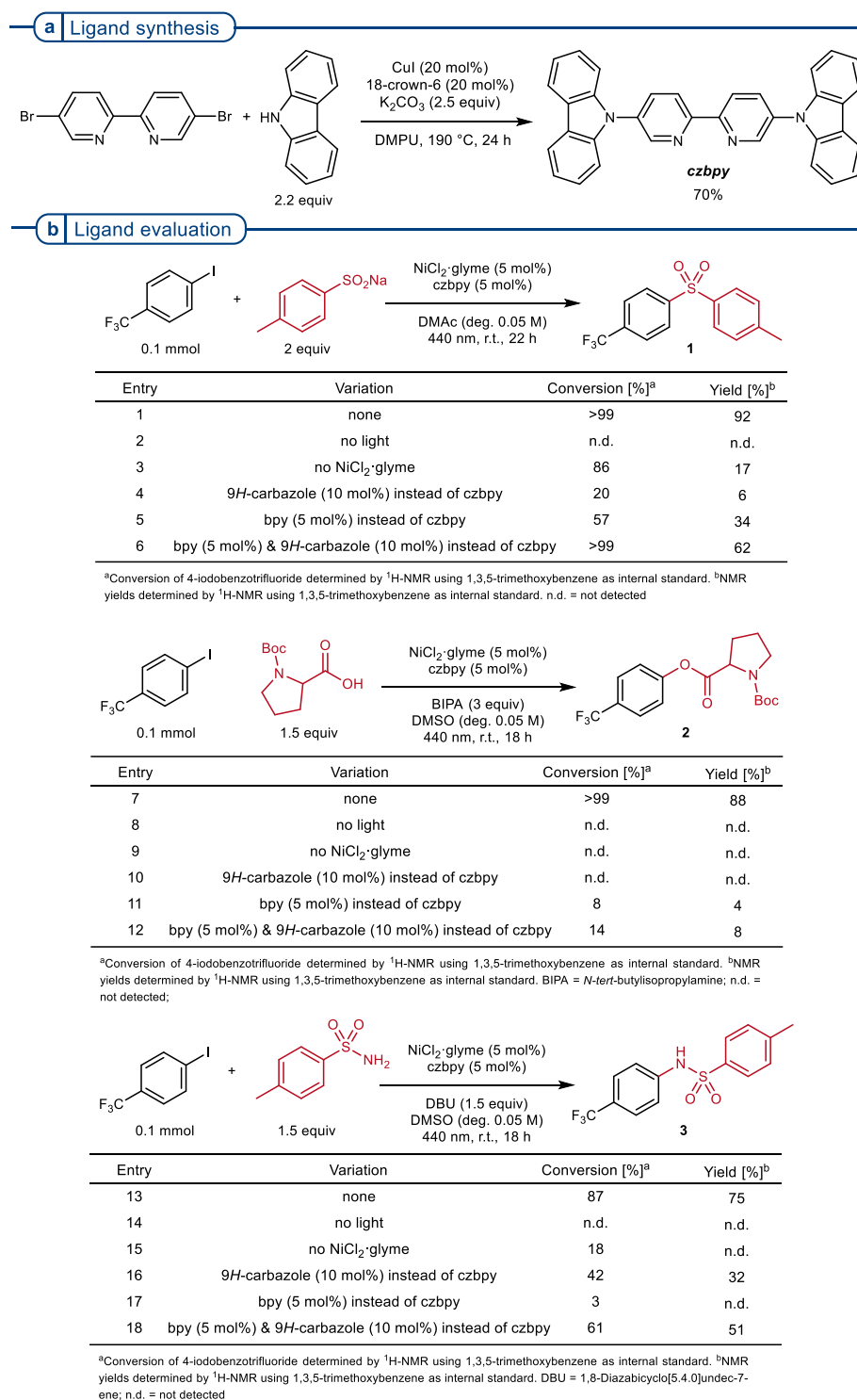
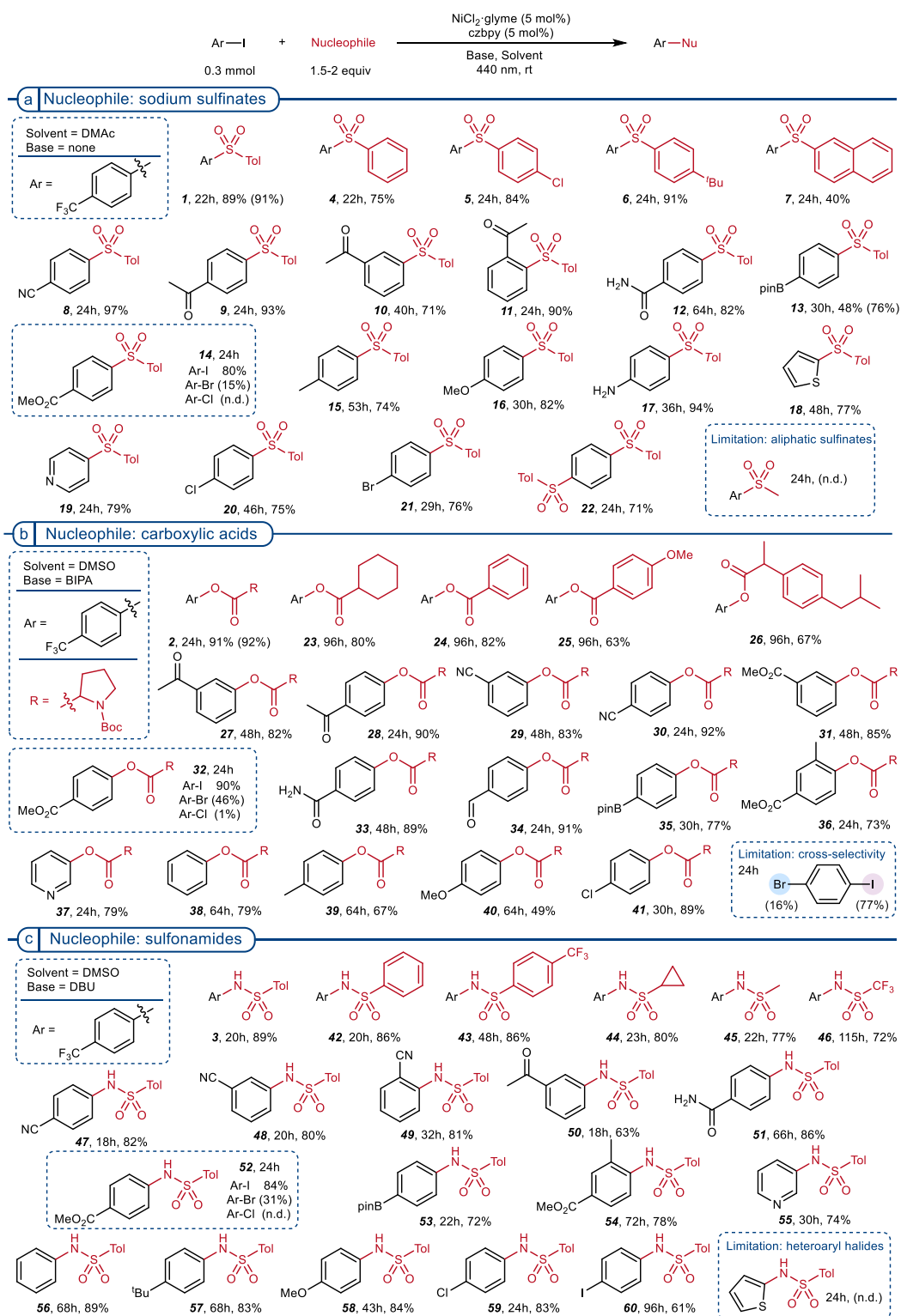


Figure 5.2. Ligand synthesis, optimized reaction conditions and control experiments. a, The ligand for photocatalyst-free, visible-light-mediated nickel catalysis was synthesized via an Ullmann C–N coupling. b, Optimized conditions and control experiments for the coupling of 4-iodobenzotrifluoride and sodium *p*-toluenesulfonate, *N*-Boc-proline and *p*-toluenesulfonamide.

Next, we explored the scope and limitations of these photocatalyst-free, visible-light-mediated carbon–heteroatom cross-couplings (Table 5.1). Several aromatic sulfinate salts were successfully coupled with 4-iodobenzotrifluoride (Table 5.1a, **1**, **4–7**). Optimized reaction conditions did not result in the desired product from the aliphatic sodium methane sulfinate. It is noteworthy that this substrate was earlier reported as a successful coupling partner when $\text{NiCl}_2 \cdot \text{bpy}$ was used in combination with tris(2,2'-bipyridyl)dichlororuthenium(II) hexahydrate as exogenous photocatalyst.³³ With regard to the aryl iodide, the reaction affords the corresponding sulfones in presence of electron withdrawing groups such as trifluoromethyl (**1**), nitrile (**8**), ketone (**9–11**), amide (**12**), boron pinacolate ester (**13**), and methyl ester (**14**). Para- (**9**) and ortho- (**11**) substitution showed similar reactivity, whereas meta-substitution (**10**) required a longer reaction time for full conversion. Electron-rich aryl iodides, such as 4-iodotoluene (**15**) and 4-iodoanisole (**16**), were suitable substrates and the presence of an unprotected amine group (**17**) was tolerated. Coupling of 2-iodothiophene (**18**) and 4-iodopyridine (**19**) showed that heteroaryl iodides are suitable substrates. A comparison of different aryl halides showed that an aryl iodide reacts significantly faster than the corresponding bromide (**14**). This is in contrast to dual nickel/photocatalytic protocols in which iodides and bromides exhibit similar reactivity.^{31–32} Aryl chlorides undergo nickel/photocatalytic reactions when more electron-donating 4,4'-dimethoxy-bpy ligand was used,³¹ but *czbpy* was not suitable for aryl chloride. These observations were applied for selective couplings of aryl iodides that contain a chloride (**20**) or a bromide substituent (**21**). Moreover, diarylated product **22** was synthesized from 1,4-diiodobenzene using 3 equivalents of sodium *p*-toluenesulfinate.

Good to excellent isolated yields were obtained for the C–O arylation of 4-iodobenzotrifluoride with aliphatic and aromatic carboxylic acids (Table 5.1b, **2**, **23–26**). Further, a range of aryl iodides containing electron-withdrawing groups afforded the corresponding products (**2**, **27–35**). The influence of substituents on reactivity is highlighted by the longer reaction times required for the coupling of meta-substituted (**27**, **29**, **31**) aryl iodides, compared to their para-substituted analogues (**28**, **30**, **32**). The coupling of ortho-substituted aryl iodides was not possible in case of 2-iodoacetophenone, 2-iodobenzonitrile, but **36** was successfully synthesized from methyl 3-methyl-4-iodobenzoate. A heteroaryl iodide was also susceptible to the optimized reaction conditions (**37**). High electron densities on the aryl iodide decreased their reactivity towards the C–O coupling, as showcased for the series 4-iodobenzene (**38**), 4-iodotoluene (**39**) and 4-iodoanisole (**40**). Similar to the C–S coupling described above, aryl iodides work best in the reaction (**32**, 90% from Ar-I).

Table 5.1. Visible-light-mediated nickel-catalyzed C–S, C–O and C–N cross-couplings.^a

^aReaction conditions: aryl halide (300 μmol), nucleophile (a, sodium sulfinate, 600 μmol ; b, carboxylic acid, 450 μmol ; c, sulfonamide, 450 μmol), NiCl₂-glyme (15 μmol), czbpy (15 μmol), base (b, *N*-*tert*-butylisopropylamine, 900 μmol ; c, 1,8-diazabicyclo[5.4.0]undec-7-ene, 450 μmol), solvent (a, DMAc, 6 mL; b, DMSO, 3 or 6 mL; c, DMSO, 6 mL), 440 nm LED (2 lamps at full power) at room temperature. Isolated yields are reported. NMR yields are in parantheses and were calculated via ¹H-NMR analysis using 1,3,5-trimethoxybenzene or maleic acid as internal standard. n.d. = not detected. Bpin = boronic acid pinacolate ester.

The reaction is rather slow using the corresponding bromide (46% NMR yield from Ar-Br), and a chloride afforded only traces of the desired product. As a result, 1-chloro-4-iodobenzene (**41**) coupled selectively on the iodo-position, but 1-bromo-4-iodobenzene reacted unselectively. All of these results are in agreement with previous reports on the dual nickel/photocatalytic cross-coupling of carboxylic acids with aryl halides, indicating that the photocatalyst-free strategy follows a similar mechanism.^{14, 26, 35, 38-39}

Aromatic as well as aliphatic sulfonamides (**3**, **42-46**) gave selective C–N cross-couplings with 4-iodobenzotrifluoride (Table 5.1c). Long reaction times were necessary in presence of electron-withdrawing groups on the nucleophile (**43**, **46**). In contrast to the previous C–S and C–O coupling, reactivity is not affected by the substitution pattern of the aryl iodide (**47-49**, **54**), or by the presence of either electron-withdrawing or electron-donating functional groups (**3**, **47-53**, **56-58**). Heteroaryl halides are problematic substrates in dual nickel/photocatalytic sulfonamidation protocols and require a ligand-free approach at elevated temperature.⁴⁰ Under our optimized conditions 3-iodopyridine gave **55** in good yield, but no product was observed for 2-iodothiophene. Aryl bromides were previously coupled with sulfonamides using combinations of nickel and iridium catalysts.⁴⁰ Our screening of different halides, showed that bromides are suitable substrates but reactivity of iodides is superior (**52**, 84% from Ar-I, 31% NMR yield from Ar-Br within 24h). Aryl chlorides are not suitable and therefore **59** was obtained with good selectivity from 1-chloro-4-iodobenzene.

5.3 Polymerization of czbpy for heterogeneous, visible-light-mediated nickel catalysis

Having shown that czbpy serves as a versatile ligand for visible-light-mediated cross-couplings via homogeneous nickel-catalysis without an exogenous photocatalyst, we aimed to extend this approach to develop a heterogeneous, recyclable catalytic system.⁴¹ Defined porous materials are ideal candidates for immobilization of metal catalysts, as they enable optimal access to the catalytic sites. The microporous organic polymer network poly-czbpy was synthesized from czbpy via oxidative polymerization with iron(III) chloride and exhibits a Brunauer-Emmett-Teller (BET) surface area of 853 m² g⁻¹ (Figure 5.3a).²⁷ Ni@poly-czbpy was subsequently prepared by refluxing a suspension of poly-czbpy and NiCl₂ in methanol. Investigation of the porosity by nitrogen sorption measurements after metalation showed a decreased BET surface of 470 m² g⁻¹ due to the immobilization of the Ni(II) complex. Presence of nickel shifts light

absorption of the material up to 650 nm (Figure 5.3b), while the metal-free ligand framework poly-czbp_y absorbs until 550 nm. Characterization of Ni@poly-czbp_y by X-ray photoelectron spectroscopy (XPS) confirmed successful immobilization of Ni(II) species on the polymeric material. The N 1s core spectrum (Figure 5.3c) contains three signals for nitrogen: i) an intense peak at 400.4 eV corresponding to polymerized carbazole moieties, ii) a signal at 399.7 eV which is assigned to N-Ni coordination of the Ni(II)-complex and iii) a low-intensity peak at 400.2 eV deriving from bipyridine nitrogen species which are not coordinated to nickel. The Ni 2p spectrum (Figure 5.3d) shows a doublet and its corresponding satellites. Peaks located at 855.6 eV and 873.3 eV are assigned to 2p_{3/2} and 2p_{1/2} signals for Ni(II) species, respectively. ICP-OES analysis indicated presence of 3.7% w/w of nickel on the material Ni@poly-czbp_y, corresponding to occupation of 40% of bipyridine functionalities.

After confirming that poly-czbp_y is suitable to coordinate and immobilize nickel atoms, its use in the previously optimized coupling reactions was studied (Figure 5.3e). The desired C–S, C–O and C–N coupling products were obtained by irradiation at 440 nm of mixtures of NiCl₂·glyme (5 mol%) and poly-czbp_y (5 mol%), but the selectivity of the reactions was lower than using homogeneous conditions.

Next, we sought to study the recyclability of the heterogeneous catalytic system. Poly-czbp_y was recovered after the C–S coupling reaction by centrifugation and was, after washing, reused for the same reaction (Figure 5.3f). Initial results confirmed that poly-czbp_y can be recycled ten times without significant loss in reactivity (orange bars). The addition of the nickel salt at each reaction cycle was unnecessary, as confirmed in a second set of experiments (green bars) and selectivity of the reaction improved upon washing and reusing the material without addition of fresh nickel salt (1st cycle: 78% yield, 2nd cycle: 90% yield). According to previous ICP-OES analysis, 40% of the pyridine sites in poly-czbp_y coordinate to nickel. Therefore, equimolar amounts of nickel and poly-czbp_y lead to an excess of unligated nickel in solution, which presumably has a detrimental effect on the selectivity. This was confirmed by reactions using lower nickel salt/ligand ratio (2.5 mol% of NiCl₂·glyme, 5 mol% poly-czbp_y) that improved selectivity for all the three transformations (Table 5.28, 5.29, 5.30).

A final recycling experiment in which 2.5 mol% of NiCl₂·glyme was loaded only for the first reaction (Figure 5.3f, blue bars) resulted in excellent yields for the C–S coupling reaction without any loss in activity over ten recycling experiments.

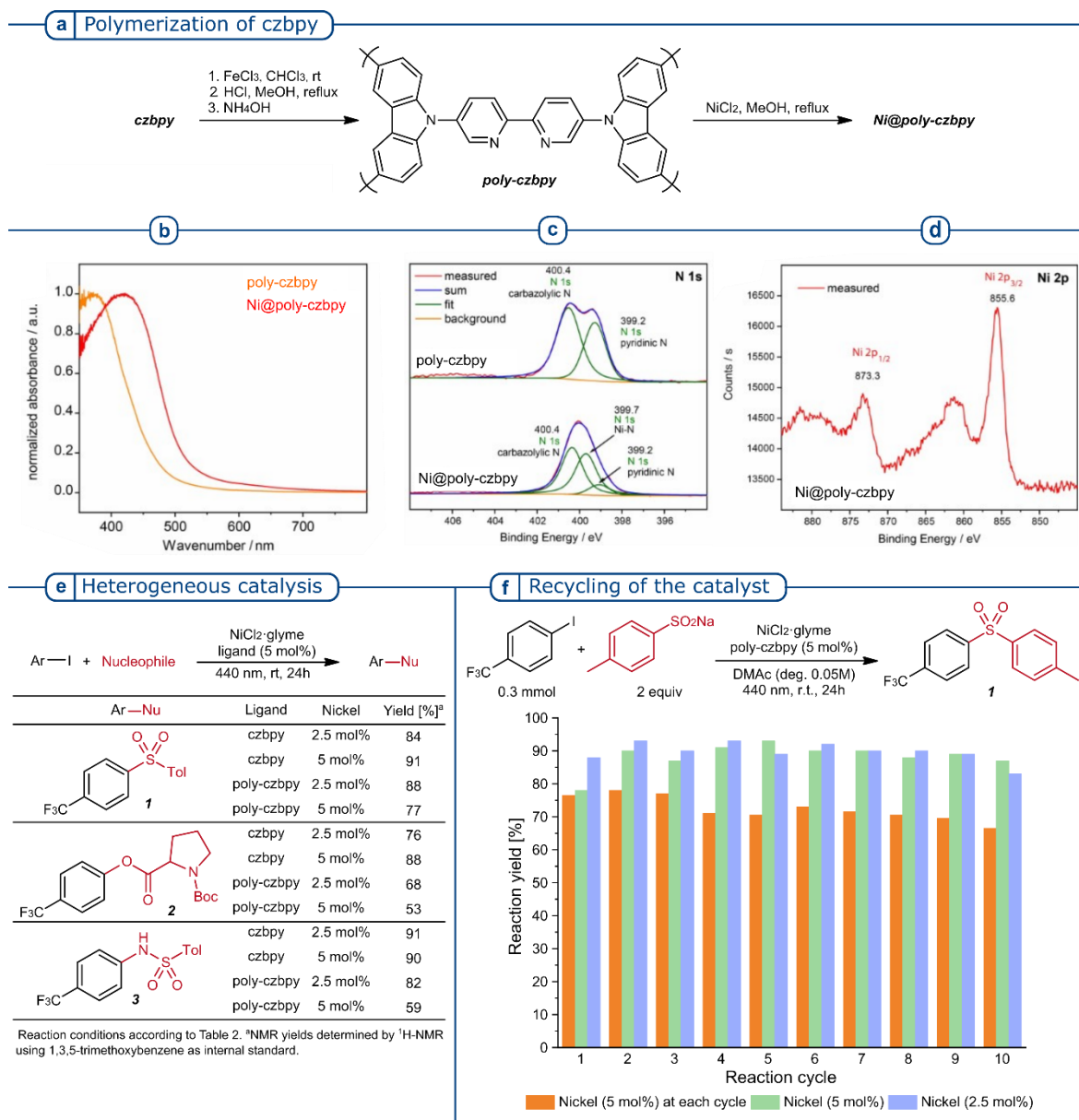


Figure 5.3. Heterogeneous visible-light-mediated nickel catalysis with poly-czbpy. **a**, Preparation of the porous organic polymer poly-czbpy and metalation with nickel. **b**, Characterization of poly-czbpy and Ni@poly-czbpy by UV-visible spectroscopy. XPS analysis of Ni@poly-czbpy: N 1s (**c**) and Ni 2p core-level spectra (**d**). **e**, Heterogeneous visible-light-mediated nickel catalysis using poly-czbpy. **f**, Recycling of the catalyst in the C–S coupling reaction. Reaction conditions: 4-iodobenzotrifluoride (300 μ mol), sodium *p*-toluenesulfonate (600 μ mol), NiCl₂·glyme (7.5–15 μ mol), poly-czbpy (7.43 mg), DMAc (6 mL), 440 nm LED (2 lamps at full power) at room temperature. Yields were calculated via ¹H-NMR analysis using 1,3,5-trimethoxybenzene as internal standard. Orange: 5 mol% of NiCl₂·glyme at each reaction cycle; green: 5 mol% of NiCl₂·glyme only for the first cycle; blue: 2.5 mol% of NiCl₂·glyme only for the first cycle.

5.4 Conclusion

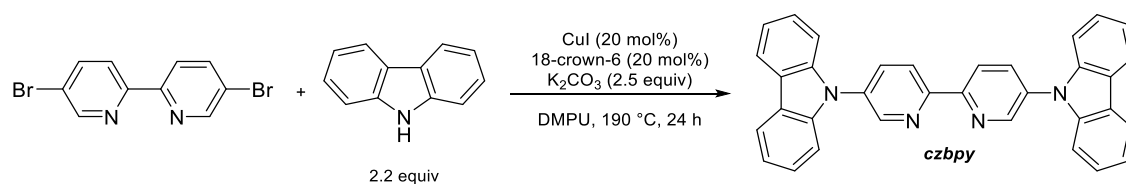
A nickel complex that forms *in situ* from NiCl₂·glyme and the carbazole-functionalized bipyridyl ligand czbpy absorbs light up to 450 nm and catalyzes the cross-coupling of aryl halides and nucleophiles under visible light irradiation, without an exogenous photocatalyst. This approach enables the formation of C–S, C–O and C–N bonds, by coupling aryl iodides with sodium sulfinates, carboxylic acids or sulfonamides. Scope and limitations of the optimized reaction protocols were evaluated on substrates presenting different functional groups and electronic properties. Polymerization of czbpy resulted in the polymeric ligand framework poly-czbpy that complexes nickel salts and enables heterogeneous, visible-light-mediated nickel catalysis. The catalytic system is recyclable, the material was reused 10 times maintaining excellent yield and selectivity and did not require addition of the nickel salt upon recycling.

5.5 Supporting information

5.5.1 General remarks

All reagents and solvents were purchased from commercial suppliers and used without further purification. Sodium 2-naphthalenesulfinate,⁴² sodium 4-*tert*-butylbenzenesulfinate⁴² and 1-((trimethylsilyl)methyl)piperidine³⁰ were prepared according to previously reported procedures. LED lamps for photocatalytic experiments were purchased from Kessil Lightning.⁴³ ¹H-, ¹³C-, and ¹⁹F spectra were recorded on a Varian 400 spectrometer (400 MHz, Agilent), an Ascend™ 400 spectrometer (400 MHz, cryoprobe, Bruker) and a Varian 600 spectrometer (600 MHz, Agilent) at 298 K, and are reported in ppm relative to the residual solvent peaks. Peaks are reported as: s = singlet, d = doublet, t = triplet, q = quartet, m = multiplet or unresolved, with coupling constants in Hz. Analytical thin layer chromatography (TLC) was performed on pre-coated TLC-sheets (ALUGRAM Xtra SIL G/UV₂₅₄ sheets, Macherey-Nagel) and visualized with 254 nm light or staining solutions followed by heating. Purification of final compounds was carried out by flash chromatography using Silica 60 M (0.04-0.063 mm) silica gel (Sigma Aldrich). UV/Vis spectra were recorded using a UV-1900 spectrometer (Shimadzu) for samples in solution and a Cary 5000 UV–Vis–NIR spectrometer (Agilent, USA) for solid samples. High-resolution mass spectral data were obtained using a Waters XEVO G2-XS 4K spectrometer with the XEVO G2-XS QTOF capability kit (ESI) and a Micromass GC-TOF micro (Water Inc.) (EI). X-ray photoelectron spectroscopy (XPS) data were obtained from an ESCA-Lab220i-XL electron spectrometer. The Brunauer–Emmett–Teller specific surface area (S_{BET}) was calculated based on the nitrogen sorption isotherms collected at 77 K using a 3-flex surface characterization analyzer (Micromeritics Instrument Corporation, USA). Nickel contents were measured by inductively coupled plasma-optical emission spectroscopy (ICP-OES 715 ES, Varian, USA) after digesting the polymers in a mixture of nitric acid and sulfuric acid (V:V = 2:1).

5.5.2 Preparation czbpy, poly-czbpy and Ni@poly-czbpy



5,5'-Di(9H-carbazol-9-yl)-2,2'-bipyridine (czbpy) was prepared by adapting a literature procedure.²⁷

In an Argon atmosphere, a mixture of 5,5'-dibromo-2,2'-bipyridine (500 mg, 1.59 mmol), carbazole (586 mg, 3.5 mmol), copper(I) iodide (61 mg, 0.32 mmol), 18-crown-6 (84 mg, 0.32 mmol), potassium carbonate (549 mg, 3.98 mmol) in 1,3-dimethyl-3,4,5,6-tetrahydro-2(1H)-pyrimidinone (DMPU, 1.67 mL) was placed in a pre-heated 100 mL Schlenk flask. The flask was connected to a reflux condenser before the mixture was stirred for 24 h at 190 °C using an oil bath. The yellow reaction solution turned to a black viscous oil after 24 h, at which point was quenched with 2 M HCl (100 mL). The mixture was extracted with dichloromethane (2x125 mL) and washed with NH₃·H₂O (25%, 60 mL) and water (100 mL). The organic layer was dried over magnesium sulfate and the solvent was removed in vacuo. The crude product was purified by column chromatography on amino-functionalized silica gel (gradient 0-50% dichloromethane/cyclohexane). The obtained yellow solid was further purified by recrystallization from cyclohexane/dichloromethane (9:1) to afford the title compound as a light-yellow crystalline solid (540 mg, 1.11 mmol, 70 %).

¹H NMR (400 MHz, CDCl₃) δ 9.03 (d, J = 1.8 Hz, 2H), 8.81 (d, J = 7.7 Hz, 2H), 8.19 (d, J = 7.7 Hz, 4H), 8.15 (dd, J = 8.4, 2.6 Hz, 2H), 7.55 – 7.44 (m, 8H), 7.36 (m, 4H). ¹³C NMR (101 MHz, CDCl₃) δ 153.5, 147.5, 140.6, 135.5, 135.2, 126.6, 124.0, 122.5, 121.0, 120.8, 109.6. HRMS (ESI) m/z calcd for C₃₄H₂₃N₄ [(M+H)⁺] 487.1923, found 487.1918. This data are in full agreement with those reported in literature.⁴⁴

The porous organic polymer **poly-czbpy** was prepared by oxidative polymerization of 5,5'-di(9H-carbazol-9-yl)-2,2'-bipyridine (czbpy), according to literature.²⁷

Preparation of Ni@poly-czbp

Poly-czbp (100 mg, 0.21 mmol based on monomer) was dispersed in a methanolic solution of NiCl₂ (42 mL, 5 mM) under inert atmosphere and refluxed for 24 hours while gently stirring. After filtration through a glass frit, the residue was washed with chloroform and dried in an oven at 80 °C to afford Ni@poly-czbp as a brown solid.

5.5.3 Experimental setup for photochemical experiments

Photochemical experiments involving visible light irradiation were carried out using Kessil PR160L-440 (440nm, blue light) or Kessil PR160L-525 (525 nm, green light) LED lamps with the respective power settings.⁴³ One or two lamps were used, depending on the required light intensity to irradiate reaction vessels located on a stirring plate (lamp-vessel distance: 4.5 cm; stirring speed: 800 rpm, Figure 5.5). To avoid heating of the reaction mixture, fans were used for cooling.

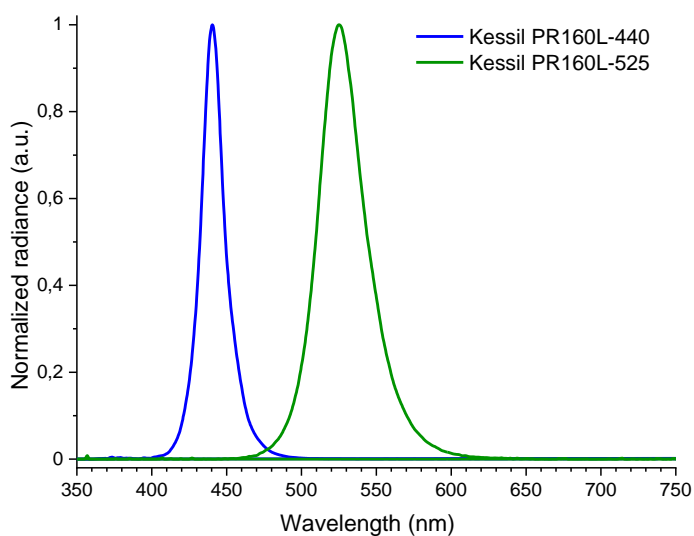


Figure 5.4. Emission spectra of Kessil PR160L-400 (blue) and Kessil PR160L-525 (green) LED lamps.



Figure 5.5. Configuration of the experimental setup using one or two LED lamps.

5.5.4 UV-visible spectroscopy measurements

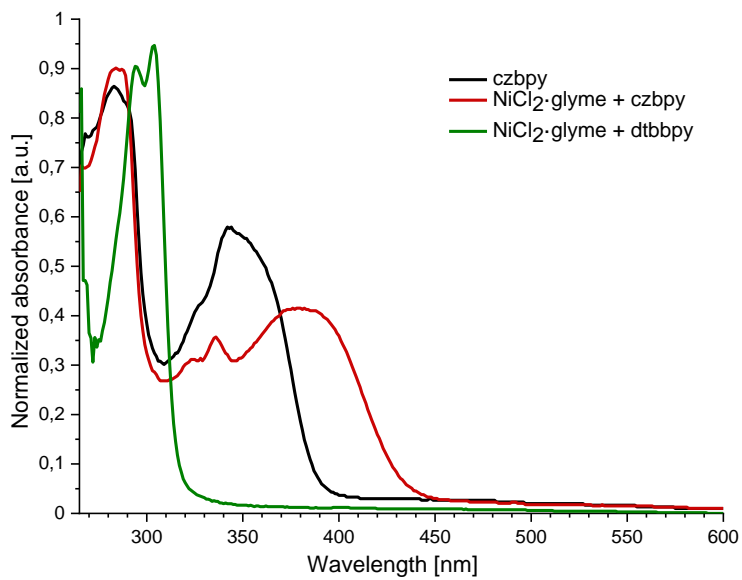


Figure 5.6. UV-visible spectra of 5,5'-di-carbazolyl-2,2'-bipyridyl (czbpy) and mixtures of NiCl₂·glyme and czbpy or 4,4'-di-*tert*-butyl-2,2'-bipyridyne (dtbbpy) in DMAc (10 μ M).

5.5.5 Unsuccessful coupling reactions using homogeneous visible-light-mediated nickel catalysis

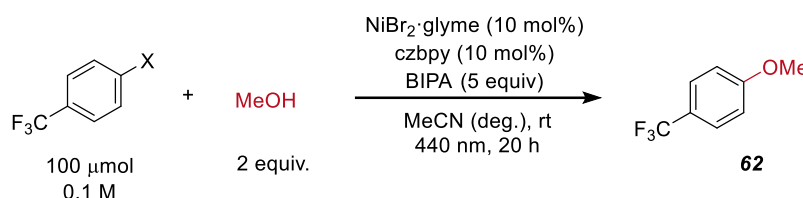
Table 5.2. Screenings for the coupling of 4-halobenzotrifluorides and pyrrolidine.^{a, 45-46}



Entry	Aryl halide	Conversion [%] ^b	61 [%] ^c
1	Bromide	2	n.d.
2	Iodide	5	n.d.

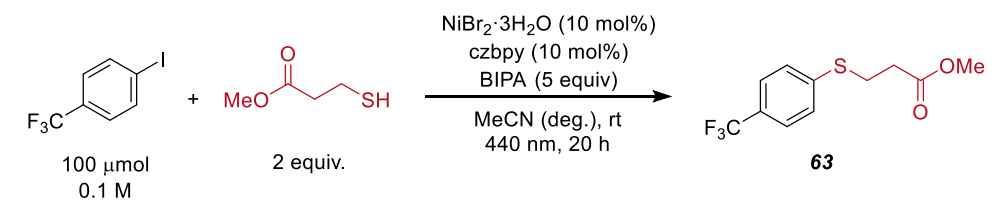
^aReaction conditions: 4-iodobenzotrifluoride (200 μ mol), pyrrolidine (600 μ mol), $\text{NiBr}_2 \cdot 3\text{H}_2\text{O}$ (10 μ mol), 5,5'-dicarbazolyl-2,2'-bipyridyl (czbpy, 10 μ mol), DMSO (anhydrous, 1 mL), 440 nm LED (1 lamp at 50% power). ^bConversion of aryl halide determined by ¹H-NMR using 1,3,5-trimethoxybenzene as internal standard. ^cNMR yields determined by ¹H-NMR using 1,3,5-trimethoxybenzene as internal standard. n.d. = not detected.

Table 5.3. Screenings for the coupling of 4-halobenzotrifluorides and methanol.^{a, 47-48}



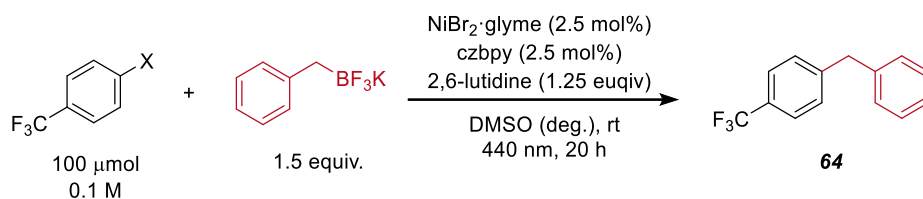
Entry	Aryl halide	Conversion [%] ^b	62 [%] ^c
1	Bromide	1	n.d.
2	Iodide	<1	n.d.

^aReaction conditions: aryl halide (100 μ mol), methanol (100 μ mol), $\text{NiBr}_2 \cdot \text{glyme}$ (10 μ mol), 5,5'-dicarbazolyl-2,2'-bipyridyl (czbpy, 10 μ mol), *N,N*-*tert*-butylisopropylamine (BIPA, 500 μ mol), MeCN (anhydrous, 1 mL), 440 nm LED (1 lamp at 50% power). ^bConversion of aryl halide determined by ¹H-NMR using 1,3,5-trimethoxybenzene as internal standard. ^cNMR yields determined by ¹H-NMR using 1,3,5-trimethoxybenzene as internal standard. glyme = 1,2-dimethoxyethane. n.d. = not detected.

Table 5.4. Screenings for the coupling of 4-iodobenzotrifluoride and methyl 3-mercaptopropanoate.^{a, 48}

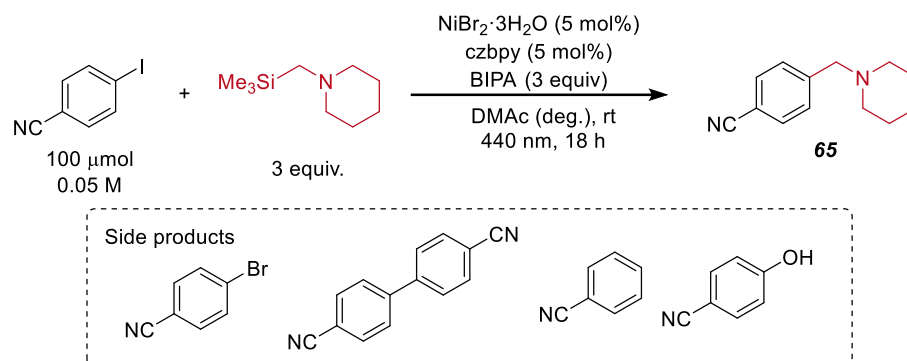
Entry	Conversion [%] ^b	63 [%] ^c
1	3	n.d.

^aReaction conditions: 4-iodobenzotrifluoride (100 μmol), methyl 3-mercaptopropanoate (200 μmol), $\text{NiBr}_2 \cdot \text{glyme}$ (10 μmol), 5,5'-dicarbazolyl-2,2'-bipyridyl (czbpy, 10 μmol), *N,N*-tert-butylisopropylamine (BIPA, 500 μmol), MeCN (anhydrous, 1 mL), 440 nm LED (1 lamp at 50% power). ^bConversion of 4-iodobenzotrifluoride determined by ¹H-NMR using 1,3,5-trimethoxybenzene as internal standard. ^cNMR yields determined by ¹H-NMR using 1,3,5-trimethoxybenzene as internal standard. n.d. = not detected.

Table 5.5. Screenings for the coupling of 4-halobenzotrifluorides and potassium benzyltrifluoroborate.^{a, 29}

Entry	Aryl halide	Conversion [%] ^b	64 [%] ^c
1	Bromide	2	n.d.
2	Iodide	-	n.d.

^aReaction conditions: aryl halide (100 μmol), potassium benzyltrifluoroborate (150 μmol), $\text{NiBr}_2 \cdot \text{glyme}$ (2.5 μmol), 5,5'-dicarbazolyl-2,2'-bipyridyl (czbpy, 2.5 μmol), 2,6-lutidine (125 μmol), DMSO (anhydrous, 1 mL), 440 nm LED (1 lamp at 50% power). ^bConversion of aryl halide determined by ¹H-NMR using 1,3,5-trimethoxybenzene as internal standard. ^cNMR yields determined by ¹H-NMR using 1,3,5-trimethoxybenzene as internal standard. glyme = 1,2-dimethoxyethane. n.d. = not detected.

Table 5.6. Screenings for the coupling of 4-iodobenzonitrile and 1-((trimethylsilyl)methyl)piperidine.^{a, 30}

Entry	Variation	Conversion [%] ^b	65 [%] ^c	Ar-Br [%] ^c	Ar-Ar [%] ^c	Ar-H [%] ^c	Ar-OH [%] ^c
1	None	>99	38	n.d.	25	10	n.d.
2	NiCl ₂ ·glyme	>99	29	n.d.	23	20	n.d.
3	NiBr ₂ ·glyme	88	28	8	22	11	1
4	No NiBr ₂ ·3H ₂ O	>99	n.d.	n.d.	n.d.	70	n.d.
5	DMSO	53	n.d.	9	0	20	0
6	DMF	>99	27	n.d.o.	10	n.d.o.	4
7	4-iodoanisole	>99	32	n.d.	33	n.d.	n.d.
11	No czbpy	>99	7	n.d.	n.d.	25	n.d.
12	No light	-	n.d.	n.d.	n.d.	n.d.	n.d.

^aReaction conditions: 4-iodobenzonitrile (100 μmol), 1-((trimethylsilyl)methyl)piperidine (300 μmol), NiBr₂·3H₂O (5 μmol), 5,5'-dicarbazolyl-2,2'-bipyridyl (czbpy, 5 μmol), *N,N*-*tert*-butylisopropylamine (BIPA, 300 μmol), DMAc (anhydrous, 2 mL), 440 nm LED (1 lamp at full power). ^bConversion of 4-iodobenzonitrile determined by ¹H-NMR using 1,3,5-trimethoxybenzene as internal standard. ^cDetermined by ¹H-NMR using 1,3,5-trimethoxybenzene as internal standard. Glyme = 1,2-dimethoxyethane. n.d. = not detected. n.d.o. = not detected due to overlap with solvent signal.

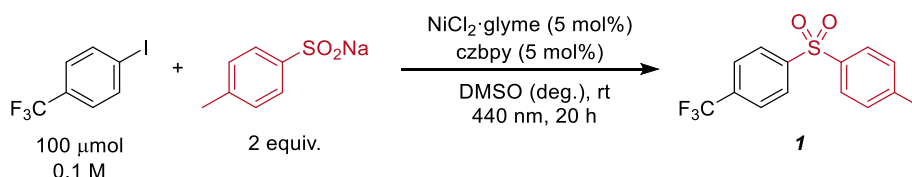
5.5.6 Optimization of the C–S cross-coupling using homogeneous visible-light-mediated nickel catalysis

General procedure for screening experiments

An oven dried vial (19 x 100 mm) equipped with a stir bar was charged with a nickel salt (5-10 μmol), 5,5'-dicarbazyl-2,2'-bipyridyl (czbpy, 5-10 μmol), 4-iodobenzotrifluoride (100-200 μmol) and sodium *p*-toluensulfinate (100-200 μmol). The solvent (anhydrous, 1-2 mL) was added and the vessel was sealed with a septum and Parafilm. The mixture was stirred for 1 minute at high speed, followed by sonication for 5 minutes and degassing by bubbling argon for 10 minutes. The reaction mixture was stirred at 800 rpm and irradiated with 440 nm LED lamps using the reported power settings. After the respective reaction time, 1,3,5-trimethoxybenzene (16.8 mg, 100 μmol , 1 equiv) was added to the reaction vessel, the mixture was shaken and an aliquote (20 μL) was removed, diluted with DMSO-*d*₆ and analyzed by ¹H NMR.

Initial screening experiments

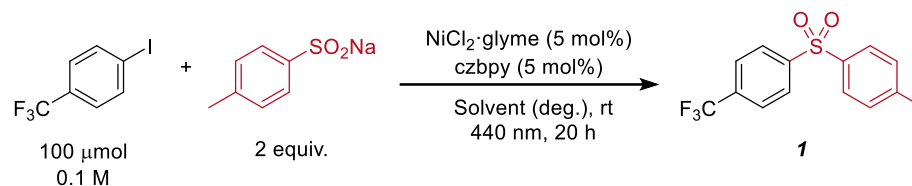
Table 5.7. Screening experiments for the coupling of 4-iodobenzotrifluoride and sodium *p*-toluensulfinate.^a



Entry	Variation	Conversion [%] ^b	1 [%] ^c
1	None	18	18
2	$\text{NiCl}_2 \cdot \text{glyme}$ (10 mol%), czbpy (10 mol%)	41	34
3	525 nm (1 lamp at 50% power)	-	n.d.
4	No irradiation	-	n.d.
5	dtbbpy instead of czbpy	9	6

^aReaction conditions: 4-iodobenzotrifluoride (100 μmol), sodium *p*-toluensulfinate (200 μmol), $\text{NiCl}_2 \cdot \text{glyme}$ (5 μmol), 5,5'-dicarbazyl-2,2'-bipyridyl (czbpy, 5 μmol), DMSO (anhydrous, 1 mL), 440 nm LED (1 lamp at 50% power). ^bConversion of 4-iodobenzotrifluoride determined by ¹H-NMR using 1,3,5-trimethoxybenzene as internal standard. ^cNMR yields determined by ¹H-NMR using 1,3,5-trimethoxybenzene as internal standard. glyme = 1,2-dimethoxyethane. dtbbpy = 4,4'-di-*tert*-butyl-2,2'-bipyridyl. n.d. = not detected.

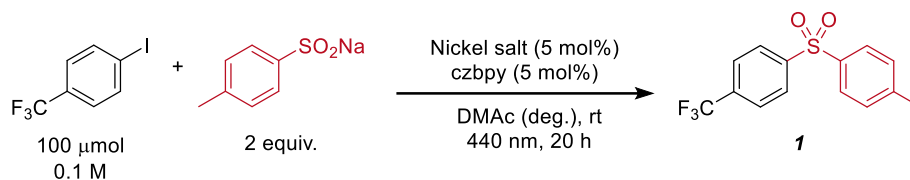
Solvent screening

Table 5.8. Solvent screening for the coupling of 4-iodobenzotrifluoride and sodium *p*-toluensulfinate.^a

Entry	Solvent	Conversion [%] ^b	1 [%] ^c
1	DMSO	18	18
2	DMF ^d	-	16
3	DMAc	31	27
4	MeCN	-	n.d.
5	Acetone ^e	-	n.d.
6	THF ^e	-	n.d.
7	Dioxane	-	n.d.

^aReaction conditions: 4-iodobenzotrifluoride (100 μmol), sodium *p*-toluensulfinate (200 μmol), NiCl₂·glyme (5 μmol), 5,5'-dicarbazolyl-2,2'-bipyridyl (czbpy, 5 μmol), Solvent (anhydrous, 1 mL), 440 nm LED (1 lamp at 50% power). ^bConversion of 4-iodobenzotrifluoride determined by ¹H-NMR using 1,3,5-trimethoxybenzene as internal standard. ^cNMR yields determined by ¹H-NMR using 1,3,5-trimethoxybenzene as internal standard. ^dSubstrate and product ratios calculated from ¹⁹F NMR. ^eDegassed by three cycles of freeze-pump-thaw. glyme = 1,2-dimethoxyethane. n.d. = not detected.

Screening of nickel salts

Table 5.9. Screening of nickel salts for the coupling of 4-iodobenzotrifluoride and sodium *p*-toluensulfinate.^a

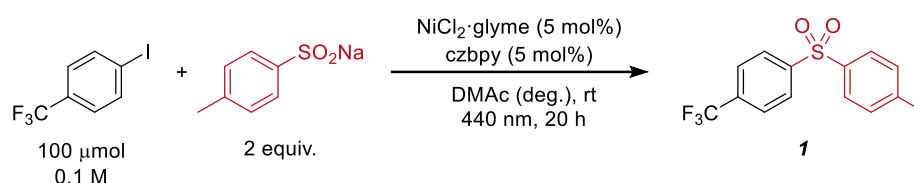
Entry	Nickel salt	Conversion [%] ^b	1 [%] ^c
1	NiCl ₂ ·glyme	31	27
2	NiCl ₂	12	12
3	NiCl ₂ ·6H ₂ O	9	8
4	NiBr ₂ ·glyme	19	19
5	NiBr ₂	4	4
6	NiBr ₂ ·3H ₂ O	22	20
7	NiI ₂	6	6
8	Ni(SO ₄) ₂ ·6H ₂ O	-	n.d.
9	Ni(ClO ₄) ₂ ·6H ₂ O	13	10
10	Ni(NO ₃) ₂ ·6H ₂ O	10	10
11	Ni(OAc) ₂ ·4H ₂ O	12	3
12	Ni(OTf) ₂	-	n.d.
13	Ni(acac) ₂	-	n.d.
14	Ni(COD)(DQ)	12	3

^aReaction conditions: 4-iodobenzotrifluoride (100 μmol), sodium *p*-toluenesulfinate (200 μmol), nickel salt (5 μmol), 5,5'-dicarbazolyl-2,2'-bipyridyl (czbpy, 5 μmol), DMAc (anhydrous, 1 mL), 440 nm LED (1 lamp at 50% power). ^bConversion of 4-iodobenzotrifluoride determined by ¹H-NMR using 1,3,5-trimethoxybenzene as internal standard. ^cNMR yields determined by ¹H-NMR using 1,3,5-trimethoxybenzene as internal standard. n.d. = not detected. glyme = 1,2-dimethoxyethane. acac = acetylacetonate. COD = 1,5-cyclooctadiene. DQ = duroquinone.

After showing that NiCl₂·glyme as nickel source gives best results, different conditions were compared.

NiCl₂·glyme and czbpy were mixed in THF in the reaction flask and gently heated for 10 minutes to preform the nickel complex. After removing THF under vacuum, 4-iodobenzotrifluoride, sodium *p*-toluensulfinate and DMAc were added and the reaction mixture was irradiated for the corresponding time. This preligation procedure provided lower yield (Table 5.10, entry 2). Further, a ligand-to-nickel ratio of 2:1 didn't improve the yield as well (entry 3).

Table 5.10. Screening of different ligation conditions.^a



Entry	Variation	Conversion [%] ^b	1 [%] ^c
1	None	31	27
2	Preligation	21	15
3	czbpy (10 mol%)	30	26

^aReaction conditions: 4-iodobenzotrifluoride (100 μmol), sodium *p*-toluensulfinate (200 μmol), NiCl₂·glyme (5 μmol), 5,5'-dicarbazolyl-2,2'-bipyridyl (czbpy, 5-10 μmol), DMAc (anhydrous, 1 mL), 440 nm LED (1 lamp at 50% power). ^bConversion of 4-iodobenzotrifluoride determined by ¹H-NMR using 1,3,5-trimethoxybenzene as internal standard. ^cNMR yields determined by ¹H-NMR using 1,3,5-trimethoxybenzene as internal standard. glyme = 1,2-dimethoxyethane.

Base screening

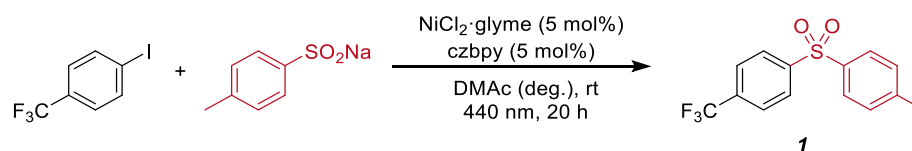
Table 5.11. Base screening for the coupling of 4-iodobenzotrifluoride and sodium *p*-toluenesulfinate.^a

Entry	Base	Conversion [%] ^b	1 [%] ^c
1	None	31	27
2	BIPA	30	22
3	DIPEA	34	30
4	NBu ₃	29	26
5	NEt ₃	27	20
6	Pyridine	32	25
7	2,6-Lutidine	19	19
8	DBU	33	n.d.
9	Quinuclidine	22	15
10	DABCO	36	30
11	Na ₂ HPO ₄	36	31
12	Na ₂ CO ₃	18	18

^aReaction conditions: 4-iodobenzotrifluoride (100 μmol), sodium *p*-toluenesulfinate (200 μmol), NiCl₂·glyme (5 μmol), 5,5'-dicarbazolyl-2,2'-bipyridyl (czbpy, 5 μmol), Base (20 μmol), DMAc (anhydrous, 1 mL), 440 nm LED (1 lamp at 50% power). ^bConversion of 4-iodobenzotrifluoride determined by ¹H-NMR using 1,3,5-trimethoxybenzene as internal standard. ^cNMR yields determined by ¹H-NMR using 1,3,5-trimethoxybenzene as internal standard. glyme = 1,2-dimethoxyethane. BIPA = *N*-*tert*-butylisopropylamine. DIPEA = *N,N*-diisopropylethylamine. DBU = 1,8-diazabicyclo[5.4.0]undec-7-ene. DABCO = 1,4-diazabicyclo[2.2.2]octane. n.d. = not detected.

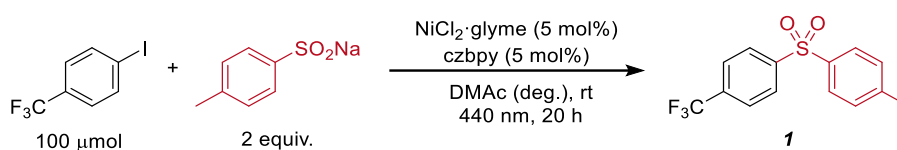
Although the nucleophile is already a salt, the addition of a base was evaluated. Only slightly better yields were obtained using 20 mol% of *N,N*-diisopropylethylamine (DIPEA, Table 5.11, Entry 3), 1,4-diazabicyclo[2.2.2]octane (DABCO, entry 10) and sodium hydrogen phosphate (Na₂HPO₄, entry 11).

Optimization of stoichiometry, light irradiation and concentration

Table 5.12. Optimization of stoichiometry and light irradiation for the coupling of 4-iodobenzotrifluoride and sodium *p*-toluensulfinate.^a

Entry	Ar-I	Ar-SO ₂ Na	Lamps, power	Conversion [%] ^b	1 [%] ^c
1	100 μmol	200 μmol	1, 50%	31	27
2	100 μmol	200 μmol	1, 100%	36	36
3	100 μmol	200 μmol	2, 100%	92	89
4	100 μmol	150 μmol	1, 100%	47	39
5	100 μmol	120 μmol	1, 100%	40	36
6	100 μmol	120 μmol	2, 100%	73	62
7	100 μmol	110 μmol	1, 100%	42	35
8	150 μmol	100 μmol	1, 100%	26	21

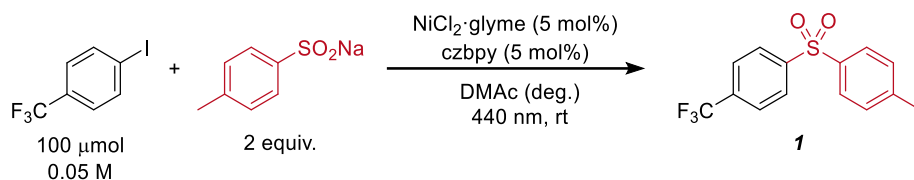
^aReaction conditions: 4-iodobenzotrifluoride (100-150 μmol), sodium *p*-toluensulfinate (100-200 μmol), NiCl₂·glyme (5 μmol), 5,5'-dicarbazolyl-2,2'-bipyridyl (czbpy, 5 μmol), DMAc (anhydrous, 1 mL), 440 nm LED. ^bConversion of 4-iodobenzotrifluoride determined by ¹H-NMR using 1,3,5-trimethoxybenzene as internal standard. ^cNMR yields determined by ¹H-NMR using 1,3,5-trimethoxybenzene as internal standard. glyme = 1,2-dimethoxyethane.

Table 5.13. Different concentrations for the coupling of 4-iodobenzotrifluoride and sodium *p*-toluensulfinate.^a

Entry	Concentration	Conversion [%] ^b	1 [%] ^c
1	0.05 M	60	55
2	0.1 M	36	36
3	0.2 M	32	32

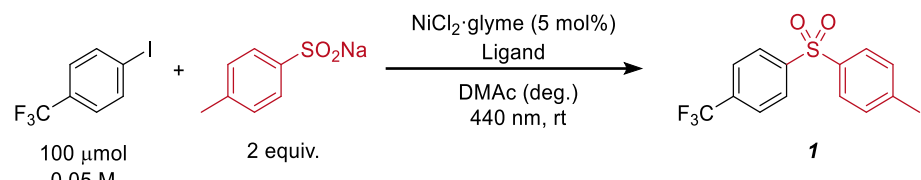
^aReaction conditions: 4-iodobenzotrifluoride (100 μmol), sodium *p*-toluensulfinate (200 μmol), NiCl₂·glyme (5 μmol), 5,5'-dicarbazolyl-2,2'-bipyridyl (czbpy, 5 μmol), DMAc (anhydrous, 0.5-2.0 mL), 440 nm LED (1 lamp at full power). ^bConversion of 4-iodobenzotrifluoride determined by ¹H-NMR using 1,3,5-trimethoxybenzene as internal standard. ^cNMR yields determined by ¹H-NMR using 1,3,5-trimethoxybenzene as internal standard. glyme = 1,2-dimethoxyethane.

Optimized conditions and control experiments

Table 5.14. Optimized conditions and control experiments for the coupling of 4-iodobenzotrifluoride and sodium *p*-toluenesulfinate.^a

Entry	Variation	Time [h]	Conversion [%] ^b	1 [%] ^c
1	None	22	> 99	92
3	NiCl ₂ ·glyme (2.5 mol%) & czbpy (2.5 mol%)	22	82	71
4	Solvent = DMAC/H ₂ O 99:1	22	> 99	90
5	T = 70 °C	7	> 99	88
6	No NiCl ₂ ·glyme	22	86	17
7	no light	22	-	n.d.
8	525 nm	22	-	n.d.
9	4-bromobenzotrifluoride	22	32	27

^aReaction conditions: 4-iodobenzotrifluoride (100 μmol), sodium *p*-toluenesulfinate (200 μmol), NiCl₂·glyme (2.5-5 μmol), 5,5'-dicarbazolyl-2,2'-bipyridyl (czbpy, 2.5-5 μmol), DMAC (anhydrous, 2 mL), 440 or 525 nm LED (2 lamps at full power). ^bConversion of 4-iodobenzotrifluoride determined by ¹H-NMR using 1,3,5-trimethoxybenzene as internal standard. ^cNMR yields determined by ¹H-NMR using 1,3,5-trimethoxybenzene as internal standard. glyme = 1,2-dimethoxyethane. n.d. = not detected.

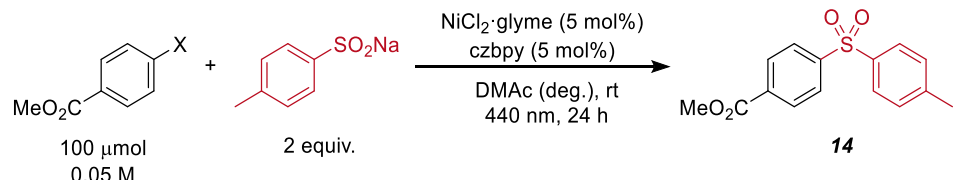
Table 5.15. Comparison of different ligands for the coupling of 4-iodobenzotrifluoride and sodium *p*-toluenesulfinate.^a


Entry	Ligand system	Time [h]	Conversion [%] ^b	1 [%] ^c
1	czbpy (5 mol%)	22	> 99	92
2	carbazole (10 mol%)	22	20	6
3	bpy (5 mol%)	22	57	34
4	bpy (5 mol%) & carbazole (10 mol%)	22	>99	62
5	poly-czbpy (5 mol%) ^d	24	95	77

^aReaction conditions: 4-iodobenzotrifluoride (100 μmol), sodium *p*-toluenesulfinate (200 μmol), NiCl₂·glyme (5 μmol), ligand, DMAc (anhydrous, 2 mL), 440 nm LED (2 lamps at full power).

^bConversion of 4-iodobenzotrifluoride determined by ¹H-NMR using 1,3,5-trimethoxybenzene as internal standard. ^cNMR yields determined by ¹H-NMR using 1,3,5-trimethoxybenzene as internal standard. ^dThe amount of poly-czbpy was calculated using the molecular weight of the monomer. glyme = 1,2-dimethoxyethane. czbpy = 5,5'-dicarbazolyl-2,2'-bipyridyl. bpy = 2,2'-bipyridyl.

Reactivity of different aryl halides

Table 5.16. Coupling of sodium *p*-toluenesulfinate and methyl 4-halobenzoates.^a


Entry	Aryl halide	Conversion [%] ^b	14 [%] ^c
1	Methyl 4-chlorobenzoate	-	n.d.
2	Methyl 4-bromobenzoate	27	15
3	Methyl 4-iodobenzoate	>99	92

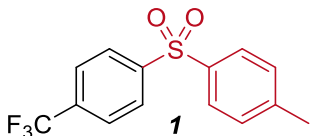
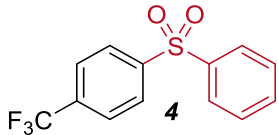
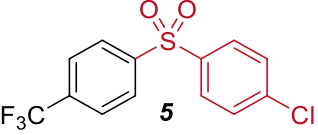
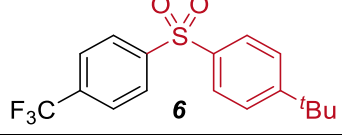
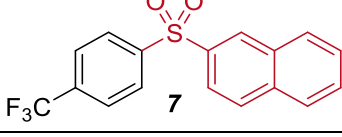
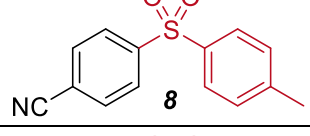
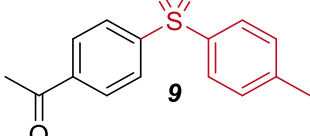
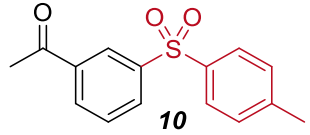
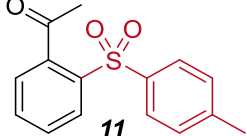
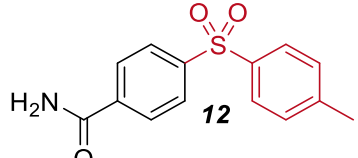
^aReaction conditions: aryl halide (100 μmol), sodium *p*-toluenesulfinate (200 μmol), NiCl₂·glyme (5 μmol), 5,5'-dicarbazolyl-2,2'-bipyridyl (czbpy, 5 μmol), DMAc (anhydrous, 2 mL), 440 nm LED (2 lamps at full power). ^bConversion of aryl halide determined by ¹H-NMR using 1,3,5-trimethoxybenzene as internal standard. ^cNMR yields determined by ¹H-NMR using 1,3,5-trimethoxybenzene as internal standard. glyme = 1,2-dimethoxyethane. n.d. = not detected.

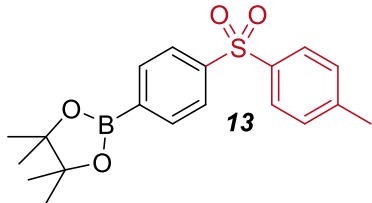
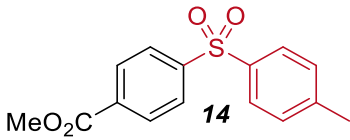
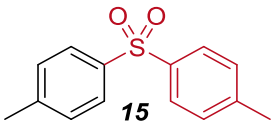
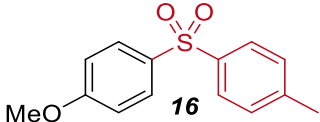
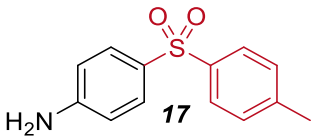
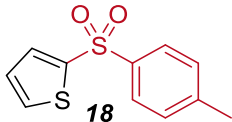
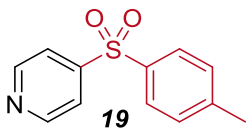
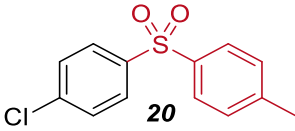
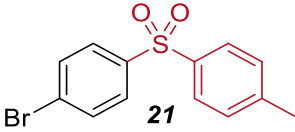
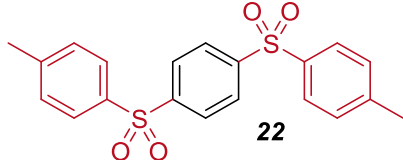
5.5.7 Scope of the C–S cross-coupling using homogeneous visible-light-mediated nickel catalysis

General procedure

An oven dried vial (19 x 100 mm) equipped with a stir bar was charged with NiCl₂·glyme (3.3 mg, 15 μmol, 5 mol%), 5,5'-dicarbazolyl-2,2'-bipyridyl (czbpy, 7.3 mg, 15 μmol, 5 mol%), the aryl iodide (300 μmol) and the sodium sulfinate (600 μmol, 2 equiv). DMAc (anhydrous, 6 mL) was added and the vessel was sealed with a septum and Parafilm. The mixture was stirred for 1 minute at high speed, followed by sonication for 5 minutes and degassing by bubbling argon for 10 minutes. The reaction mixture was stirred at 800 rpm and irradiated with two LED lamps (440 nm) at full power. After the respective reaction time, maleic acid (34.9 mg, 300 μmol, 1 equiv) was added to the reaction vessel, the mixture was shaken and an aliquote (20 μL) was diluted in DMSO-*d*₆ and analyzed by ¹H NMR. The NMR sample and the reaction mixture were combined, diluted with aqueous hydrochloric acid (0.5 M, 60 mL) and extracted with ethyl acetate (3 x 40 mL). The combined organic layers were washed with brine (2 x 40 mL), dried over Na₂SO₄ and concentrated under reduced pressure. The residue was purified by flash chromatography on silica gel using mixtures of hexane/ethyl acetate to obtain the desired product.

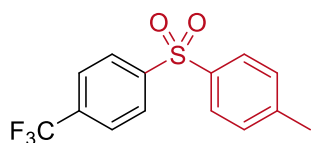
Table 5.17. Scope of the C–S coupling reaction.^a

Product	Reaction time	NMR yield ^b	Isolated yield
 1	22 hours	91%	89%
 4	22 hours	90%	75%
 5	24 hours	85%	84%
 6	24 hours	97%	91%
 7	24 hours	-	40%
 8	24 hours	98%	97%
 9	24 hours	93%	93%
 10	40 hours	77%	71%
 11	24 hours	95%	90%
 12	64 hours	87%	82%

Product	Reaction time	NMR yield ^b	Isolated yield
 13	30 hours	76%	48%
 14	24 hours	86%	80%
 15	53 hours	74%	74%
 16	30 hours	87%	82%
 17	36 hours	97%	94%
 18	48 hours	80%	77%
 19	24 hours	82%	79%
 20	46 hours	80%	75%
 21	29 hours	-	76%
 22	24 hours	82%	71%

^aReaction conditions according to general procedure. ^bNMR yields determined by ¹H-NMR using maleic acid as internal standard

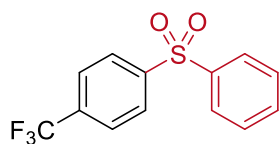
Experimental data



4-Tosylbenzotrifluoride (1) was obtained from 4-iodobenzotrifluoride (81.6 mg, 300 μmol) and sodium *p*-toluenesulfinate (106.9 mg, 600 μmol). Purification by flash chromatography (10% ethyl acetate/hexane) afforded the title compound as a yellowish solid (79.8 mg, 266 μmol , 89%).

Reaction time: 22 hours. NMR yield: 91%.

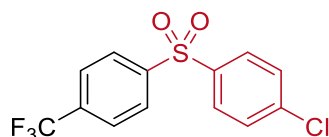
^1H NMR (400 MHz, CDCl_3) δ 8.05 (d, $J = 8.2$ Hz, 2H), 7.84 (d, $J = 8.3$ Hz, 2H), 7.75 (d, $J = 8.3$ Hz, 2H), 7.33 (d, $J = 8.0$ Hz, 2H), 2.41 (s, 3H). ^{13}C NMR (101 MHz, CDCl_3) δ 145.71, 145.08, 137.70, 134.77 (q, $J = 33.1$ Hz), 130.31, 128.17, 128.08, 126.51 (q, $J = 3.7$ Hz), 123.25 (q, $J = 273.1$ Hz), 21.75. ^{19}F NMR (376 MHz, CDCl_3) δ -63.19. These data are in full agreement with those reported in literature.³¹



1-(Phenylsulfonyl)-4-(trifluoromethyl)benzene (4) was obtained from 4-iodobenzotrifluoride (81.6 mg, 300 μmol) and sodium benzenesulfinate (98.5 mg, 600 μmol). Purification by flash chromatography (gradient 5-15% ethyl acetate/hexane) afforded the title compound as a white solid (64.0 mg, 224 μmol , 75%).

Reaction time: 22 hours. NMR yield: 90%.

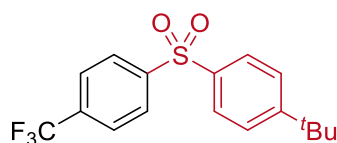
^1H NMR (400 MHz, CDCl_3) δ 8.07 (d, $J = 8.2$ Hz, 2H), 7.96 (d, $J = 7.5$ Hz, 2H), 7.76 (d, $J = 8.3$ Hz, 2H), 7.61 (t, $J = 7.4$ Hz, 1H), 7.53 (t, $J = 7.5$ Hz, 2H). ^{13}C NMR (101 MHz, CDCl_3) δ 145.31, 140.65, 134.93 (q, $J = 33.1$ Hz), 133.92, 129.67, 128.33, 128.01, 126.57 (q, $J = 3.7$ Hz), 123.21 (q, $J = 273.1$ Hz). ^{19}F NMR (376 MHz, CDCl_3) δ -63.21. These data are in full agreement with those reported in literature.³²



1-Chloro-4-((4-(trifluoromethyl)phenyl)sulfonyl)benzene (5) was obtained from 4-iodobenzotrifluoride (81.6 mg, 300 μmol) and sodium 4-chlorobenzenesulfinate (119.2 mg, 600 μmol). Purification by flash chromatography (gradient 3-10% ethyl acetate/hexane) afforded the title compound as a white solid (81.0 mg, 253 μmol , 84%).

Reaction time: 24 hours. NMR yield: 85%

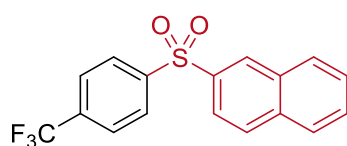
^1H NMR (400 MHz, CDCl_3) δ 8.06 (d, $J = 8.1$ Hz, 2H), 7.89 (d, $J = 8.7$ Hz, 2H), 7.78 (d, $J = 8.3$ Hz, 2H), 7.51 (d, $J = 8.7$ Hz, 2H). ^{13}C NMR (101 MHz, CDCl_3) δ 144.94, 140.80, 139.20, 135.25 (q, $J = 33.1$ Hz), 130.05, 129.49, 128.35, 126.73 (q, $J = 3.6$ Hz), 123.17 (q, $J = 273.2$ Hz). ^{19}F NMR (376 MHz, CDCl_3) δ -63.24. HRMS (EI) m/z calcd for $\text{C}_{13}\text{H}_8\text{ClF}_3\text{O}_2\text{S}$ [(M) $^+$] 319.9886, found: 319.9884.



1-tert-Butyl-4-((4-(trifluoromethyl)phenyl)sulfonyl)benzene (6) was obtained from 4-iodobenzotrifluoride (81.6 mg, 300 μmol) and sodium 4-*tert*-butylbenzenesulfinate (132.2 mg, 600 μmol). Purification by flash chromatography (5% ethyl acetate/hexane) afforded the title compound as a white solid (93.8 mg, 274 μmol , 91%).

Reaction time: 24 hours. NMR yield: 97%

^1H NMR (400 MHz, CDCl_3) δ 8.07 (d, $J = 8.1$ Hz, 2H), 7.87 (d, $J = 8.6$ Hz, 2H), 7.76 (d, $J = 8.3$ Hz, 2H), 7.54 (d, $J = 8.6$ Hz, 2H), 1.31 (s, 9H). ^{19}F NMR (376 MHz, CDCl_3) δ -63.16. ^{13}C NMR (101 MHz, CDCl_3) δ 157.96, 145.66, 137.57, 134.75 (q, $J = 33.0$ Hz), 128.25, 127.90, 126.71, 126.51 (q, $J = 3.7$ Hz), 123.27 (q, $J = 273.0$ Hz), 35.38, 31.10. These data are in full agreement with those reported in literature.⁴⁹

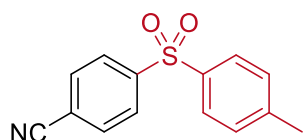


2-((4-(Trifluoromethyl)phenyl)sulfonyl)naphthalene (7) was obtained from 4-iodobenzotrifluoride (81.6 mg, 300 μmol) and sodium 2-naphthalensulfinate (128.5 mg, 600

μmol). Purification by flash chromatography (gradient 5-10% ethyl acetate/hexane) afforded the title compound as a yellowish solid (40.5 mg, 120 μmol , 40%).

Reaction time: 24 hours. NMR yield: not determined due to signal overlap.

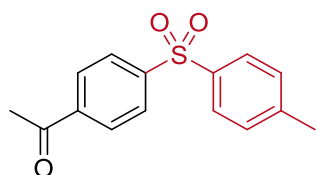
^1H NMR (400 MHz, CDCl_3) δ 8.60 (s, 1H), 8.13 (d, $J = 8.3$ Hz, 2H), 8.00 (d, $J = 7.5$ Hz, 1H), 7.96 (d, $J = 8.7$ Hz, 1H), 7.90 (d, $J = 9.3$ Hz, 1H), 7.85 (dd, $J = 8.7, 2.0$ Hz, 1H), 7.77 (d, $J = 8.5$ Hz, 2H), 7.70 – 7.60 (m, 2H). ^{13}C NMR (101 MHz, CDCl_3) δ 145.40, 137.44, 135.37, 134.97 (q, $J = 33.1$ Hz), 132.36, 130.13, 129.79, 129.69, 129.61, 128.40, 128.14, 128.04, 126.60 (q, $J = 3.7$ Hz), 123.23 (q, $J = 274.1$ Hz), 122.65. ^{19}F NMR (376 MHz, CDCl_3) δ -63.21. HRMS (EI) m/z calcd for $\text{C}_{17}\text{H}_{11}\text{F}_3\text{O}_2\text{S}$ [M^+] 336.0432, found: 336.0438.



4-Tosylbenzonitrile (8) was obtained from 4-iodobenzonitrile (68.7 mg, 300 μmol) and sodium *p*-toluenesulfinate (106.9 mg, 600 μmol). Purification by flash chromatography (15% ethyl acetate/hexane) afforded the title compound as a yellowish solid (74.7 mg, 290 μmol , 97%).

Reaction time: 24 hours. NMR yield: 98%

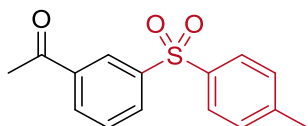
^1H NMR (400 MHz, CDCl_3) δ 8.03 (d, $J = 8.3$ Hz, 2H), 7.82 (d, $J = 8.1$ Hz, 2H), 7.78 (d, $J = 8.3$ Hz, 2H), 7.33 (d, $J = 8.0$ Hz, 2H), 2.41 (s, 3H). ^{13}C NMR (101 MHz, CDCl_3) δ 146.31, 145.36, 137.18, 133.13, 130.38, 128.21, 128.12, 117.31, 116.78, 21.75. These data are in full agreement with those reported in literature.³¹



4-Tosylacetophenone (9) was obtained from 4-iodoacetophenone (73.8 mg, 300 μmol) and sodium *p*-toluenesulfinate (106.9 mg, 600 μmol). Purification by flash chromatography (gradient 15-25% ethyl acetate/hexane) afforded the title compound as a white solid (76.8 mg, 280 μmol , 93%).

Reaction time: 24 hours. NMR yield: 93%

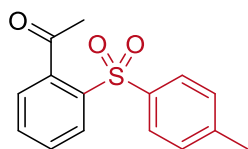
^1H NMR (400 MHz, CDCl_3) δ 8.07 – 7.96 (m, 4H), 7.83 (d, $J = 8.4$ Hz, 2H), 7.31 (d, $J = 8.1$ Hz, 2H), 2.61 (s, 3H), 2.40 (s, 3H). ^{13}C NMR (101 MHz, CDCl_3) δ 196.83, 145.96, 144.90, 140.29, 137.91, 130.24, 129.15, 128.04, 127.95, 27.02, 21.75. These data are in full agreement with those reported in literature.³¹



3-Tosylacetophenone (10) was obtained from 3-iodoacetophenone (73.8 mg, 300 μmol) and sodium *p*-toluenesulfinate (106.9 mg, 600 μmol). Purification by flash chromatography (gradient 10-30% ethyl acetate/hexane) afforded the title compound as a colorless oil (58.2 mg, 212 μmol , 71%).

Reaction time: 40 hours. NMR yield: 77%

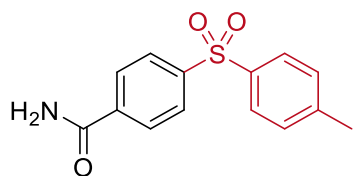
^1H NMR (400 MHz, CDCl_3) δ 8.51 – 8.39 (m, 1H), 8.15 – 8.02 (m, 2H), 7.83 (d, $J = 8.3$ Hz, 2H), 7.60 (t, $J = 7.8$ Hz, 1H), 7.30 (d, $J = 8.1$ Hz, 2H), 2.62 (s, 3H), 2.39 (s, 3H). ^{13}C NMR (101 MHz, CDCl_3) δ 196.30, 144.77, 143.03, 138.02, 137.99, 132.52, 131.64, 130.20, 129.89, 127.91, 127.27, 26.81, 21.69. HRMS (EI) m/z calcd for $\text{C}_{15}\text{H}_{14}\text{O}_3\text{S}$ [M^+] 274.0664, found: 274.0666.



2-Tosylacetophenone (11) was obtained from 2-iodoacetophenone (73.8 mg, 300 μmol) and sodium *p*-toluenesulfinate (106.9 mg, 600 μmol). Purification by flash chromatography (gradient 10-20% ethyl acetate/hexane) afforded the title compound as a colorless oil (73.8 mg, 269 μmol , 90%).

Reaction time: 24 hours. NMR yield: 95%

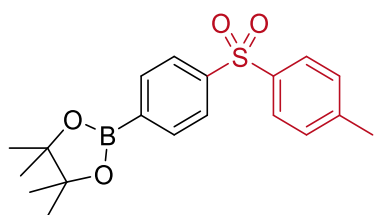
^1H NMR (400 MHz, CDCl_3) δ 8.02 (d, $J = 7.8$ Hz, 1H), 7.81 (d, $J = 8.3$ Hz, 2H), 7.58 (td, $J = 7.5, 1.3$ Hz, 1H), 7.52 (td, $J = 7.7, 1.3$ Hz, 1H), 7.31 – 7.25 (m, 3H, contains residual solvent signal of CDCl_3), 2.67 (s, 3H), 2.37 (s, 3H). ^{13}C NMR (101 MHz, CDCl_3) δ 203.49, 144.53, 142.29, 138.40, 138.38, 133.30, 129.92, 129.88, 129.82, 128.15, 126.01, 32.10, 21.68. HRMS (EI) m/z calcd for $\text{C}_{15}\text{H}_{14}\text{O}_3\text{S}$ [M^+] 274.0664, found: 274.0667.



4-Tosylbenzamide (12) was obtained from 4-iodobenzamide (74.1 mg, 300 μmol) and sodium *p*-toluenesulfinate (106.9 mg, 600 μmol). Purification by flash chromatography (gradient 50-100% ethyl acetate/hexane) afforded the title compound as a white solid (67.4 mg, 245 μmol , 82%).

Reaction time: 64 hours. NMR yield: 87%

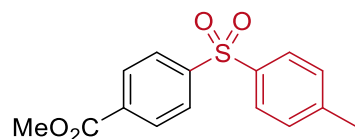
^1H NMR (400 MHz, CDCl_3) δ 8.01 (d, $J = 8.4$ Hz, 2H), 7.90 (d, $J = 8.5$ Hz, 2H), 7.83 (d, $J = 8.3$ Hz, 2H), 7.32 (d, $J = 7.9$ Hz, 2H), 2.41 (s, 3H). ^1H NMR (400 MHz, DMSO-d_6) δ 8.17 (s, 1H), 8.08 – 7.94 (m, 4H), 7.86 (d, $J = 8.2$ Hz, 2H), 7.63 (s, 1H), 7.43 (d, $J = 8.1$ Hz, 2H), 2.36 (s, 3H). ^{13}C NMR (101 MHz, DMSO-d_6) δ 166.53, 144.67, 143.57, 138.76, 137.77, 130.30, 128.71, 127.57, 127.27, 21.06. These data are in full agreement with those reported in literature.³⁴



4,4,5,5-tetramethyl-2-(4-tosylphenyl)-1,3,2-dioxaborolane (13) was obtained from 2-(4-iodophenyl)-4,4,5,5-tetramethyl-1,3,2-dioxaborolane (99.0 mg, 300 μmol) and sodium *p*-toluenesulfinate (106.9 mg, 600 μmol). Purification by flash chromatography (gradient 10-40% ethyl acetate/hexane) afforded the title compound as a yellowish solid (51.3 mg, 143 μmol , 48%). The low isolated yield is a result of product decomposition that was also observed during TLC analysis.

Reaction time: 30 hours. NMR yield: 76%

^1H NMR (400 MHz, CDCl_3) δ 7.99 – 7.85 (m, 4H), 7.80 (d, $J = 8.2$ Hz, 2H), 7.27 (d, $J = 8.5$ Hz, 2H, contains residual solvent signal of CDCl_3), 2.37 (s, 3H), 1.32 (s, 12H). ^{13}C NMR (101 MHz, CDCl_3) δ 144.32, 144.15, 138.62, 135.56, 133.11 (br. s), 130.02, 127.82, 126.58, 84.53, 24.95, 21.68. HRMS (EI) m/z calcd for $\text{C}_{19}\text{H}_{23}\text{BO}_4\text{S}$ $[(\text{M})^+]$ 358.1410, found: 358.1416.

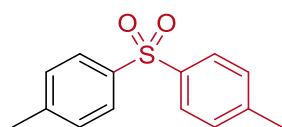


Methyl 4-tosylbenzoate (14) was obtained from methyl 4-iodobenzoate (78.6 mg, 300 μmol) and sodium *p*-toluenesulfinate (106.9 mg, 600 μmol). Purification by flash chromatography (gradient 15-25% ethyl acetate/hexane) afforded the title compound as a white solid (70.1 mg, 241 μmol , 80%)

Reaction time: 24 hours. NMR yield: 86%

^1H NMR (400 MHz, CDCl_3) δ 8.13 (d, $J = 8.6$ Hz, 2H), 7.98 (d, $J = 8.6$ Hz, 2H), 7.83 (d, $J = 8.3$ Hz, 2H), 7.31 (d, $J = 8.1$ Hz, 2H), 3.92 (s, 3H), 2.39 (s, 3H). ^{13}C NMR (101 MHz, CDCl_3) δ 165.63, 145.98, 144.85, 137.91, 134.19, 130.51, 130.21, 128.02, 127.64, 52.78, 21.73.

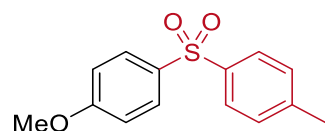
These data are in full agreement with those reported in literature.³¹



4,4'-Sulfonylbis(methylbenzene) (15) was obtained from 4-iodotoluene (65.4 mg, 300 μmol) and sodium *p*-toluenesulfinate (106.9 mg, 600 μmol). Purification by flash chromatography (gradient 5-10% ethyl acetate/hexane) afforded the title compound as a white solid (54.4 mg, 221 μmol , 74%).

Reaction time: 53 hours. NMR yield: 74%

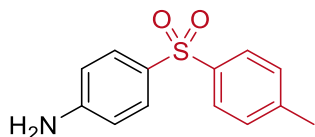
^1H NMR (400 MHz, CDCl_3) δ 7.81 (d, $J = 8.3$ Hz, 4H), 7.28 (d, $J = 7.9$ Hz, 4H, contains residual solvent signal of CDCl_3), 2.38 (s, 6H). ^{13}C NMR (101 MHz, CDCl_3) δ 144.05, 139.16, 129.98, 127.68, 21.68. These data are in full agreement with those reported in literature.⁵⁰



4-Tosylanisole (16) was obtained from 4-iodoanisole (70.2 mg, 300 μmol) and sodium *p*-toluenesulfinate (106.9 mg, 600 μmol). Purification by flash chromatography (gradient 20-40% ethyl acetate/hexane) afforded the title compound as a white solid (64.9 mg, 247 μmol , 82%).

Reaction time: 30 hours. NMR yield: 87%

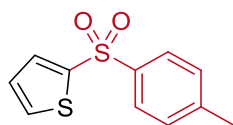
^1H NMR (400 MHz, CDCl_3) δ 7.85 (d, $J = 9.0$ Hz, 2H), 7.79 (d, $J = 8.3$ Hz, 2H), 7.34 – 7.17 (m, 2H, contains residual solvent signal of CDCl_3), 6.94 (d, $J = 8.9$ Hz, 2H), 3.83 (s, 3H), 2.38 (s, 3H). ^{13}C NMR (101 MHz, CDCl_3) δ 163.32, 143.85, 139.51, 133.63, 129.94, 129.81, 127.47, 114.55, 55.75, 21.66. These data are in full agreement with those reported in literature.³⁴



4-Tosylaniline (17) was obtained from 4-iodoaniline (65.7 mg, 300 μmol) and sodium *p*-toluenesulfinate (106.9 mg, 600 μmol). Purification by flash chromatography (gradient 0-4% ethyl acetate/dichloromethane) afforded the title compound as a white solid (70.1 mg, 283 μmol , 94%).

Reaction time: 36 hours. NMR yield: 97%

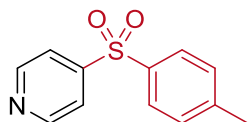
^1H NMR (400 MHz, CDCl_3) δ 7.77 (d, $J = 8.3$ Hz, 2H), 7.69 (d, $J = 8.7$ Hz, 2H), 7.25 (d, $J = 7.9$ Hz, 2H, contains residual solvent signal of CDCl_3), 6.64 (d, $J = 8.7$ Hz, 2H), 4.12 (br. s, 2H), 2.38 (s, 3H). ^{13}C NMR (101 MHz, CDCl_3) δ 150.93, 143.44, 140.16, 130.17, 129.86, 129.84, 127.29, 114.30, 21.65. These data are in full agreement with those reported in literature.³¹



2-Tosylthiophene (18) was obtained from 4-iodoanisole (63.0 mg, 300 μmol) and sodium *p*-toluenesulfinate (106.9 mg, 600 μmol). Purification by flash chromatography (gradient 5-10% ethyl acetate/hexane) afforded the title compound as a white solid (54.9 mg, 230 μmol , 77 %).

Reaction time: 48 hours. NMR yield: 80%.

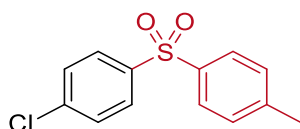
^1H NMR (400 MHz, CDCl_3) δ 7.87 (d, $J = 8.4$ Hz, 2H), 7.67 (dd, $J = 3.8, 1.4$ Hz, 1H), 7.62 (dd, $J = 5.0, 1.4$ Hz, 1H), 7.31 (d, $J = 7.9$ Hz, 2H), 7.06 (dd, $J = 5.0, 3.8$ Hz, 1H), 2.41 (s, 3H). ^{13}C NMR (101 MHz, CDCl_3) δ 144.47, 143.62, 139.25, 133.69, 133.17, 130.08, 127.89, 127.51, 21.73. These data are in full agreement with those reported in literature⁵⁰



4-Tosylpyridine (19) was obtained from 4-iodopyridine (61.5 mg, 300 μmol) and sodium *p*-toluenesulfonate (106.9 mg, 600 μmol). Purification by flash chromatography (gradient 20-50% ethyl acetate/hexane) afforded the title compound as a white solid (55.2 mg, 237 μmol , 79%).

Reaction time: 24 hours. NMR yield: 82%

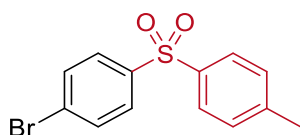
^1H NMR (400 MHz, CDCl_3) δ 8.79 (d, $J = 5.7$ Hz, 2H), 7.83 (d, $J = 8.3$ Hz, 2H), 7.74 (d, $J = 6.0$ Hz, 2H), 7.33 (d, $J = 8.1$ Hz, 2H), 2.41 (s, 3H). ^{13}C NMR (101 MHz, CDCl_3) δ 151.21, 150.23, 145.53, 136.72, 130.37, 128.28, 120.59, 21.77. These data are in full agreement with those reported in literature.⁵¹



1-Chloro-4-tosylbenzene (20) was obtained from 1-chloro-4-iodobenzene (71.5 mg, 300 μmol) and sodium *p*-toluenesulfonate (106.9 mg, 600 μmol). Purification by flash chromatography (5% ethyl acetate/hexane) afforded the title compound as a yellowish solid (60.0 mg, 225 μmol , 75%).

Reaction time: 46 hours. NMR yield: 80%

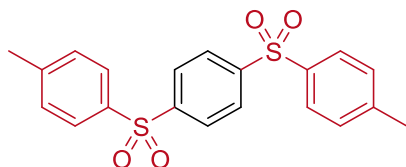
^1H NMR (400 MHz, CDCl_3) δ 7.86 (d, $J = 8.7$ Hz, 2H), 7.81 (d, $J = 8.4$ Hz, 2H), 7.46 (d, $J = 8.6$ Hz, 2H), 7.30 (d, $J = 8.1$ Hz, 2H), 2.40 (s, 3H). ^{13}C NMR (101 MHz, CDCl_3) δ 144.64, 140.66, 139.80, 138.36, 130.18, 129.68, 129.11, 127.84, 21.73. These data are in full agreement with those reported in literature.⁵⁰



1-Bromo-4-tosylbenzene (21) was obtained from 1-bromo-4-iodobenzene (84.9 mg, 300 μmol) and sodium *p*-toluenesulfonate (106.9 mg, 600 μmol). Purification by flash chromatography (gradient 5-20% ethyl acetate/hexane) afforded the title compound as a yellowish solid (70.9 mg, 228 μmol , 76%).

Reaction time: 29 hours. NMR yield: not calculated due to signal overlap.

^1H NMR (400 MHz, CDCl_3) δ 7.85 – 7.67 (m, 4H), 7.61 (d, J = 8.6 Hz, 2H), 7.30 (d, J = 8.2 Hz, 2H), 2.39 (s, 3H). ^{13}C NMR (101 MHz, CDCl_3) δ 144.65, 141.11, 138.20, 132.62, 130.16, 129.13, 128.30, 127.79, 21.71. These data are in full agreement with those reported in literature.⁵²



1,4-Ditosylbenzene (22) was obtained from 1,4-diiodobenzene (99.0 mg, 300 μmol) and sodium *p*-toluenesulfinate (160.4 mg, 900 μmol). Purification by flash chromatography (gradient 20-100% ethyl acetate/hexane) afforded the title compound as a yellowish solid (81.9 mg, 212 μmol , 71%).

Reaction time: 24 hours. NMR yield: 82%

^1H NMR (400 MHz, CDCl_3) δ 8.01 (s, 4H), 7.80 (d, J = 8.3 Hz, 4H), 7.31 (d, J = 8.1 Hz, 4H), 2.40 (s, 6H). ^{13}C NMR (101 MHz, CDCl_3) δ 146.40, 145.27, 137.35, 130.35, 128.51, 128.16, 21.78. These data are in full agreement with those reported in literature.⁵⁰

5.5.8 Optimization of the C–O cross-coupling using homogeneous visible-light-mediated nickel catalysis

General procedure for screening experiments

An oven dried vial (19 x 100 mm) equipped with a stir bar was charged with a nickel salt (5 μmol), 5,5'-dicarbazolyl-2,2'-bipyridyl (czbpy, 2.4 mg, 5 μmol), 4-iodobenzotrifluoride (27.2 mg, 100 μmol) and *N*-(*tert*-butoxycarbonyl)proline (32.3 mg, 150 μmol). DMSO (anhydrous, 2 mL) and *N*-*tert*-butylisopropylamine (BIPA, 34.6 mg, 300 μmol) were added and the vessel was sealed with a septum and Parafilm. The mixture was stirred for 1 minute at high speed, followed by sonication for 5 minutes and degassing by bubbling argon for 10 minutes. The reaction mixture was stirred at 800 rpm and irradiated with 440 nm LED lamps using the respective power settings. After the respective reaction time, 1,3,5-trimethoxybenzene (16.8 mg, 100 μmol , 1 equiv) was added to the reaction vessel, the mixture was shaken and an aliquote (300 μL) was removed, diluted with DMSO-*d*₆ and analyzed by ¹H NMR.

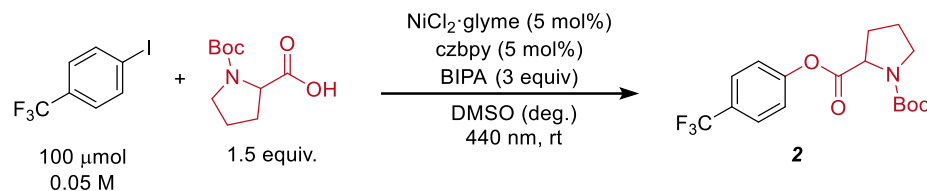
Screening of nickel salts

Table 5.18. Screening of nickel salts for the coupling of 4-iodobenzotrifluoride and *N*-Boc-proline.^a

Entry	Nickel salt	Conversion [%] ^b	2 [%] ^c
1	NiCl ₂ ·glyme	>99	88
2	NiBr ₂ ·glyme	46	39
3	NiBr ₂ ·3H ₂ O	>99	90

^aReaction conditions: 4-iodobenzotrifluoride (100 μmol), (*tert*-butoxycarbonyl)proline (*N*-Boc-proline, 150 μmol), *N*-*tert*-butylisopropylamine (BIPA, 150 μmol), nickel salt (5 μmol), 5,5'-dicarbazolyl-2,2'-bipyridyl (czbpy, 5 μmol), DMSO (anhydrous, 2 mL), 440 nm LED (1 lamp at full power). ^bConversion of 4-iodobenzotrifluoride determined by ¹H-NMR using 1,3,5-trimethoxybenzene as internal standard. ^cNMR yields determined by ¹H-NMR using 1,3,5-trimethoxybenzene as internal standard. glyme = 1,2-dimethoxyethane.

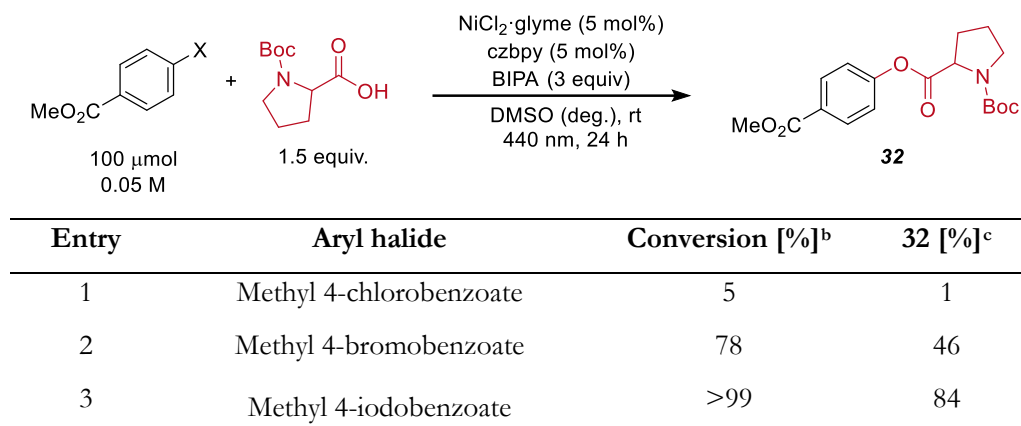
Optimized conditions and control experiments

Table 5.19. Optimized conditions and control experiments for the coupling of 4-iodobenzotrifluoride and *N*-Boc-proline.^a

Entry	Variation	Time [h]	Conversion [%] ^b	2 [%] ^c
1	None	18	>99	88
2	carbazole (10 mol%) instead of czbpy	18	0	n.d.
3	bpy (5 mol%) instead of czbpy	18	8	4
4	bpy (5 mol%) & carbazole (10 mol%) instead of czbpy	18	14	8
5	No NiCl ₂ ·glyme	18	0	n.d.
6	No czbpy	18	0	n.d.
7	No BIPA	18	5	5
8	No light	18	0	n.d.
9	poly-czbpy (5 mol%) ^d	24	75	53

^aReaction conditions: 4-iodobenzotrifluoride (100 μmol), (*tert*-butoxycarbonyl)proline (*N*-Boc-proline, 150 μmol), *N*-*tert*-butylisopropylamine (BIPA, 150 μmol) NiCl₂·glyme (5 μmol), 5,5'-dicarbazolyl-2,2'-bipyridyl (czbpy, 5 μmol), DMSO (anhydrous, 2 mL), 440 nm LED (1 lamp at full power). ^bConversion of 4-iodobenzotrifluoride determined by ¹H-NMR using 1,3,5-trimethoxybenzene as internal standard. ^cNMR yields determined by ¹H-NMR using 1,3,5-trimethoxybenzene as internal standard. ^dThe amount of poly-czbpy was calculated using the molecular weight of the monomer. glyme = 1,2-dimethoxyethane. bpy = 2,2'-bipyridyl.

Reactivity of different aryl halides

Table 5.20. Coupling of *N*-Boc-proline and methyl 4-halobenzoates.^a

^aReaction conditions: aryl halide (100 μmol), (*tert*-butoxycarbonyl)proline (*N*-Boc-proline, 150 μmol), *N-tert*-butylisopropylamine (BIPA, 150 μmol) NiCl₂·glyme (5 μmol), 5,5'-dicarbazoyl-2,2'-bipyridyl (czbpy, 5 μmol), DMSO (anhydrous, 2 mL), 440 nm LED (2 lamps at full power).

^bConversion of 4-iodobenzotrifluoride determined by ¹H-NMR using 1,3,5-trimethoxybenzene as internal standard. ^cNMR yields determined by ¹H-NMR using 1,3,5-trimethoxybenzene as internal standard. glyme = 1,2-dimethoxyethane.

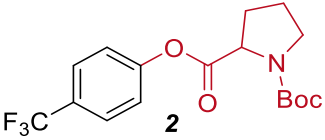
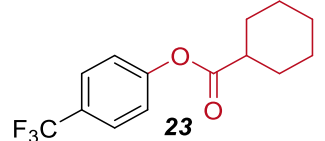
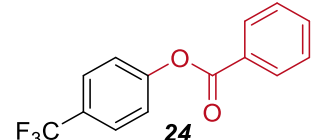
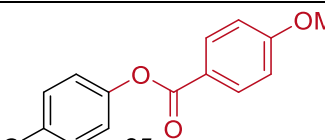
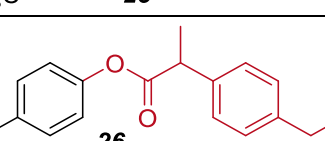
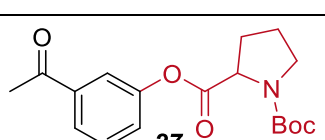
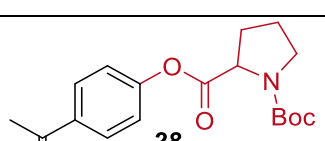
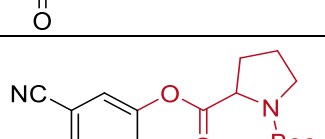
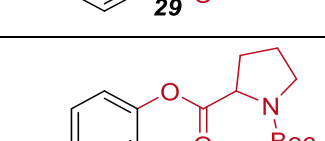
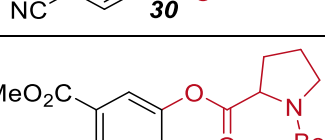
5.5.9 Scope of the C–O cross-coupling using homogeneous visible-light-mediated nickel catalysis

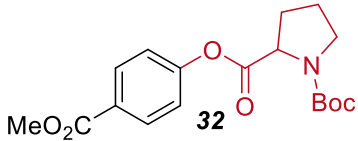
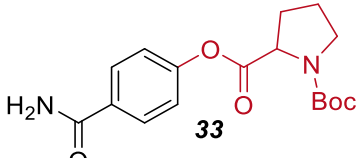
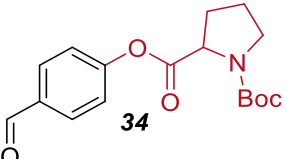
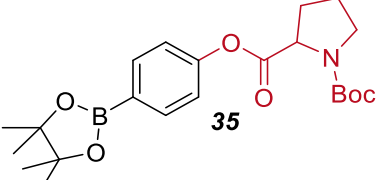
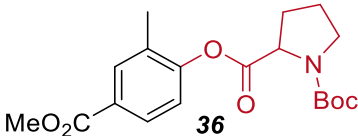
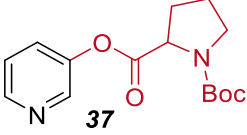
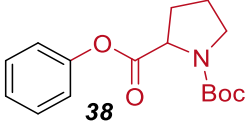
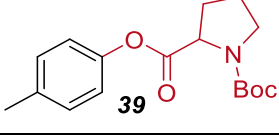
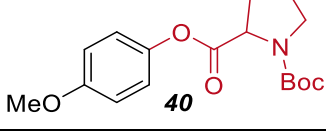
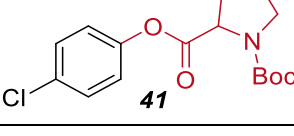
General procedure

An oven dried vial (19 x 100 mm) equipped with a stir bar was charged with NiCl₂·glyme (3.3 mg, 15 μmol, 5 mol%), 5,5'-dicarbazolyl-2,2'-bipyridyl (czbpy, 7.3 mg, 15 μmol, 5 mol%), the aryl iodide (300 μmol) and the carboxylic (450 μmol, 1.5 equiv). DMSO (anhydrous, 3 mL) was added, followed by *N*-*tert*-butylisopropylamine (BIPA, 103.8 mg, 0.9 mmol, 3.0 equiv), before sealing the vessel with a septum and Parafilm. The mixture was sonicated for 5 minutes and degassed by bubbling argon for 10 minutes. The reaction mixture was stirred at 800 rpm and irradiated with two LED lamps (440 nm) at full power. After the respective reaction time, maleic acid (34.9 mg, 300 μmol, 1.0 equiv) was added to the reaction vessel, the mixture was stirred and an aliquote (~200 μL) was removed, diluted with DMSO-*d*₆ and analyzed by ¹H NMR. The NMR sample was combined with the reaction mixture, diluted with H₂O (40 mL) and extracted with dichloromethane (3 x 40 mL). The combined organic phases were washed with brine (50 mL), dried over Na₂SO₄ and concentrated. The residue was purified by flash chromatography on silica gel using mixtures of hexane/ethyl acetate to obtain the desired product.

In case of **23**, **24**, **25** and **26**, the reaction was slow using the above reported conditions. Less concentrated conditions (300 μmol of the aryl iodide in 6 mL of DMSO) resulted in faster reactions for these substrates.

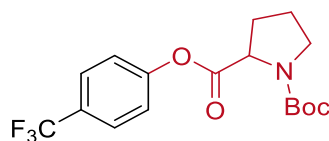
Table 5.21. Scope of the C–O coupling reaction.^a

Product	Reaction time	NMR yield ^b	Isolated yield
 2	24 hours	92%	91%
 23	96 hours	85%	80%
 24	96 hours	87%	82%
 25	96 hours	full conversion	63%
 26	96 hours	70%	67%
 27	48 hours	86%	82%
 28	24 hours	92%	90%
 29	48 hours	88%	83%
 30	24 hours	94%	92%
 31	48 hours	87%	85%

Product	Reaction time	NMR yield ^b	Isolated yield
 32	24 hours	91%	90%
 33	48 hours	94%	89%
 34	24 hours	96%	91%
 35	30 hours	96%	77%
 36	24 hours	74%	73%
 37	24 hours	85%	79%
 38	64 hours	81% yield	79%
 39	64 hours	73%	67%
 40	64 hours	65%	49%
 41	30 hours	93%	89%

^aReaction conditions according to general procedure. ^bNMR yields determined by ¹H-NMR using maleic acid as internal standard

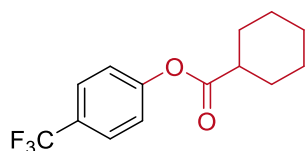
Experimental data



1-(*tert*-Butyl) 2-(4-(trifluoromethyl)phenyl) pyrrolidine-1,2-dicarboxylate (2) was obtained from 4-iodobenzotrifluoride (81.6 mg, 300 μmol) and (*tert*-butoxycarbonyl)proline (96.9 mg, 450 μmol). Purification by flash chromatography (gradient 0-5% ethyl acetate/hexane) afforded the title compound as a colorless oil (98.5 mg, 274 μmol , 91%).

Reaction time: 24 hours. NMR yield: 92%

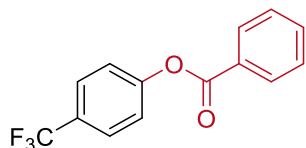
^1H NMR (400 MHz, CDCl_3) rotameric mixture δ 7.67 (m, 2H), 7.30 – 7.22 (m, 2H, contains residual solvent signal of CDCl_3), 4.51 (dd, $J = 8.5, 4.4$ Hz, 0.4H), 4.44 (dd, $J = 8.7, 4.4$ Hz, 0.6H), 3.71 – 3.42 (m, 2H), 2.44 – 2.27 (m, 1H), 2.24 – 2.12 (m, 1H), 2.12 – 1.93 (m, 2H), 1.52 – 1.45 (m, 9H). ^{13}C NMR (101 MHz, CDCl_3) rotameric mixture, resonances for minor rotamer are enclosed in parenthesis δ (171.27) 171.16, (154.50) 153.63, (153.31) 153.07, 128.16 (d, $J = 32.6$ Hz) (127.99 (d, $J = 32.8$ Hz)), 126.91 (q, $J = 3.7$ Hz) (126.74 (q, $J = 3.8$ Hz)), (123.83 (d, $J = 271.9$ Hz)) 123.74 (d, $J = 272.1$ Hz). (122.03) 121.66, 80.37 (80.18), 59.16 (59.08), (46.66) 46.47, 31.04 (29.99), 28.41, (24.58) 23.74. ^{19}F NMR (564 MHz, CDCl_3) rotameric mixture δ -62.22, -62.28. These data are in full agreement with those previously published in the literature.³⁸



4-(Trifluoromethyl)phenyl cyclohexanecarboxylate (23) was obtained from 4-iodobenzotrifluoride (81.6 mg, 300 μmol) and cyclohexanecarboxylic acid (57.7 mg, 450 μmol), using 6 mL of DMSO as solvent. Purification by flash chromatography (gradient 0-3% ethyl acetate/hexane) afforded the title compound as a white solid (65.3 mg, 240 μmol , 80%).

Reaction time: 96 hours. NMR yield: 85%

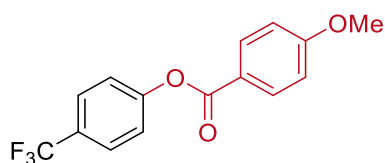
^1H NMR (400 MHz, CDCl_3) δ 7.64 (d, $J = 8.4$ Hz, 2H), 7.19 (d, $J = 8.4$ Hz, 2H), 2.58 (tt, $J = 11.2, 3.7$ Hz, 1H), 2.13 – 2.02 (m, 2H), 1.87 – 1.78 (m, 2H), 1.75 – 1.66 (m, 1H), 1.66 – 1.53 (m, 2H), 1.46 – 1.22 (m, 3H). ^{13}C NMR (101 MHz, CDCl_3) δ 174.02, 153.45, 127.89 (q, $J = 32.8$ Hz), 126.73 (q, $J = 3.8$ Hz), 123.92 (q, $J = 272.1$ Hz), 122.09, 43.17, 28.89, 25.66, 25.31. ^{19}F NMR (564 MHz, CDCl_3) δ -62.21. These data are in full agreement with those reported in literature.⁵³



4-(Trifluoromethyl)phenyl benzoate (24) was obtained from 4-iodobenzotrifluoride (81.6 mg, 300 μmol) and benzoic acid (55.0 mg, 450 μmol), using 6 mL of DMSO as solvent. Purification by flash chromatography (gradient 0-3% ethyl acetate/hexane) afforded the title compound as a white solid (65.4 mg, 246 μmol , 82%).

Reaction time: 96 hours. NMR yield: 87%

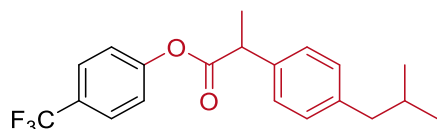
^1H NMR (400 MHz, CDCl_3) δ 8.22 (d, $J = 7.0$ Hz, 2H), 7.72 (d, $J = 8.5$ Hz, 2H), 7.68 (t, $J = 7.5$ Hz, 1H), 7.54 (t, $J = 7.8$ Hz, 2H), 7.37 (d, $J = 8.5$ Hz, 2H). ^{13}C NMR (101 MHz, CDCl_3) δ 164.69, 153.51 (d, $J = 1.5$ Hz), 134.01, 130.29, 128.98, 128.73, 128.19 (q, $J = 33.0$ Hz), 126.89 (q, $J = 3.7$ Hz), 123.95 (q, $J = 271.9$ Hz), 122.31. ^{19}F NMR (564 MHz, CDCl_3) δ -62.16. These data are in full agreement with those reported in literature.²⁶



4-(Trifluoromethyl)phenyl 4-methoxybenzoate (25) was obtained from 4-iodobenzotrifluoride (81.6 mg, 300 μmol) and 4-methoxybenzoic acid (68.5 mg, 450 μmol), using 6 mL of DMSO as solvent. Purification by flash chromatography (gradient 0-3% ethyl acetate/hexane) afforded the title compound as a white solid (56.2 mg, 190 μmol , 63%).

Reaction time: 96 hours. NMR analysis: full conversion of aryl iodide.

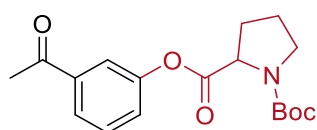
^1H NMR (400 MHz, CDCl_3) δ 8.16 (d, $J = 9.0$ Hz, 2H), 7.70 (d, $J = 8.4$ Hz, 2H), 7.34 (d, $J = 8.4$ Hz, 2H), 7.00 (d, $J = 9.0$ Hz, 2H), 3.91 (s, 3H). ^{13}C NMR (101 MHz, CDCl_3) δ 164.40, 164.20, 153.62, 132.45, 127.83, 126.82 (q, $J = 3.8$ Hz), 125.30, 122.35, 121.19, 113.99, 55.59. ^{19}F NMR (564 MHz, CDCl_3) δ -62.16. These data are in full agreement with those reported in literature.⁵⁴



4-(Trifluoromethyl)phenyl 2-(4-isobutylphenyl)propanoate (26) was obtained from 4-iodobenzotrifluoride (81.6 mg, 300 μmol) and ibuprofen (92.8 mg, 450 μmol), using 6 mL of DMSO as solvent. Purification by flash chromatography (gradient 0-3% ethyl acetate/hexane) afforded the title compound as a colorless oil (72.9 mg, 200 μmol , 67%).

Reaction time: 96 hours. NMR yield: 70%

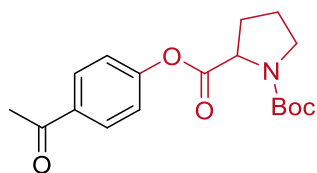
^1H NMR (400 MHz, CDCl_3) δ 7.60 (d, $J = 8.3$ Hz, 1H), 7.29 (d, $J = 8.1$ Hz, 2H), 7.15 (d, $J = 8.3$ Hz, 2H), 7.12 (d, $J = 8.2$ Hz, 1H), 3.95 (q, $J = 7.1$ Hz, 1H), 2.47 (d, $J = 7.2$ Hz, 2H), 1.87 (m, 1H), 1.61 (d, $J = 7.1$ Hz, 3H), 0.91 (d, $J = 6.6$ Hz, 6H). ^{13}C NMR (101 MHz, CDCl_3) δ 172.75, 153.41 (d, $J = 1.5$ Hz), 141.09, 136.86, 129.65, 128.02 (q, $J = 32.8$ Hz), 127.22, 126.71 (q, $J = 3.7$ Hz), 123.90 (d, $J = 271.9$ Hz), 121.97, 45.29, 45.08, 30.24, 22.41, 18.45. ^{19}F NMR (564 MHz, CDCl_3) δ -62.19. HRMS (EI) m/z calcd for $\text{C}_{20}\text{H}_{21}\text{F}_3\text{O}_2$ $[(\text{M})^+]$ 350.1491, found: 350.1491



2-(3-Acetylphenyl) 1-(*tert*-butyl) pyrrolidine-1,2-dicarboxylate (27) was obtained from 3-iodoacetophenone (78.8 mg, 300 μmol) and (*tert*-butoxycarbonyl)proline (96.9 mg, 450 μmol). Purification by flash chromatography (gradient 0-10% ethyl acetate/hexane) afforded the title compound as a colorless oil (82.4 mg, 247 μmol , 82%).

Reaction time: 48 hours. NMR yield: 86%

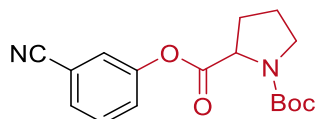
^1H NMR (400 MHz CDCl_3) rotameric mixture δ 7.84 – 7.76 (t, $J = 7.4$ Hz, 1H), 7.68 – 7.63 (m, 1H), 7.51 – 7.42 (m, 1H), 7.36 – 7.26 (m, 1H), 4.51 (dd, $J = 8.6, 4.4$ Hz, 0.4H), 4.45 (dd, $J = 8.7, 4.3$ Hz, 0.6H), 3.66 – 3.39 (m, 2H), 2.60 – 2.54 (m, 3H), 2.46 – 2.27 (m, 1H), 2.24 – 2.09 (m, 1H), 2.08 – 1.88 (m, 2H), 1.48 – 1.44 (m, 9H). ^{13}C NMR (101 MHz, CDCl_3) rotameric mixture, resonances for minor rotamer are enclosed in parenthesis δ (197.11) 196.86, (171.56) 171.53, (154.50) 153.67, (150.99) 150.82, 138.57 (138.43), 129.80 (129.64), (126.48) 126.01, 125.99 (125.76), (121.34) 120.93, 80.34 (80.11), 59.13 (59.07), (46.66) 46.47, 31.05 (30.00), 28.43, (26.72) 26.72, (24.58) 23.75. These data are in full agreement with those previously published in the literature.³⁸



2-(4-Acetylphenyl) 1-(*tert*-butyl) pyrrolidine-1,2-dicarboxylate (28) was obtained from 4-iodoacetophenone (78.8 mg, 300 μmol) and (*tert*-butoxycarbonyl)proline (96.9 mg, 450 μmol). Purification by flash chromatography (gradient 0-10% ethyl acetate/hexane) afforded the title compound as a colorless oil (89.8 mg, 269 μmol , 90%).

Reaction time: 24 hours. NMR yield: 92%

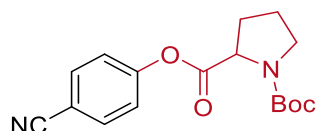
^1H NMR (400 MHz, CDCl_3) rotameric mixture δ 8.02 – 7.94 (m, 2H), 7.23 – 7.15 (m, 2H), 4.50 (dd, $J = 8.6, 4.4$ Hz, 0.4H), 4.44 (dd, $J = 8.7, 4.4$ Hz, 0.6H), 3.67 – 3.42 (m, 2H), 2.60 – 2.55 (m, 3H), 2.45 – 2.27 (m, 1H), 2.23 – 2.11 (m, 1H), 2.08 – 1.89 (m, 2H), 1.49 – 1.40 (m, 9H). ^{13}C NMR (101 MHz, CDCl_3) rotameric mixture, resonances for minor rotamer are enclosed in parenthesis δ (196.96) 196.79, (171.21) 171.15, 154.53 (154.48), 154.24 (153.63), 134.81 (134.70), 130.05 (129.92), (121.70) 121.34, 80.34 (80.15), 59.18 (59.10), (46.66) 46.47, 31.04 (29.99), 28.41, 26.65, (24.58) 23.76. These data are in full agreement with those previously published in the literature.³⁹



1-(*tert*-Butyl) 2-(3-cyanophenyl) pyrrolidine-1,2-dicarboxylate (29) was obtained from 3-iodobenzonitrile (68.7 mg, 300 μmol) and (*tert*-butoxycarbonyl)proline (96.9 mg, 450 μmol). Purification by flash chromatography (gradient 0-10% ethyl acetate/hexane) afforded the title compound as a colorless oil (78.6 mg, 248 μmol , 82%).

Reaction time: 48 hours. NMR yield: 88%

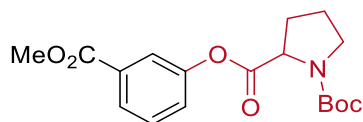
^1H NMR (400 MHz, CDCl_3) rotameric mixture δ 7.58 – 7.32 (m, 4H), 4.52 – 4.42 (m, 1H), 3.67 – 3.39 (m, 2H), 2.48 – 2.27 (m, 1H), 2.22 – 1.87 (m, 3H), 1.54 – 1.37 (m, 9H). ^{13}C NMR (101 MHz, CDCl_3) rotameric mixture, resonances for minor rotamer are enclosed in parenthesis δ (171.22) 171.09, (154.50) 153.55, (150.91) 150.69, 130.55 (130.38), 129.69 (129.59), (126.61) 126.15, (125.29) 124.92, (117.86) 117.75, (113.59) 113.38, 80.42 (80.27), (59.07) 59.03, (46.66) 46.46, 31.04 (29.97), 28.43 (28.41), 24.63 (23.74). These data are in full agreement with those previously published in the literature.³⁸



1-(*tert*-Butyl) 2-(4-cyanophenyl) pyrrolidine-1,2-dicarboxylate (30) was obtained from 4-iodobenzonitrile (68.7 mg, 300 μmol) and (*tert*-butoxycarbonyl)proline (96.9 mg, 450 μmol). Purification by flash chromatography (gradient 0-10% ethyl acetate/hexane) afforded the title compound as a colorless oil (87.6 mg, 277 μmol , 92%).

Reaction time: 24 hours. NMR yield: 94%

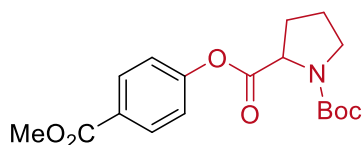
^1H NMR (400 MHz, CDCl_3) rotameric mixture, δ 7.74 – 7.65 (m, 2H), 7.29 – 7.22 (m, 2H, contains residual solvent signal of CDCl_3), 4.49 (dd, $J = 8.6, 4.6$ Hz, 0.5H), 4.44 (dd, $J = 8.7, 4.4$ Hz, 0.5H), 3.65 – 3.38 (m, 2H), 2.48 – 2.30 (m, 1H), 2.20 – 1.88 (m, 3H), 1.51 – 1.44 (m, 9H). ^{13}C NMR (101 MHz, CDCl_3) rotameric mixture, resonances for minor rotamer are enclosed in parenthesis δ (171.01) 170.88, (154.50) 154.11, 153.82 (153.54), 133.81 (133.66), (122.71) 122.31, (118.33) 118.15, (109.91) 109.71, 80.43 (80.28), 59.14 (59.07), (46.66) 46.47, (31.03) 29.96, 28.41, (24.63) 23.76. These data are in full agreement with those previously published in the literature.³⁸



1-(*tert*-Butyl) 2-(3-(methoxycarbonyl)phenyl) pyrrolidine-1,2-dicarboxylate (31) was obtained from methyl 3-iodobenzoate (78.6 mg, 300 μmol) and (*tert*-butoxycarbonyl)proline (96.9 mg, 450 μmol). Purification by flash chromatography (gradient 0-10% ethyl acetate/hexane) afforded the title compound as a colorless oil (89.2 mg, 255 μmol , 85%).

Reaction time: 48 hours. NMR yield: 87%

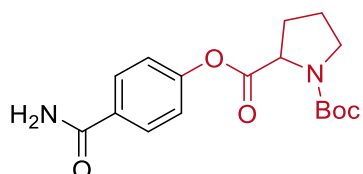
^1H NMR (400 MHz, CDCl_3) rotameric mixture δ 7.94 – 7.87 (m, 1H), 7.77 – 7.73 (m, 1H), 7.49 – 7.40 (m, 1H), 7.36 – 7.27 (m, 1H), 4.52 (dd, $J = 8.6, 4.3$ Hz, 0.4H), 4.45 (dd, $J = 8.7, 4.3$ Hz, 0.6H), 3.92 – 3.88 (m, 3H), 3.67 – 3.39 (m, 2H), 2.46 – 2.27 (m, 1H), 2.23 – 2.11 (m, 1H), 2.11 – 1.89 (m, 2H), 1.51 – 1.41 (m, 9H). ^{13}C NMR (101 MHz, CDCl_3) rotameric mixture, resonances for minor rotamer are enclosed in parenthesis δ 171.47, (166.19) 166.05, (154.48) 153.70, (150.71) 150.53, 131.76 (131.59), 129.56 (129.41), 127.12 (127.04), (126.34) 125.81, (122.67) 122.48, 80.37 (80.09), 59.15 (59.05), 52.37 (52.28), (46.64) 46.48, 31.05 (30.00), 28.42, (24.55) 23.74. These data are in full agreement with those previously published in the literature.³⁸



1-(*tert*-Butyl) 2-(4-(methoxycarbonyl)phenyl) pyrrolidine-1,2-dicarboxylate (32) was obtained from methyl 4-iodobenzoate (78.6 mg, 300 μmol) and (*tert*-butoxycarbonyl)proline (96.9 mg, 450 μmol). Purification by flash chromatography (gradient 0-10% ethyl acetate/hexane) afforded the title compound as a colorless oil (94.5 mg, 270 μmol , 90%).

Reaction time: 24 hours. NMR yield: 91%

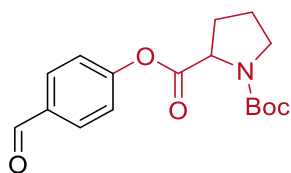
^1H NMR (400 MHz, CDCl_3) rotameric mixture, δ 8.10 – 8.01 (m, 2H), 7.20 – 7.13 (m, 2H), 4.52 (dd, $J = 8.6, 4.3$ Hz, 0.4H), 4.46 (dd, $J = 8.7, 4.3$ Hz, 0.6H), 3.93 – 3.85 (m, 3H), 3.67 – 3.41 (m, 2H), 2.45 – 2.26 (m, 1H), 2.21 – 2.09 (m, 1H), 2.08 – 1.88 (m, 2H), 1.50 – 1.38 (m, 9H). ^{13}C NMR (101 MHz, CDCl_3) rotameric mixture, resonances for minor rotamer are enclosed in parenthesis δ (171.17) 171.12, (166.34) 166.20, (154.47) 154.19, 153.64, 131.25 (131.11), 127.83 (127.67), (121.52) 121.16, 80.34 (80.13), 59.19 (59.10), 52.24 (52.18), (46.65) 46.46, 31.02 (29.97), 28.41, (24.55) 23.73. These data are in full agreement with those previously published in the literature.³⁸



1-(*tert*-Butyl) 2-(4-carbamoylphenyl) pyrrolidine-1,2-dicarboxylate (33) was obtained from 4-iodobenzamide (74.1 mg, 300 μmol) and (*tert*-butoxycarbonyl)proline (96.9 mg, 450 μmol). Purification by flash chromatography (50% ethyl acetate/hexane) afforded the title compound as a colorless oil (90.2 mg, 270 μmol , 89%).

Reaction time: 48 hours. NMR yield: 94%

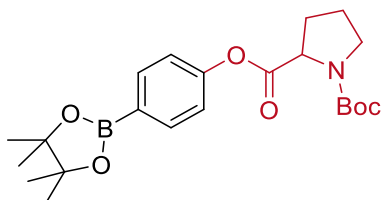
^1H NMR (400 MHz, CDCl_3) rotameric mixture δ 7.89 – 7.76 (m, 2H), 7.12 (d, $J = 8.7$ Hz, 2H), 6.74 – 6.22 (m, 2H), 4.52 (dd, $J = 8.6, 4.4$ Hz, 0.4H), 4.45 (dd, $J = 8.7, 4.4$ Hz, 0.6H), 3.66 – 3.38 (m, 2H), 2.43 – 2.25 (m, 1H), 2.21 – 2.09 (m, 1H), 2.06 – 1.84 (m, 2H), 1.51 – 1.35 (m, 9H). ^{13}C NMR (101 MHz, CDCl_3) rotameric mixture, resonances for minor rotamer are enclosed in parenthesis δ (171.42) 171.33, (168.93) 168.79, 154.55 (153.72), (153.42) 153.23, 131.25 (131.11), 129.11 (128.98), (121.58) 121.26, 80.39 (80.22), 59.17 (59.10), (46.69) 46.47, 30.99 (29.98), 28.40, (24.54) 23.72. HRMS (ESI) m/z calcd for $\text{C}_{17}\text{H}_{24}\text{N}_2\text{NaO}_5$ [(M+Na) $^+$] 357.1421, found: 357.1397.



1-(*tert*-Butyl) 2-(4-formylphenyl) pyrrolidine-1,2-dicarboxylate (34) was obtained from 4-iodobenzaldehyde (69.6 mg, 300 μmol) and (*tert*-butoxycarbonyl)proline (96.9 mg, 450 μmol). Purification by flash chromatography (gradient 0-10% ethyl acetate/hexane) afforded the title compound as a colorless oil (87.2 mg, 273 μmol , 91%).

Reaction time: 24 hours. NMR yield: 96%

^1H NMR (400 MHz, CDCl_3) rotameric mixture δ 9.98 (s, 0.6H), 9.97 (s, 0.4H), 7.95 – 7.86 (m, 2H), 7.32 – 7.24 (m, 2H, contains residual solvent signal of CDCl_3), 4.51 (dd, $J = 8.5, 4.4$ Hz, 0.4H), 4.45 (dd, $J = 8.7, 4.4$ Hz, 0.6H), 3.66 – 3.40 (m, 2H), 2.46 – 2.29 (m, 1H), 2.22 – 2.10 (m, 1H), 2.11 – 1.90 (m, 2H), 1.51 – 1.41 (m, 9H). ^{13}C NMR (101 MHz, CDCl_3) rotameric mixture, resonances for minor rotamer are enclosed in parenthesis δ (190.989) 190.81, (171.10) 171.02, (155.55) 155.24, (154.49) 153.60, 134.09 (134.00), 131.30 (131.19), (122.31) 121.93, 80.38 (80.20), 59.20 (59.11), (46.66) 46.47, 31.04 (29.99), 28.42, (24.59) 23.75. These data are in full agreement with those previously published in the literature.³⁸



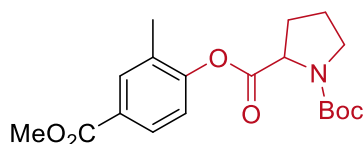
1-(*tert*-Butyl) 2-(4-(4,4,5,5-tetramethyl-1,3,2-dioxaborolan-2-yl)phenyl) pyrrolidine-1,2-dicarboxylate (35) was obtained from 4-iodophenylboronic acid pinacol ester (99.0 mg, 300 μmol) and (*tert*-butoxycarbonyl)proline (96.9 mg, 450 μmol). Purification by flash chromatography (gradient 0-10% ethyl acetate/hexane) afforded the title compound as a white solid (96.1 mg, 230 μmol , 77%).

In order to avoid hydrolysis of the boronic acid ester, no washing with a NaOH solution can be carried out and mixed fractions have to be discarded or further purified by a second column chromatography step.

Reaction time: 30 hours. NMR yield: 96%

^1H NMR (400 MHz, CDCl_3) rotameric mixture δ 7.87 – 7.77 (m, 2H), 7.14 – 7.05 (m, 2H), 4.51 (dd, $J = 8.6, 4.2$ Hz, 0.4H), 4.43 (dd, $J = 8.7, 4.3$ Hz, 0.6H), 3.67 – 3.38 (m, 2H), 2.44 – 2.26 (m,

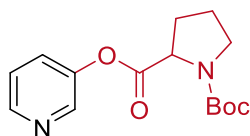
1H), 2.25 – 2.14 (m, 1H), 2.10 – 1.86 (m, 2H), 1.49 – 1.41 (m, 9H), 1.33 (s, 12H). ¹³C NMR (101 MHz, CDCl₃) rotameric mixture, resonances for minor rotamer are enclosed in parenthesis δ 171.35, (154.46) 153.75, (153.34) 153.10, 136.24 (136.13), 126.65 (br s), (120.85) 120.50, 83.94 (83.87), 80.26 (79.99), 59.23 (59.11), (46.64) 46.46, 31.03 (30.00), (28.43) 28.40, 24.86, (24.51) 23.73. These data are in full agreement with those previously published in the literature.³⁸



1-(*tert*-Butyl) 2-(4-(methoxycarbonyl)-2-methylphenyl) pyrrolidine-1,2-dicarboxylate (36) was obtained from methyl 4-iodo-3-methylbenzoate (77.8 mg, 300 μmol) and (*tert*-butoxycarbonyl)proline (96.9 mg, 450 μmol). Purification by flash chromatography (gradient 0–10% ethyl acetate/hexane) afforded the title compound as a colorless oil (79.3 mg, 218 μmol, 73%).

Reaction time: 24 hours. NMR yield: 74%

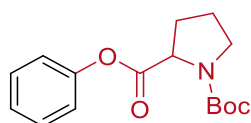
¹H NMR (400 MHz, CDCl₃) rotameric mixture δ 7.96 – 7.83 (m, 2H), 7.12 – 7.05 (m, 1H), 4.57 – 4.48 (m, 1H), 3.89 – 3.85 (m, 3H), 3.65 – 3.40 (m, 2H), 2.45 – 2.28 (m, 1H), 2.27 – 2.11 (m, 4H), 2.10 – 1.89 (m, 2H), 1.50 – 1.41 (m, 9H). ¹³C NMR (101 MHz, CDCl₃) rotameric mixture, resonances for minor rotamer are enclosed in parenthesis δ (170.95) 170.71, (166.52) 166.39, (154.42) 153.71, 153.02 (152.77), 132.76 (132.63), (130.69) 130.23, 128.64 (128.53), 127.91 (127.80), (122.00) 121.56, 80.37 (80.06), 59.06 (59.01), 52.18 (52.12), (46.62) 46.43, 31.16 (30.11), 28.42, (24.56) 23.62, 16.25 (16.18). These data are in full agreement with those previously published in the literature.³⁸



1-(*tert*-Butyl) 2-(pyridin-3-yl) pyrrolidine-1,2-dicarboxylate (37) was obtained from 3-iodopyridine (77.8 mg, 300 μmol) and (*tert*-butoxycarbonyl)proline (96.9 mg, 450 μmol). Purification by flash chromatography (gradient 15–33% ethyl acetate/hexane) afforded the title compound as a colorless oil (68.9 mg, 236 μmol, 79%).

Reaction time: 24 hours. NMR yield: 85%

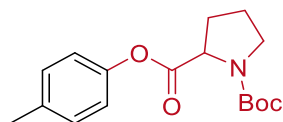
^1H NMR (400 MHz, CDCl_3) rotameric mixture δ 8.50 – 8.37 (m, 2H), 7.55 – 7.44 (m, 1H), 7.37 – 7.28 (m, 1H), 4.50 (dd, $J = 8.5, 4.5$ Hz, 0.4H), 4.45 (dd, $J = 8.7, 4.4$ Hz, 0.6H), 3.64 – 3.39 (m, 2H), 2.44 – 2.27 (m, 1H), 2.11 – 2.09 (m, 1H), 2.06 – 1.87 (m, 2H), 1.48 – 1.38 (m, 9H). ^{13}C NMR (101 MHz, CDCl_3) rotameric mixture, resonances for minor rotamer are enclosed in parenthesis δ (171.26) 171.24, (154.47) 153.57, (147.55) 147.29, 147.02 (146.72), (143.06) 142.96, (129.46) 128.86, 124.04 (123.96), 80.39 (80.21), 59.06 (59.02), (46.64) 46.45, 31.06 (30.00), 28.40, (24.59) 23.74. HRMS (ESI) m/z calcd for $\text{C}_{15}\text{H}_{20}\text{N}_2\text{NaO}_4$ [(M+H) $^+$] 293.1495, found: 293.1465.



1-(*tert*-Butyl) pyrrolidine-1,2-dicarboxylate (38) was obtained from iodobenzene (61.2 mg, 300 μmol) and (*tert*-butoxycarbonyl)proline (96.9 mg, 450 μmol). Purification by flash chromatography (gradient 0-8% ethyl acetate/hexane) afforded the title compound as a colorless oil (69.0 mg, 237 μmol , 79%).

Reaction time: 64 hours. NMR yield: 81%

^1H NMR (400 MHz CDCl_3) rotameric mixture δ 7.42 – 7.31 (m, 2H), 7.26 – 7.17 (m, 1H), 7.14 – 7.05 (m, 2H), 4.51 (dd, $J = 8.6, 4.4$ Hz, 0.4H), 4.45 (dd, $J = 8.7, 4.3$ Hz, 0.6H), 3.67 – 3.39 (m, 2H), 2.44 – 2.26 (m, 2H), 2.22 – 2.11 (m, 1H), 2.11 – 1.87 (m, 2H), 1.52 – 1.40 (m, 9H). ^{13}C NMR (101 MHz, CDCl_3) rotameric mixture, resonances for minor rotamer are enclosed in parenthesis δ 171.63, (154.46) 153.76, (150.80) 150.59, 129.51 (129.36), 125.95 (125.79), (121.48) 121.15, 80.21 (79.96), 59.19 (59.09), (46.64) 46.46, 31.07 (30.03), 28.44, (24.50) 23.71. These data are in full agreement with those previously published in the literature.⁵⁵

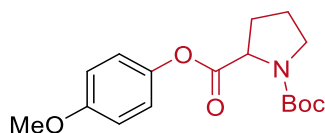


1-(*tert*-Butyl) 2-(4-tolyl) pyrrolidine-1,2-dicarboxylate (39) was obtained from 4-iodotoluene (65.4 mg, 300 μmol) and (*tert*-butoxycarbonyl)proline (96.9 mg, 450 μmol). Purification by flash chromatography (gradient 0-10% ethyl acetate/hexane) afforded the title compound as a colorless oil (61.5 mg, 201 μmol , 67%).

Reaction time: 64 hours. NMR yield: 73%

^1H NMR (400 MHz, CDCl_3) rotameric mixture δ 7.20 – 7.11 (m, 2H), 7.00 – 6.93 (m, 2H), 4.51 (dd, $J = 8.6, 4.4$ Hz, 0.4H), 4.43 (dd, $J = 8.7, 4.4$ Hz, 0.6H), 3.68 – 3.39 (m, 2H), 2.41 – 2.26 (m,

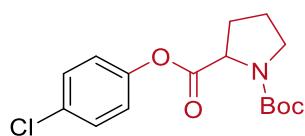
4H), 2.22 – 2.10 (m, 1H), 2.09 – 1.87 (m, 2H), 1.51 – 1.43 (m, 9H). ¹³C NMR (101 MHz, CDCl₃) rotameric mixture, resonances for minor rotamer are enclosed in parenthesis δ 171.80, (154.48) 153.79, (148.55) 148.35, 135.59 (135.38), 130.00 (129.85), (121.14) 120.82, 80.17 (79.92), 59.19 (59.07), (46.63) 46.45, 31.07 (30.03), (28.58) 28.44, (24.49) 23.71, 20.88. HRMS (ESI) m/z calcd for C₁₇H₂₃NNaO₄ [(M+Na)⁺] 328.1519, found: 328.1493.



1-(*tert*-Butyl) 2-(4-methoxyphenyl) pyrrolidine-1,2-dicarboxylate (40) was obtained from 4-iodoanisole (70.2 mg, 300 μmol) and (*tert*-butoxycarbonyl)proline (96.9 mg, 450 μmol). Purification by flash chromatography (gradient 0-10% ethyl acetate/hexane) afforded the title compound as a colorless oil (47.1 mg, 147 μmol, 49%).

Reaction time: 64 hours. NMR yield: 65%

¹H NMR (400 MHz, CDCl₃) rotameric mixture δ 7.05 – 6.95 (m, 2H), 6.91 – 6.82 (m, 2H), 4.49 (dd, *J* = 8.6, 4.4 Hz, 0.4H), 4.42 (dd, *J* = 8.7, 4.4 Hz, 0.6H), 3.80 – 3.76 (m, 3H), 3.65 – 3.39 (m, 2H), 2.42 – 2.24 (m, 1H), 2.21 – 2.09 (m, 1H), 2.08 – 1.89 (m, 2H), 1.48 – 1.44 (m, 9H). ¹³C NMR (101 MHz, CDCl₃) rotameric mixture, resonances for minor rotamer are enclosed in parenthesis δ 171.97, 157.29 (157.22), (154.45) 153.78, (144.28) 144.06, (122.22) 121.90, 114.50 (114.37), (80.17) 79.93, 59.15 (59.04), 55.60, (46.63) 46.45, 31.07 (30.03), 28.44, (24.50) 23.71. HRMS (ESI) m/z calcd for C₁₇H₂₃NNaO₅ [(M+Na)⁺] 344.1468, found : 344.1443.



1-(*tert*-Butyl) 2-(4-chlorophenyl) pyrrolidine-1,2-dicarboxylate (41) was obtained from 1-chloro-4-iodobenzene (71.6 mg, 300 μmol) and (*tert*-butoxycarbonyl)proline (96.9 mg, 450 μmol). Purification by flash chromatography (gradient 0-5% ethyl acetate/hexane) afforded the title compound as a colorless oil (86.9 mg, 267 μmol, 89%).

Reaction time: 30 hours. NMR yield: 93%

¹H NMR (400 MHz CDCl₃) rotameric mixture δ 7.37 – 7.29 (m, 2H), 7.08 – 7.00 (m, 2H), 4.49 (dd, *J* = 8.6, 4.3 Hz, 0.4H), 4.42 (dd, *J* = 8.7, 4.4 Hz, 0.6H), 3.64 – 3.39 (m, 2H), 2.43 – 2.26 (m, 1H), 2.20 – 1.87 (m, 3H), 1.49 – 1.42 (m, 9H). ¹³C NMR (101 MHz, CDCl₃) rotameric mixture,

Chapter 5

resonances for minor rotamer are enclosed in parenthesis δ (171.48) 171.41, (154.47) 153.67, (149.27) 149.05, 131.31 (131.15), 129.57 (129.41), (122.88) 122.51, 80.28 (80.09), 59.14 (59.04), (46.64) 46.45, 31.04 (29.99), 28.42, (24.55) 23.73. These data are in full agreement with those previously published in the literature.³⁸

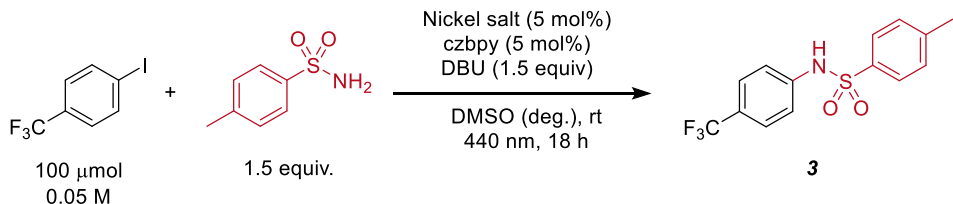
5.5.10 Optimization of the C–N cross-coupling using homogeneous visible-light-mediated nickel catalysis

General procedure for screening experiments

An oven dried vial (19 x 100 mm) equipped with a stir bar was charged with a nickel salt (5 μmol), 5,5'-dicarbazyl-2,2'-bipyridyl (czbpy, 5 μmol), 4-iodobenzotrifluoride (100 μmol) and the *p*-toluensulfonamide (150 μmol). The solvent (anhydrous, 2 mL) was added, followed by the base (150 μmol), before sealing the vessel with a septum and Parafilm. The mixture was stirred for 1 minute at high speed, followed by sonication for 5 minutes and degassing by bubbling argon for 10 minutes. The reaction mixture was stirred at 800 rpm and irradiated with one LED lamp (440 nm) using full power. After the respective reaction time, 1,3,5-trimethoxybenzene (16.8 mg, 100 μmol , 1 equiv) was added to the reaction vessel, the mixture was shaken and an aliquote (20 μL) was removed, diluted with DMSO- d_6 and analyzed by ^1H NMR.

Screening of nickel salts

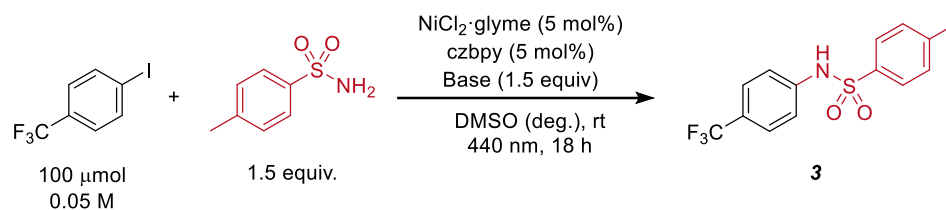
Table 5.22. Screening of nickel salts for the coupling of 4-iodobenzotrifluoride and *p*-toluensulfonamide.^a



Entry	Nickel salt	Conversion [%] ^b	3 [%] ^c
1	NiCl ₂ ·glyme	98	80
2	NiBr ₂ ·glyme	69	55
3	NiBr ₂ ·3H ₂ O	63	46

^aReaction conditions: 4-iodobenzotrifluoride (100 μmol), *p*-toluensulfonamide (150 μmol), 1,8-diazabicyclo[5.4.0]undec-7-ene (DBU, 150 μmol), nickel salt (5 μmol), 5,5'-dicarbazyl-2,2'-bipyridyl (czbpy, 5 μmol), DMSO (anhydrous, 2 mL), 440 nm LED (2 lamps at full power). ^bConversion of 4-iodobenzotrifluoride determined by ^1H -NMR using 1,3,5-trimethoxybenzene as internal standard. ^cNMR yields determined by ^1H -NMR using 1,3,5-trimethoxybenzene as internal standard. glyme = 1,2-dimethoxyethane.

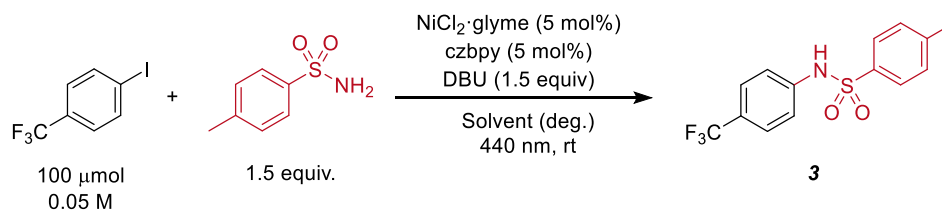
Base screening

Table 5.23. Base screening for the coupling of 4-iodobenzotrifluoride and *p*-toluenesulfonamide.^a

Entry	Base	Conversion [%] ^b	3 [%] ^c
1	1,8-Diazabicyclo[5.4.0]undec-7-ene (DBU)	98	80
2	7-Methyl-1,5,7-triazabicyclo[4.4.0]dec-5-en (MTBD)	98	74
3	1,1,3,3-Tetramethylguanidine (TMG)	65	61
4	2- <i>tert</i> -Butyl-1,1,3,3-tetramethylguanidine (BTMG)	18	18

^aReaction conditions: 4-iodobenzotrifluoride (100 μmol), *p*-toluenesulfonamide (150 μmol), base (150 μmol), NiCl₂·glyme (5 μmol), 5,5'-dicarbazyl-2,2'-bipyridyl (czbpy, 5 μmol), DMSO (anhydrous, 2 mL), 440 nm LED (2 lamps at full power). ^bConversion of 4-iodobenzotrifluoride determined by ¹H-NMR using 1,3,5-trimethoxybenzene as internal standard. ^cNMR yields determined by ¹H-NMR using 1,3,5-trimethoxybenzene as internal standard. glyme = 1,2-dimethoxyethane.

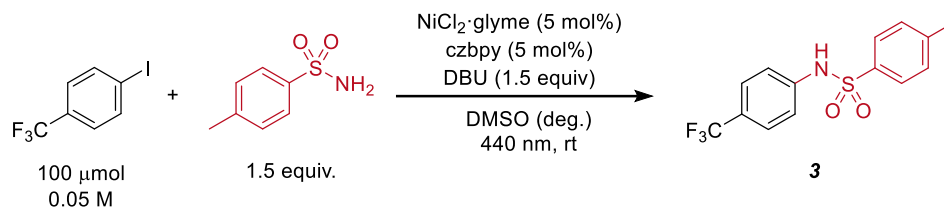
Solvent screening

Table 5.24. Solvent screening for the coupling of 4-iodobenzotrifluoride and *p*-toluenesulfonamide.^a

Entry	Solvent	Time [h]	Conversion [%] ^b	3 [%] ^c
1	DMSO	18	98	80
2	MeCN	18	43	40
3	DMAc	18	62	39

^aReaction conditions: 4-iodobenzotrifluoride (100 μmol), *p*-toluenesulfonamide (150 μmol), 1,8-diazabicyclo[5.4.0]undec-7-ene (DBU, 150 μmol), NiCl₂·glyme (5 μmol), 5,5'-dicarbazyl-2,2'-bipyridyl (czbpy, 5 μmol), solvent (anhydrous, 2 mL), 440 nm LED (2 lamps at full power). ^bConversion of 4-iodobenzotrifluoride determined by ¹H-NMR using 1,3,5-trimethoxybenzene as internal standard. ^cNMR yields determined by ¹H-NMR using 1,3,5-trimethoxybenzene as internal standard. glyme = 1,2-dimethoxyethane.

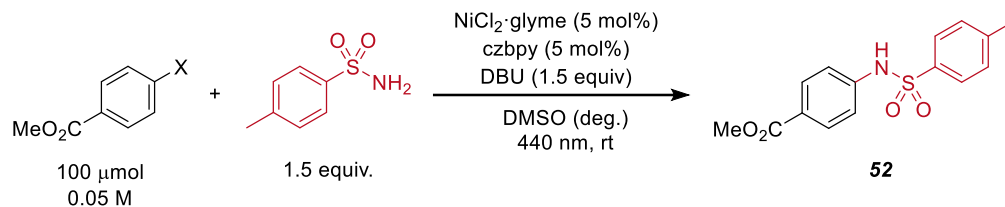
Optimized conditions and control experiments

Table 5.25. Optimized conditions and control experiments for the coupling of 4-iodobenzotrifluoride and *p*-toluenesulfonamide.^a

Entry	Variation	Time [h]	Conversion [%] ^b	3 [%] ^c
1	None	18	87	75
2	carbazole (10 mol%) instead of czbpy	18	42	32
3	bpy (5 mol%) instead of czbpy	18	3	n.d.
4	bpy (5 mol%) & carbazole (10 mol%) instead of czbpy	18	61	51
5	No NiCl ₂ ·glyme	18	18	n.d.
6	No czbpy	18	-	n.d.
7	No DBU	18	5	5
8	No light	18	-	n.d.
9	poly-czbpy (5 mol%) ^d	24	98	59

^aReaction conditions: 4-iodobenzotrifluoride (100 μmol), *p*-toluenesulfonamide (150 μmol), 1,8-diazabicyclo[5.4.0]undec-7-ene (DBU, 150 μmol), NiCl₂·glyme (5 μmol), 5,5'-dicarbazyl-2,2'-bipyridyl (czbpy, 5 μmol), DMSO (anhydrous, 2 mL), 440 nm LED (2 lamps at full power). ^bConversion of 4-iodobenzotrifluoride determined by ¹H-NMR using 1,3,5-trimethoxybenzene as internal standard. ^cNMR yields determined by ¹H-NMR using 1,3,5-trimethoxybenzene as internal standard. ^dThe amount of poly-czbpy was calculated using the molecular weight of the monomer. glyme = 1,2-dimethoxyethane. bpy = 2,2'-bipyridyl. n.d. = not detected.

Reactivity of different aryl halides

Table 5.26. Coupling of *p*-toluensulfonamide and methyl 4-halobenzoates.^a

Entry	Aryl halide	Time [h]	Conversion [%] ^b	52 [%] ^c
1	Methyl 4-chlorobenzoate	24	-	n.d.
2	Methyl 4-bromobenzoate	24	57	31
3	Methyl 4-iodobenzoate	24	>99	82

^aReaction conditions: aryl halide (100 μmol), *p*-toluensulfonamide (150 μmol), 1,8-diazabicyclo[5.4.0]undec-7-ene (DBU, 150 μmol), $\text{NiCl}_2 \cdot \text{glyme}$ (5 μmol), 5,5'-dicarbazolyl-2,2'-bipyridyl (*czbpy*, 5 μmol), DMSO (anhydrous, 2 mL), 440 nm LED (2 lamps at full power). ^bConversion of aryl halide determined by ¹H-NMR using 1,3,5-trimethoxybenzene as internal standard. ^cNMR yields determined by ¹H-NMR using 1,3,5-trimethoxybenzene as internal standard. glyme = 1,2-dimethoxyethane. n.d. = not detected.

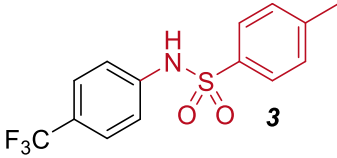
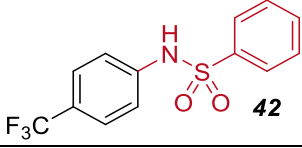
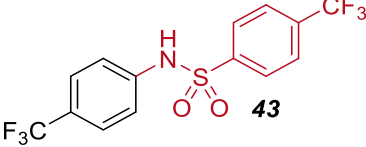
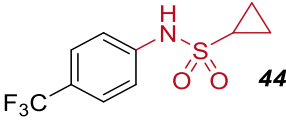
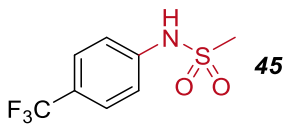
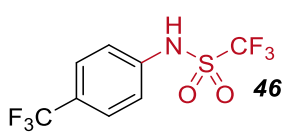
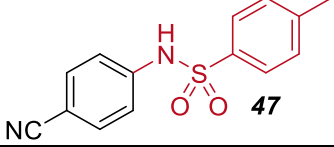
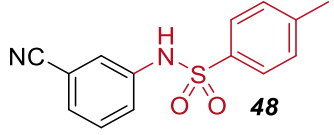
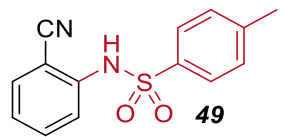
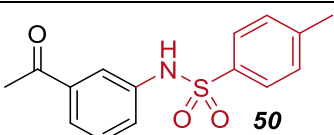
5.5.11 Scope of the C–N cross-coupling using homogeneous visible-light-mediated nickel catalysis

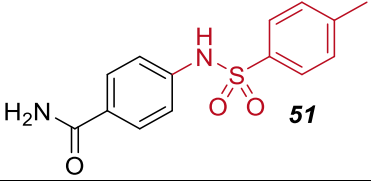
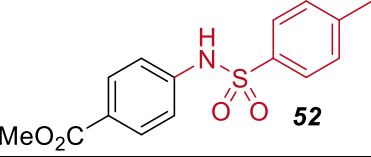
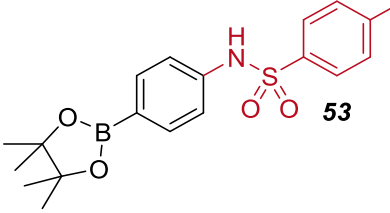
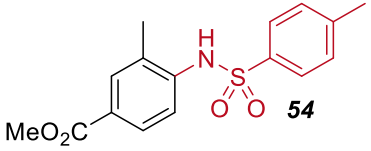
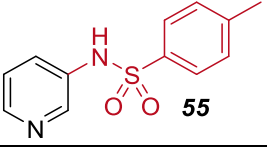
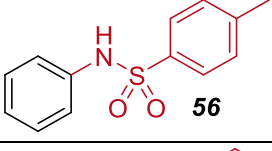
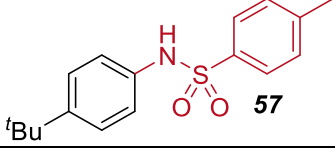
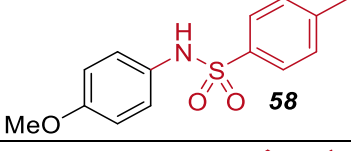
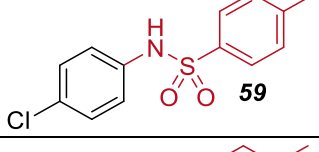
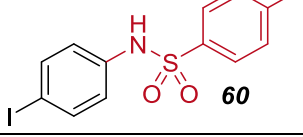
General procedure

An oven dried vial (19 x 100 mm) equipped with a stir bar was charged with NiCl₂·glyme (3.3 mg, 15 μmol, 5 mol%), 5,5-dicarbazoyl-2,2'-bipyridyl (czbpy, 7.3 mg, 15 μmol, 5 mol%), the aryl iodide (300 μmol) and the sulfonamide (450 μmol, 1.5 equiv). DMSO (anhydrous, 6 mL) was added, followed by 1,8-diazabicyclo[5.4.0]undec-7-ene (DBU, 68.5 mg, 450 μmol, 1.5 equiv), before sealing the vessel with a septum and Parafilm. The mixture was stirred for 1 minute at high speed, followed by sonication for 5 minutes and degassing by bubbling argon for 10 minutes. The reaction mixture was stirred at 800 rpm and irradiated with two LED lamps (440 nm) at full power. After the respective reaction time, maleic acid (34.8 mg, 300 μmol, 1.0 equiv) was added to the reaction vessel, the mixture was stirred and an aliquote (20 μL) was removed, diluted with DMSO-*d*₆ and analyzed by ¹H NMR. The NMR sample and the reaction mixture were combined and diluted with water (60 mL). The aqueous phase was extracted with ethyl acetate (3 x 40 mL). The combined organic layers were washed with brine (2 x 40 mL), dried over Na₂SO₄ and concentrated. The residue was purified by flash chromatography on silica gel using mixtures of hexane/ethyl acetate to obtain the desired product.

In some cases, we were not able to determine NMR yields reliably. In these cases, only consumption of the starting material (conversion) and isolated yields were determined.

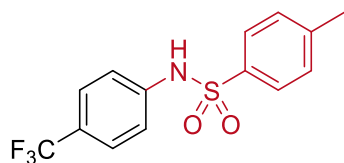
Table 5.27. Scope of the C–O coupling reaction.^a

Product	Reaction time	NMR yield ^b	Isolated yield
 3	20 hours	full conversion	89%
 42	20 hours	full conversion	86%
 43	48 hours	full conversion	86%
 44	23 hours	83% yield	80%
 45	22 hours	78% yield	77%
 46	115 hours	74% yield	72%
 47	18 hours	full conversion	82%
 48	20 hours	full conversion	80%
 49	32 hours	82% yield	81%
 50	18 hours	89% yield	63%

Product	Reaction time	NMR yield ^b	Isolated yield
 51	66 hours	89% yield	86%
 52	24 hours	95% yield	84%
 53	22 hours	full conversion	72%
 54	72 hours	full conversion	78%
 55	30 hours	76% yield	74%
 56	68 hours	full conversion	89%
 57	68 hours	-	83%
 58	43 hours	95% conversion	84%
 59	24 hours	86% yield	83%
 60	96 hours	65% yield	61%

^aReaction conditions according to general procedure. ^bNMR yields determined by ¹H-NMR using maleic acid as internal standard

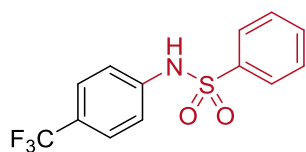
Experimental data



4-Methyl-N-(4-(trifluoromethyl)phenyl)benzenesulfonamide (3) was obtained from 4-iodobenzotrifluoride (81.6 mg, 300 μmol) and *p*-toluenesulfonamide (77.0 mg, 450 μmol). Purification by flash chromatography (gradient 5-20% ethyl acetate/hexane) afforded the title compound as a yellowish solid (84.2 mg, 267 μmol , 89%).

Reaction time: 20 hours. NMR analysis: full conversion of aryl iodide.

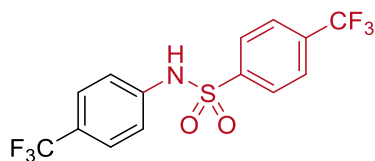
^1H NMR (400 MHz, CDCl_3) δ 7.74 (d, $J = 8.4$ Hz, 2H), 7.48 (d, $J = 8.5$ Hz, 2H), 7.42 (br. s, 1H), 7.27 (d, $J = 7.8$ Hz, 2H, contains residual solvent signal of CDCl_3), 7.19 (d, $J = 8.3$ Hz, 2H), 2.39 (s, 3H). ^{13}C NMR (101 MHz, CDCl_3) δ 144.71, 140.04, 135.77, 130.10, 127.39, 126.78 (q, $J = 3.8$ Hz), 126.78 (q, $J = 32.9$ Hz), 124.01 (d, $J = 270.9$ Hz), 119.75, 21.72. ^{19}F NMR (376 MHz, CDCl_3) δ -62.24. These data are in full agreement with those reported in literature.⁵⁶



N-(4-(Trifluoromethyl)phenyl)benzenesulfonamide (42) was obtained from 4-iodobenzotrifluoride (81.6 mg, 300 μmol) and benzenesulfonamide (70.7 mg, 450 μmol). Purification by flash chromatography (gradient 10-20% ethyl acetate/hexane) afforded the title compound as a white solid (77.6 mg, 258 μmol , 86%).

Reaction time: 20 hours. NMR analysis: full conversion of aryl iodide.

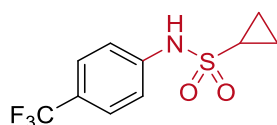
^1H NMR (400 MHz, CDCl_3) δ 7.92 – 7.86 (m, 2H), 7.82 (br. s, 1H), 7.58 (t, $J = 7.5$ Hz, 1H), 7.51 – 7.44 (m, 4H), 7.22 (d, $J = 8.2$ Hz, 2H). ^{13}C NMR (101 MHz, CDCl_3) δ 139.82, 138.57, 133.60, 129.39, 127.21, 126.89 (d, $J = 32.8$ Hz), 126.68 (q, $J = 3.7$ Hz), 123.89 (q, $J = 271.7$ Hz), 119.78. ^{19}F NMR (564 MHz, CDCl_3) δ -62.26. These data are in full agreement with those reported in literature.⁵⁷



4-(Trifluoromethyl)-N-(4-(trifluoromethyl)phenyl)benzenesulfonamide (43) was obtained from 4-iodobenzotrifluoride (81.6 mg, 300 μmol) and 4-(trifluoromethyl)benzenesulfonamide (101.3 mg, 450 μmol). Purification by flash chromatography (10% ethyl acetate/hexane) afforded the title compound as a white solid (95.2 mg, 258 μmol , 86%).

Reaction time: 48 hours. NMR analysis: full conversion of aryl iodide.

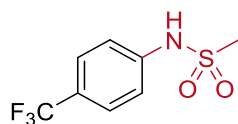
^1H NMR (400 MHz, CDCl_3) δ 7.99 (d, $J = 8.2$ Hz, 2H), 7.75 (d, $J = 8.3$ Hz, 2H), 7.61 (s, 1H), 7.52 (d, $J = 8.4$ Hz, 2H), 7.22 (d, $J = 8.4$ Hz, 2H). ^{13}C NMR (101 MHz, CDCl_3) δ 142.11, 139.09, 135.25 (q, $J = 33.3$ Hz), 127.74, 127.53 (q, $J = 32.8$ Hz), 126.91 (q, $J = 3.8$ Hz), 126.60 (q, $J = 3.7$ Hz), 123.73 (q, $J = 271.8$ Hz), 122.97 (q, $J = 273.2$ Hz), 120.20. ^{19}F NMR (564 MHz, CDCl_3) δ -62.40, -63.29. HRMS (EI) m/z calcd for $\text{C}_{14}\text{H}_9\text{F}_6\text{NO}_2\text{S}$ $[(\text{M})^+]$ 369.0258, found: 369.0256.



N-(4-(Trifluoromethyl)phenyl)cyclopropanesulfonamide (44) was obtained from 4-iodobenzotrifluoride (81.6 mg, 300 μmol) and cyclopropanesulfonamide (54.5 mg, 450 μmol). Purification by flash chromatography (gradient 10-20% ethyl acetate/hexane) afforded the title compound as a white solid (63.7 mg, 240 μmol , 80%).

Reaction time: 23 hours. NMR yield: 83%.

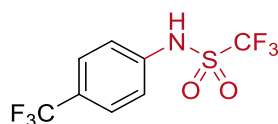
^1H NMR (400 MHz, CDCl_3) δ 7.59 (d, $J = 8.5$ Hz, 2H), 7.35 (d, $J = 8.5$ Hz, 2H), 7.16 (s, 1H), 2.60 – 2.51 (m, 1H), 1.27 – 1.21 (m, 2H), 1.05 – 0.98 (m, 2H). ^{13}C NMR (101 MHz, CDCl_3) δ 140.26, 126.87 (q, $J = 32.9$ Hz), 126.82 (q, $J = 3.8$ Hz), 123.94 (q, $J = 271.3$ Hz), 119.95, 30.41, 5.84. ^{19}F NMR (564 MHz, CDCl_3) δ -62.22. HRMS (EI) m/z calcd for $\text{C}_{10}\text{H}_{10}\text{F}_3\text{NO}_2\text{S}$ $[(\text{M})^+]$ 265.0384, found: 265.0390.



N-(4-(Trifluoromethyl)phenyl)methanesulfonamide (45) was obtained from 4-iodobenzotrifluoride (81.6 mg, 300 μmol) and methanesulfonamide (42.8 mg, 450 μmol). Purification by flash chromatography (gradient 10-20% ethyl acetate/hexane) afforded the title compound as a white solid (55.6 mg, 232 μmol , 77%).

Reaction time: 22 hours. NMR yield: 78%.

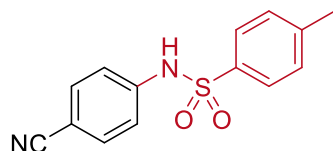
^1H NMR (400 MHz, CDCl_3) δ 7.65 – 7.57 (m, 2H), 7.39 (s, 1H), 7.36 – 7.29 (m, 2H), 3.10 (s, 3H). ^{13}C NMR (101 MHz, CDCl_3) δ 140.07, 127.04 (q, $J = 3.7$ Hz), 126.93 (q, $J = 32.9$ Hz), 123.89 (q, $J = 271.5$ Hz), 119.13, 39.88. ^{19}F NMR (564 MHz, CDCl_3) δ -62.27. These data are in full agreement with those reported in literature.⁵⁷



1,1,1-Trifluoro-N-(4-(trifluoromethyl)phenyl)methanesulfonamide (46) was obtained from 4-iodobenzotrifluoride (81.6 mg, 300 μmol) and trifluoromethanesulfonamide (42.8 mg, 450 μmol). Purification by flash chromatography (gradient 5-20% ethyl acetate/hexane) afforded the title compound as a white solid (63.2 mg, 216 μmol , 72%).

Reaction time: 115 hours. NMR yield: 74%.

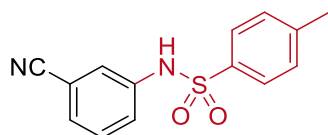
^1H NMR (400 MHz, CDCl_3) δ 7.66 (d, $J = 8.4$ Hz, 2H), 7.39 (d, $J = 8.4$ Hz, 2H), 7.29 (s, 1H). ^{13}C NMR (101 MHz, CDCl_3) δ 137.12, 129.32 (q, $J = 33.2$ Hz), 127.04 (q, $J = 3.7$ Hz), 123.5 (q, $J = 271.5$ Hz), 122.21, 119.6 (q, $J = 322.7$ Hz). ^{19}F NMR (377 MHz, CDCl_3) δ -62.65, -75.49. These data are in full agreement with those reported in literature.⁵⁸



N-(4-Cyanophenyl)-4-methylbenzenesulfonamide (47) was obtained from 4-iodobenzonitrile (68.7 mg, 300 μmol) and *p*-toluenesulfonamide (77.0 mg, 450 μmol). Purification by flash chromatography (gradient 1-3% ethyl acetate/dichloromethane) afforded the title compound as a white solid (67.3 mg, 247 μmol , 82%).

Reaction time: 18 hours. NMR analysis: full conversion of aryl iodide.

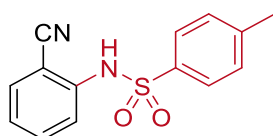
^1H NMR (400 MHz, CDCl_3) δ 7.72 (d, $J = 8.4$ Hz, 2H), 7.53 (d, $J = 8.7$ Hz, 2H), 7.28 (d, $J = 7.9$ Hz, 2H, contains residual solvent signal of CDCl_3), 7.15 (d, $J = 8.7$ Hz, 2H), 2.40 (s, 3H). ^{13}C NMR (101 MHz, CDCl_3) δ 145.00, 141.08, 135.64, 133.74, 130.19, 127.38, 119.44, 118.58, 107.87, 21.76. These data are in full agreement with those reported in literature.⁵⁹



***N*-(3-Cyanophenyl)-4-methylbenzenesulfonamide (48)** was obtained from 3-iodobenzonitrile (68.7 mg, 300 μmol) and *p*-toluenesulfonamide (77.0 mg, 450 μmol). Purification by flash chromatography (gradient 10-20% ethyl acetate/hexane) afforded the title compound as a white solid (65.3 mg, 240 μmol , 80%).

Reaction time: 20 hours. NMR yield: 80%.

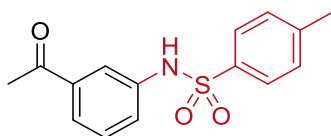
^1H NMR (400 MHz, CDCl_3) δ 7.72 (d, $J = 8.4$ Hz, 2H), 7.66 (s, 1H), 7.40 – 7.38 (m, 1H), 7.37 – 7.34 (m, 3H), 7.27 (d, $J = 8.0$ Hz, 2H), 2.39 (s, 3H). ^{13}C NMR (101 MHz, CDCl_3) δ 144.75, 137.79, 135.38, 130.35, 130.06, 128.47, 127.23, 124.98, 123.47, 118.13, 113.33, 21.63. These data are in full agreement with those reported in literature.⁶⁰



***N*-(2-Cyanophenyl)-4-methylbenzenesulfonamide (49)** was obtained from 2-iodobenzonitrile (68.7 mg, 300 μmol) and *p*-toluenesulfonamide (77.0 mg, 450 μmol). Purification by flash chromatography (gradient 10-15% ethyl acetate/hexane) afforded the title compound as a colorless oil (66.2 mg, 243 μmol , 81%).

Reaction time: 32 hours. NMR yield: 82%.

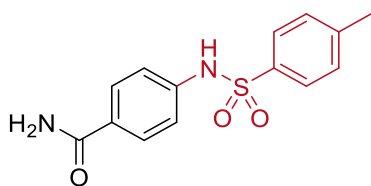
^1H NMR (400 MHz, CDCl_3) δ 7.75 – 7.67 (m, 3H), 7.58 – 7.52 (m, 1H), 7.47 (dd, $J = 7.8$ Hz, 1.6 Hz, 1H), 7.28 – 7.23 (m, 2H, contains residual solvent signal of CDCl_3), 7.17 (td, $J = 7.6$ Hz, 1.1 Hz, 1H), 7.13 (br. s, 1H), 2.39 (s, 3H). ^{13}C NMR (101 MHz, CDCl_3) δ 144.78, 139.35, 135.43, 134.22, 132.80, 129.97, 127.39, 125.18, 121.72, 115.74, 104.26, 21.64. These data are in full agreement with those reported in literature.⁶¹



N-(3-Acetylphenyl)-4-methylbenzenesulfonamide (50) was obtained from 3-iodoacetophenone (73.8 mg, 300 μmol) and *p*-toluenesulfonamide (77.0 mg, 450 μmol). Purification by flash chromatography (1st gradient 10-20% ethyl acetate/hexane; 2nd 15% ethyl acetate/hexane) afforded the title compound as a white solid (54.7 mg, 189 μmol , 63%).

Reaction time: 18 hours. NMR yield: 89%.

¹H NMR (400 MHz, CDCl₃) δ 7.75 – 7.70 (m, 3H), 7.67 (t, J = 2.0 Hz, 1H), 7.46 – 7.36 (m, 2H), 7.32 – 7.23 (m, 2H, contains residual solvent signal of CDCl₃), 2.59 (s, 3H), 2.41 (s, 3H). ¹³C NMR (101 MHz, CDCl₃) δ 197.65, 144.36, 138.20, 137.40, 135.93, 129.93, 129.81, 127.40, 125.73, 125.16, 120.82, 26.82, 21.69. These data are in full agreement with those reported in literature.⁵⁹

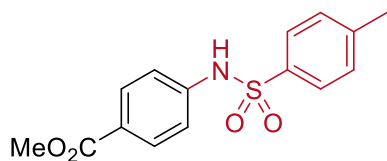


4-((4-Methylphenyl)sulfonamido)benzamide (51) was obtained from 4-iodobenzamide (74.1 mg, 300 μmol) and *p*-toluenesulfonamide (77.0 mg, 450 μmol). Purification by flash chromatography (gradient 80-100% ethyl acetate/hexane) afforded the title compound as a white solid (75.0 mg, 258 μmol , 86%).

Reaction time: 66 hours. NMR yield: 89%.

¹H NMR (400 MHz, DMSO) δ 10.59 (s, 1H), 7.82 (s, 1H), 7.72 (d, J = 8.7 Hz, 2H), 7.69 (d, J = 8.3 Hz, 2H), 7.35 (d, J = 8.1 Hz, 2H), 7.25 (s, 1H), 7.13 (d, J = 8.7 Hz, 2H), 2.32 (s, 3H). ¹³C NMR (101 MHz, DMSO-d₆) δ 167.23, 143.57, 140.58, 136.47, 129.83, 129.33, 128.76, 126.76, 118.16, 20.98.

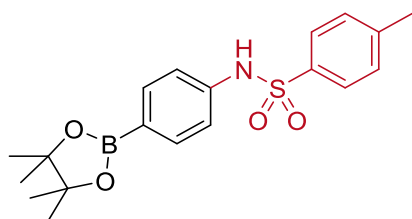
These data are in full agreement with those reported in literature.⁶²



Methyl 4-((4-methylphenyl)sulfonamido)benzoate (52) was obtained from methyl 4-iodobenzoate (78.6 mg, 300 μmol) and *p*-toluenesulfonamide (77.0 mg, 450 μmol). Purification by flash chromatography (gradient 15-30% ethyl acetate/hexane) afforded the title compound as a white solid (76.5 mg, 251 μmol , 84%).

Reaction time: 24 hours. NMR yield: 95%.

^1H NMR (400 MHz, DMSO- d_6) δ 10.80 (br. s, 1H), 7.81 (d, $J = 8.8$ Hz, 2H), 7.70 (d, $J = 8.3$ Hz, 2H), 7.36 (d, $J = 8.2$ Hz, 2H), 7.20 (d, $J = 8.8$ Hz, 2H), 3.77 (s, 3H), 2.33 (s, 3H). ^{13}C NMR (101 MHz, DMSO- d_6) δ 165.66, 143.71, 142.52, 136.36, 130.63, 129.87, 126.74, 124.25, 118.08, 51.95, 20.97. These data are in full agreement with those reported in literature.⁵⁹

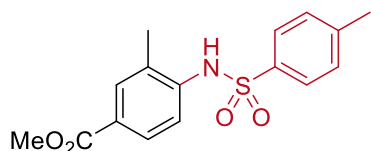


4-Methyl-N-(4-(4,4,5,5-tetramethyl-1,3,2-dioxaborolan-2-yl)phenyl)benzenesulfonamide (53) was obtained from 2-(4-iodophenyl)-4,4,5,5-tetramethyl-1,3,2-dioxaborolane (99.0 mg, 300 μmol) and *p*-toluenesulfonamide (77.0 mg, 450 μmol). Purification by flash chromatography (gradient 15-25% ethyl acetate/hexane) afforded the title compound as a white solid (80.1 mg, 215 μmol , 72%).

Reaction time: 22 hours. NMR analysis: full conversion of aryl iodide.

^1H NMR (400 MHz, CDCl_3) δ 7.71 – 7.64 (m, 4H), 7.21 (d, $J = 8.6$ Hz, 2H), 7.06 (d, $J = 8.5$ Hz, 2H), 6.74 (s, 1H), 2.36 (s, 3H), 1.31 (s, 12H). ^{13}C NMR (101 MHz, CDCl_3) δ 144.16, 139.36, 136.14, 136.05, 129.84, 127.40, 119.57, 83.98, 24.98, 21.68. The signal corresponding to the $\text{C}(\text{sp}^2)\text{-B}$ carbon was detected at 124.92 ppm in a HMBC experiment.

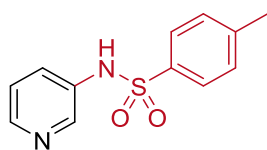
These data are in full agreement with those reported in literature.⁶³



Methyl 3-methyl-4-((4-methylphenyl)sulfonamido)benzoate (54) was obtained from methyl 4-iodo-3-methylbenzoate (77.8 mg, 300 μmol) and *p*-toluenesulfonamide (77.0 mg, 450 μmol). Purification by flash chromatography (gradient 10-15% ethyl acetate/hexane) afforded the title compound as a white solid (74.9 mg, 235 μmol , 78%).

Reaction time: 72 hours. NMR analysis: full conversion of aryl iodide.

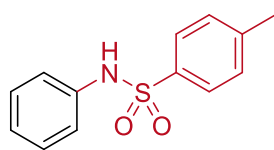
^1H NMR (400 MHz, CDCl_3) δ 7.81 – 7.77 (m, 1H), 7.77 – 7.74 (m, 1H), 7.68 (d, $J = 8.4$ Hz, 2H), 7.47 (d, $J = 8.5$ Hz, 1H), 7.22 (d, $J = 7.9$ Hz, 2H), 7.05 (s, 1H), 3.86 (s, 3H), 2.37 (s, 3H), 2.09 (s, 3H). ^{13}C NMR (101 MHz, CDCl_3) δ 166.61, 144.33, 139.17, 136.28, 132.16, 129.84, 128.80, 128.58, 127.16, 126.55, 120.96, 52.12, 21.59, 17.58. HRMS (EI) m/z calcd for $\text{C}_{16}\text{H}_{17}\text{NO}_4\text{S}$ [M] $^+$ 319.0878, found: 319.0877.



4-Methyl-N-(pyridin-3-yl)benzenesulfonamide (55) was obtained from 3-iodopyridine (61.5 mg, 300 μmol) and *p*-toluenesulfonamide (77.0 mg, 450 μmol). Purification by flash chromatography (gradient 15-50% ethyl acetate/hexane) afforded the title compound as a white solid (55.6 mg, 224 μmol , 74%).

Reaction time: 30 hours. NMR analysis: full conversion of aryl iodide; 76% NMR yield.

^1H NMR (400 MHz, DMSO-d_6) δ 10.50 (br. s, 1H), 8.27 (d, $J = 2.7$ Hz, 1H), 8.24 (dd, $J = 4.7, 1.5$ Hz, 1H), 7.65 (d, $J = 8.1$ Hz, 2H), 7.49 (ddd, $J = 8.3, 2.7, 1.5$ Hz, 1H), 7.35 (d, $J = 8.1$ Hz, 2H), 7.27 (dd, $J = 8.1, 4.7$ Hz, 1H), 2.32 (s, 3H). ^{13}C NMR (101 MHz, DMSO-d_6) δ 145.69, 144.10, 142.12, 136.63, 134.93, 130.32, 127.68, 127.18, 124.44, 21.43. These data are in full agreement with those reported in literature.⁶⁴

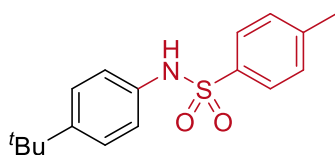


4-Methyl-N-phenylbenzenesulfonamide (56) was obtained from iodobenzene (61.2 mg, 300 μmol) and *p*-toluenesulfonamide (77.0 mg, 450 μmol). Purification by flash chromatography

(gradient 10-20% ethyl acetate/hexane) afforded the title compound as a white solid (66.4 mg, 268 μmol , 89%).

Reaction time: 68 hours. NMR analysis: full conversion of aryl iodide.

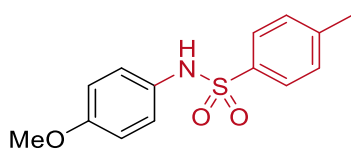
^1H NMR (400 MHz, CDCl_3) δ 7.68 (d, $J = 8.3$ Hz, 2H), 7.26 – 7.19 (m, 3H, contains residual solvent signal of CDCl_3), 7.12 – 7.06 (m, 4H), 2.37 (s, 3H). ^{13}C NMR (101 MHz, CDCl_3) δ 144.01, 136.67, 136.12, 129.78, 129.42, 127.40, 125.38, 121.60, 21.67. These data are in full agreement with those reported in literature.⁵⁹



***N*-(4-(*tert*-Butyl)phenyl)-4-methylbenzenesulfonamide (57)** was obtained from 1-iodo-4-*tert*-butylbenzene (78.0 mg, 300 μmol) and *p*-toluenesulfonamide (77.0 mg, 450 μmol). Purification by flash chromatography (gradient 10-20% ethyl acetate/hexane) afforded the title compound as a white solid (75.7 mg, 249 μmol , 83%).

Reaction time: 68 hours. NMR yield: not calculated due to signal overlap.

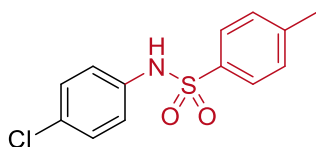
^1H NMR (400 MHz, CDCl_3) δ 7.67 (d, $J = 8.4$ Hz, 2H), 7.26 – 7.20 (m, 4H), 6.98 (d, $J = 8.6$ Hz, 2H), 6.73 (s, 1H), 2.38 (s, 3H), 1.25 (s, 9H). ^{13}C NMR (101 MHz, CDCl_3) δ 148.57, 143.85, 136.47, 133.81, 129.74, 127.39, 126.30, 121.72, 34.49, 31.41, 21.70. These data are in full agreement with those reported in literature.⁴⁰



***N*-(4-Methoxyphenyl)-4-methylbenzenesulfonamide (58)** was obtained from 4-iodoanisole (70.2 mg, 300 μmol) and *p*-toluenesulfonamide (77.0 mg, 450 μmol). Purification by flash chromatography (gradient 10-25% ethyl acetate/hexane) afforded the title compound as a white solid (69.6 mg, 251 μmol , 84%).

Reaction time: 43 hours. NMR analysis: 95% conversion of aryl iodide.

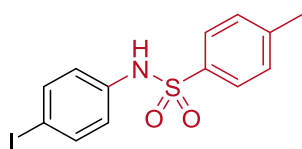
^1H NMR (400 MHz, CDCl_3) δ 7.59 (d, $J = 8.3$ Hz, 2H), 7.21 (d, $J = 7.8$ Hz, 2H), 6.98 (d, $J = 8.9$ Hz, 2H), 6.75 (d, $J = 9.0$ Hz, 2H), 6.62 (br. s, 1H), 3.75 (s, 3H), 2.38 (s, 3H). ^{13}C NMR (101 MHz, CDCl_3) δ 158.05, 143.80, 136.09, 129.68, 129.01, 127.45, 125.55, 114.52, 55.53, 21.68. These data are in full agreement with those reported in literature.⁵⁹



N-(4-Chlorophenyl)-4-methylbenzenesulfonamide (59) was obtained from 1-chloro-4-iodobenzene (71.6 mg, 300 μmol) and *p*-toluenesulfonamide (77.0 mg, 450 μmol). Purification by flash chromatography (gradient 10-15% ethyl acetate/hexane) afforded the title compound as a colorless oil (70.3 mg, 250 μmol , 83%).

Reaction time: 24 hours. NMR yield: 86%.

^1H NMR (400 MHz, CDCl_3) δ 7.68 (d, $J = 8.4$ Hz, 2H), 7.44 (s, 1H), 7.23 (d, $J = 8.4$ Hz, 2H), 7.20 – 7.14 (m, 2H), 7.07 – 7.01 (m, 2H), 2.37 (s, 3H). ^{13}C NMR (101 MHz, CDCl_3) δ 144.25, 135.57, 135.20, 130.78, 129.83, 129.41, 127.30, 122.78, 21.59. These data are in full agreement with those reported in literature.⁶⁵



N-(4-Iodophenyl)-4-methylbenzenesulfonamide (60) was obtained from 1,4-diiodobenzene (99.0 mg, 300 μmol) and *p*-toluenesulfonamide (77.0 mg, 450 μmol). Purification by flash chromatography (gradient 10-20% ethyl acetate/hexane) afforded the title compound as a white solid (68.3 mg, 183 μmol , 61%).

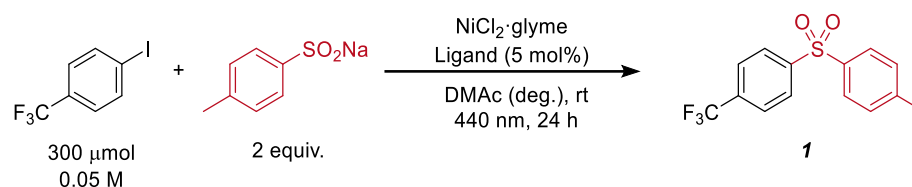
Reaction time: 96 hours. NMR analysis: 85% conversion of aryl iodide; 65% NMR yield.

^1H NMR (400 MHz, CDCl_3) δ 7.66 (d, $J = 8.4$ Hz, 2H), 7.52 (d, $J = 8.7$ Hz, 2H), 7.24 (d, $J = 8.0$ Hz, 2H), 7.00 (s, 1H), 6.84 (d, $J = 8.7$ Hz, 2H), 2.39 (s, 3H). ^{13}C NMR (101 MHz, CDCl_3) δ 144.38, 138.44, 136.53, 135.79, 129.95, 127.38, 123.21, 89.30, 21.71. These data are in full agreement with those reported in literature.⁶⁵

5.5.12 Heterogeneous visible-light-mediated nickel catalysis and recycling studies

Screening experiments

Table 5.28. Comparison of czbpy and poly-czbpy for the coupling of 4-iodobenzotrifluoride and sodium *p*-toluenesulfinate.^a



Entry	Ligand	$\text{NiCl}_2 \cdot \text{glyme}$	Conversion [%] ^b	1 [%] ^c
1	czbpy	2.5 mol%	97	84
2	czbpy	5 mol%	97	91
3	poly-czbpy	2.5 mol%	96	88
4	poly-czbpy	5 mol%	97	77

^aReaction conditions: 4-iodobenzotrifluoride (300 μmol), sodium *p*-toluenesulfinate (600 μmol), $\text{NiCl}_2 \cdot \text{glyme}$ (7.5–15 μmol), ligand (7.4 mg, 15 μmol), DMAc (anhydrous, 6 mL), 440 nm LED (2 lamps at full power). ^bConversion of 4-iodobenzotrifluoride determined by $^1\text{H-NMR}$ using 1,3,5-trimethoxybenzene as internal standard. ^cNMR yields determined by $^1\text{H-NMR}$ using 1,3,5-trimethoxybenzene as internal standard. glyme = 1,2-dimethoxyethane. czbpy = 5,5'-dicarbazolyl-2,2'-bipyridyl.

Table 5.29. Comparison of czbpy and poly-czbpy for the coupling of 4-iodobenzotrifluoride and *N*-Boc-proline.^a

Entry	Ligand	NiCl ₂ ·glyme	Conversion [%] ^b	2 [%] ^c	Ar-H [%] ^c	Ar-Cl [%] ^c
1	czbpy	2.5 mol%	98	76	14	3
2	czbpy	5 mol%	>99	88	9	n.d.
3	poly-czbpy	2.5 mol%	97	68	7	n.d.
4	poly-czbpy	5 mol%	75	53	18	n.d.

^aReaction conditions: 4-iodobenzotrifluoride (300 μmol), *N*-Boc-proline (450 μmol), *N*-*tert*-butylisopropylamine (BIPA, 450 μmol) NiCl₂·glyme (7.5-15 μmol), ligand (7.4 mg, 15 μmol), DMSO (anhydrous, 6 mL), 440 nm LED (2 lamps at full power). ^bConversion of 4-iodobenzotrifluoride determined by ¹H-NMR using 1,3,5-trimethoxybenzene as internal standard. ^cNMR yields determined by ¹H-NMR using 1,3,5-trimethoxybenzene as internal standard. glyme = 1,2-dimethoxyethane. czbpy = 5,5'-dicarbazolyl-2,2'-bipyridyl.

Table 5.30. Comparison of czbpy and poly-czbpy for the coupling of 4-iodobenzotrifluoride and *N*-Boc-proline.^a

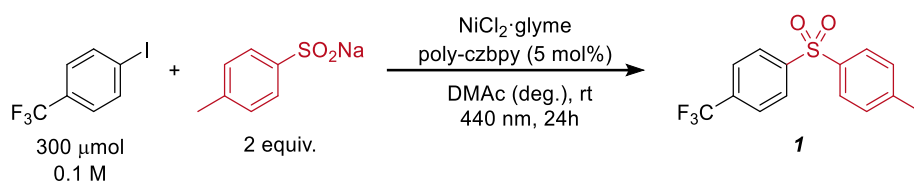
Entry	Ligand	NiCl ₂ ·glyme	Conversion [%] ^b	3 [%] ^c
1	czbpy	2.5 mol%	>99	91
2	czbpy	5 mol%	99	90
3	poly-czbpy	2.5 mol%	>99	82
4	poly-czbpy	5 mol%	99	59

^aReaction conditions: 4-iodobenzotrifluoride (300 μmol), *p*-toluene sulfonamide (450 μmol), 1,8-diazabicyclo[5.4.0]undec-7-ene (DBU, 450 μmol), NiCl₂·glyme (7.5-15 μmol), Ligand (7.4 mg, 15 μmol), DMSO (anhydrous, 6 mL), 440 nm LED (2 lamps at full power). ^bConversion of 4-iodobenzotrifluoride determined by ¹H-NMR using 1,3,5-trimethoxybenzene as internal standard. ^cNMR yields determined by ¹H-NMR using 1,3,5-trimethoxybenzene as internal standard. glyme = 1,2-dimethoxyethane. czbpy = 5,5'-dicarbazolyl-2,2'-bipyridyl.

General procedure for recycling experiments

An oven dried vial (13 x 80 mm) equipped with a stir bar was charged with poly-czbp (7.3 mg, 5 mol% calculated using monomer's molecular weight), sodium *p*-toluenesulfinate (106.9 mg, 600 μmol , 2 equiv) and $\text{NiCl}_2 \cdot \text{glyme}$ (7.5-15 μmol). Subsequently, 4-iodobenzotrifluoride (81.6 mg, 300 μmol) and DMAc (anhydrous, 6 mL) were added and the vial was sealed with a septum and Parafilm. The reaction mixture was sonicated for 5 minutes, followed by stirring to obtain a fine dispersion of the solids, before degassing by bubbling nitrogen for 10 min. The mixture was stirred at 800 rpm and irradiated with two LED lamps (440 nm) at full power. After 24 hours, 1,3,5-trimethoxybenzene (50.5 mg, 300 μmol , 1 equiv) was added and the mixture was stirred for 5 min. The reaction mixture was centrifuged at 3500 rpm for 15 min. The liquid phase was carefully separated and analyzed by $^1\text{H-NMR}$. Poly-czbp was washed two times with DMAc (anhydrous, 6 mL, followed by centrifugation at 3500 rpm for 15 min and separation of the liquid phase), lyophilized (overnight) and reused in the next reaction.

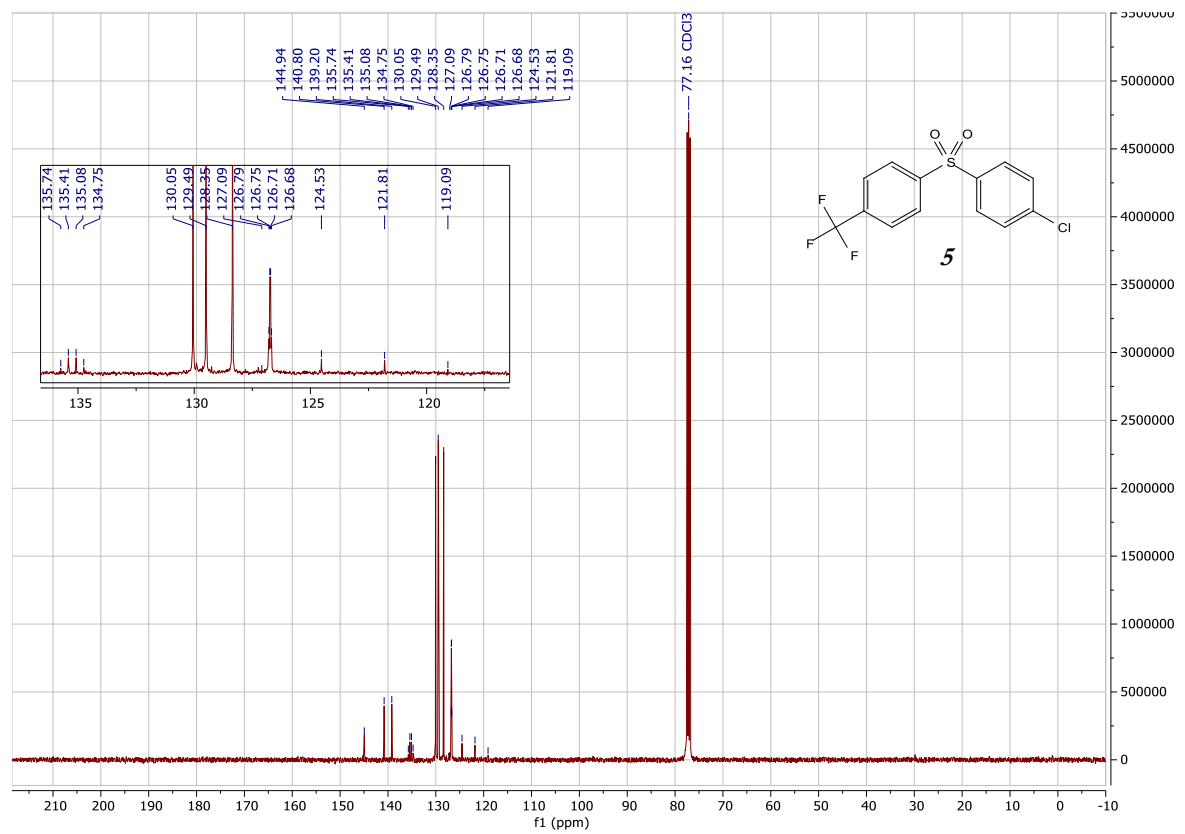
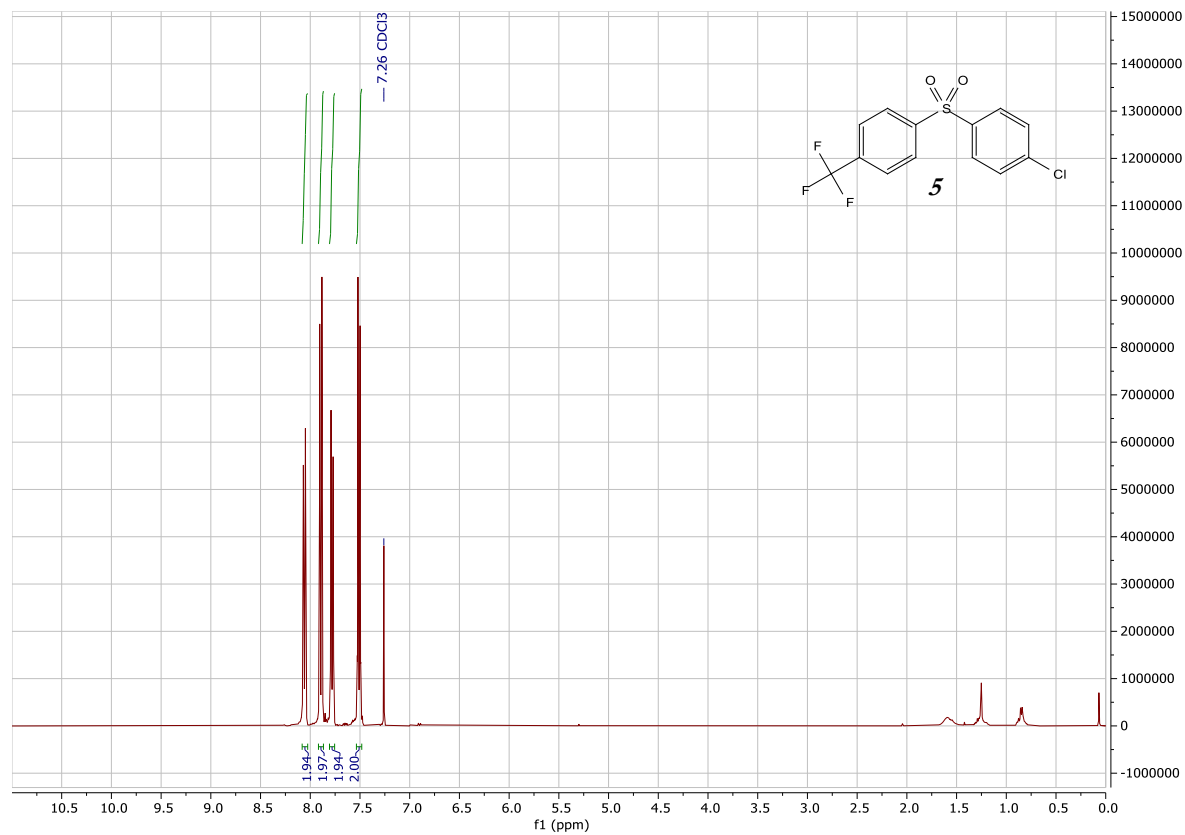
Reusability of the polymer poly-czbp was tested with and without addition of $\text{NiCl}_2 \cdot \text{glyme}$ in each cycle (Table 5.31).

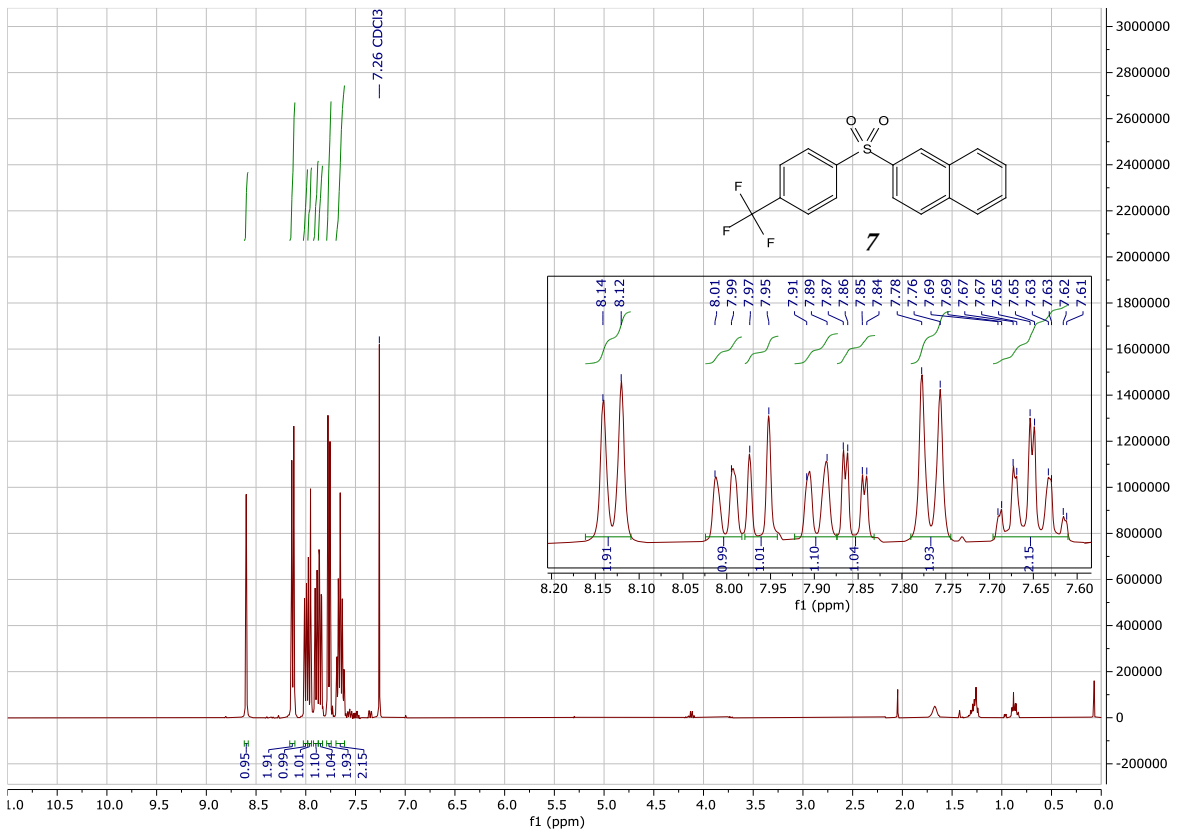
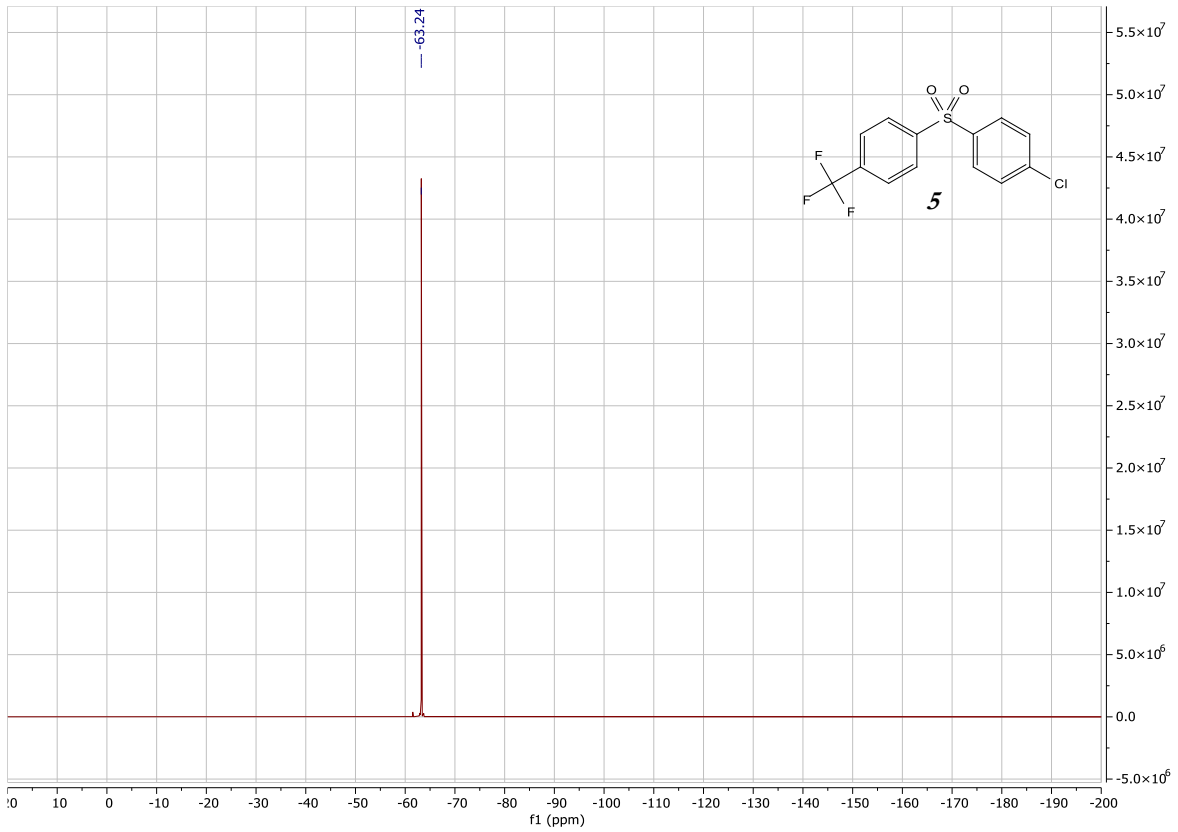
Table 5.31. Reusability of the polymer poly-czbpby.^a

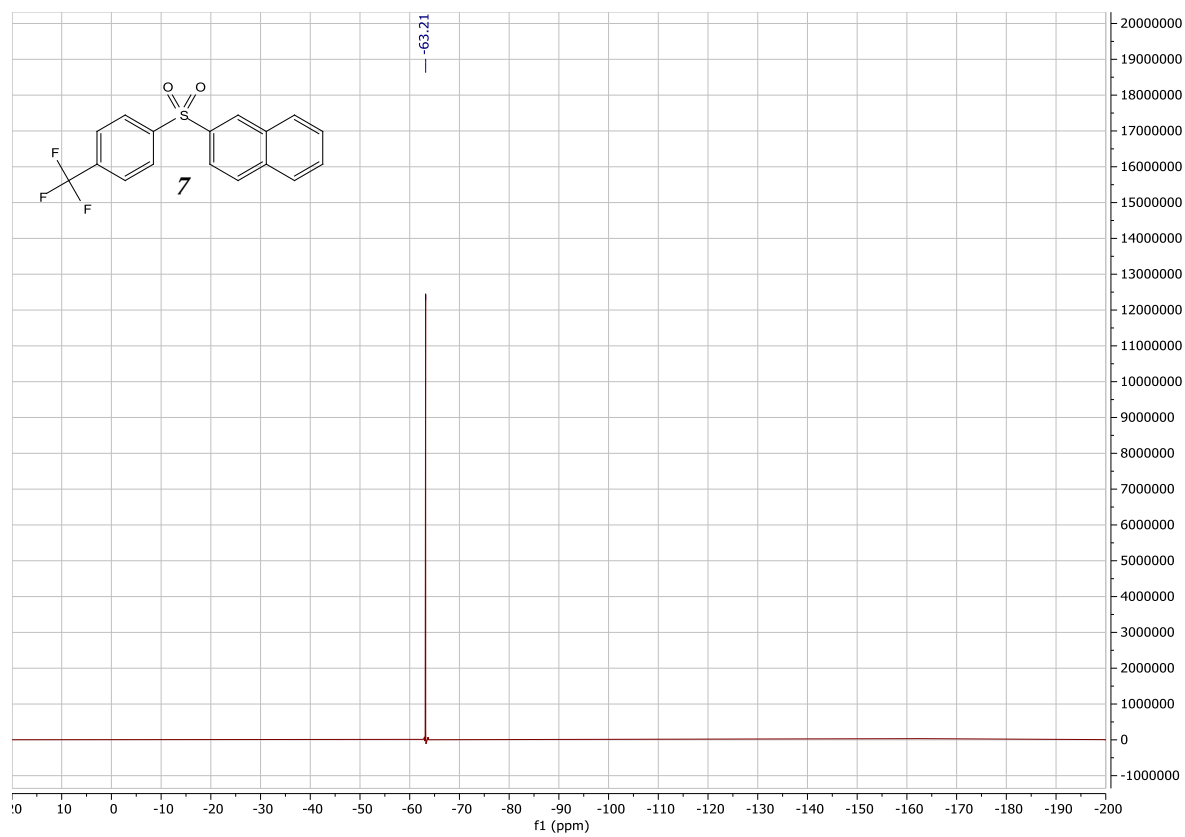
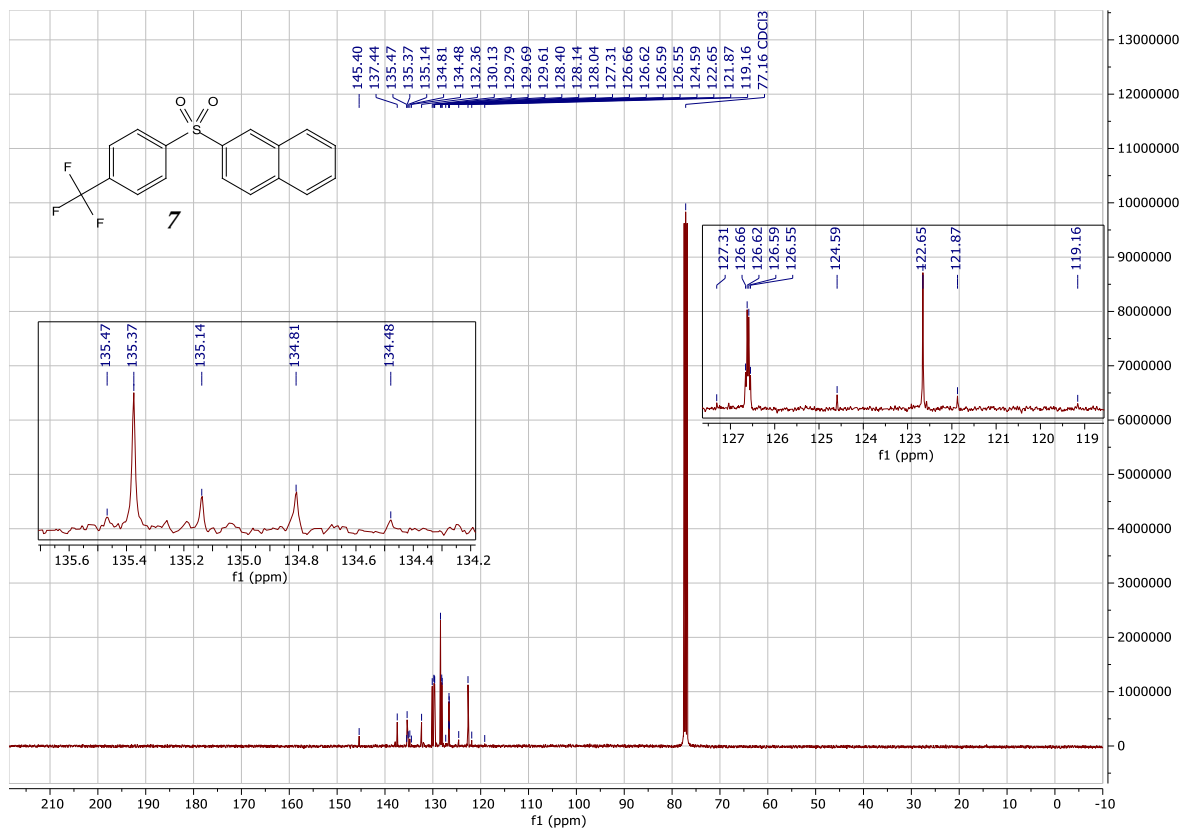
Nickel loading	5 mol% at each cycle	2.5 mol% at each cycle	5 mol% only at cycle 1	2.5 mol% only at cycle 1
Reaction Cycle	1 [%] ^b	1 [%] ^b	1 [%] ^b	1 [%] ^b
1	77	86	78	88
2	78	80	90	93
3	77	84	87	90
4	71	83	91	93
5	71	85	93	89
6	73	83	90	92
7	72	86	90	90
8	71	87	88	90
9	70	80	89	89
10	67	83	87	83

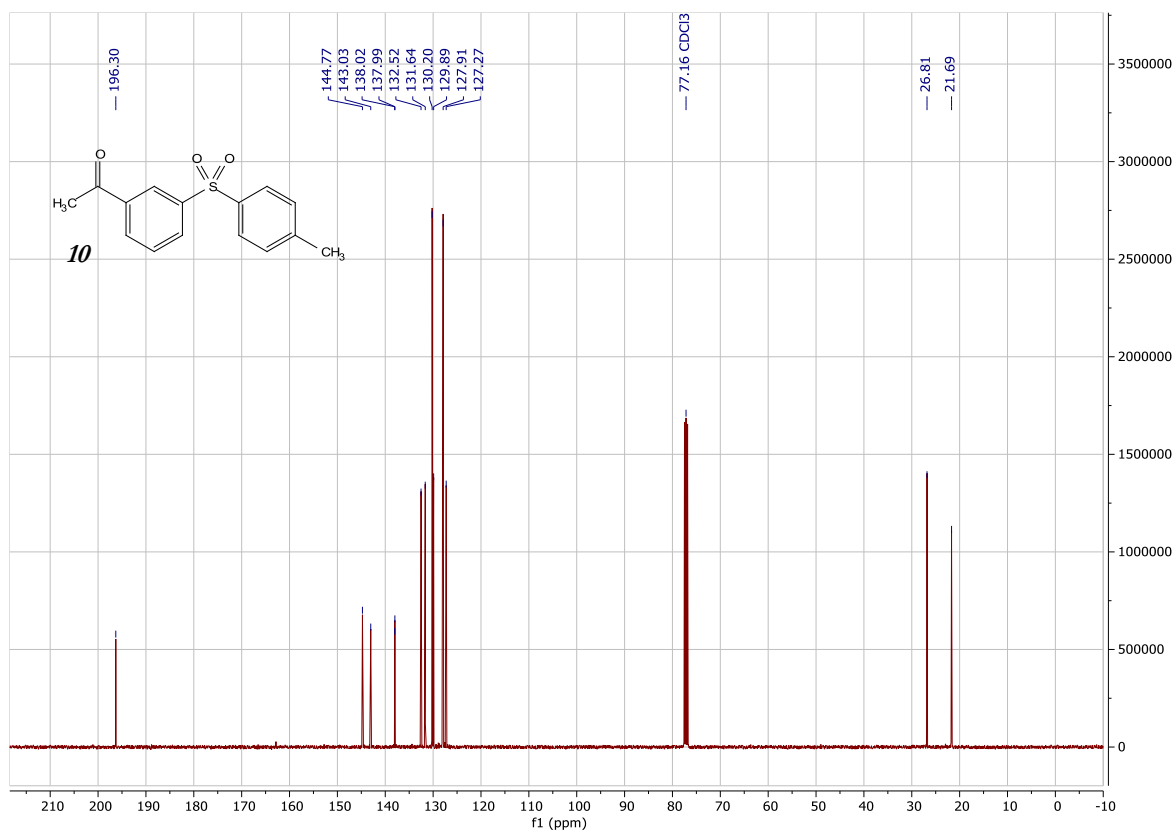
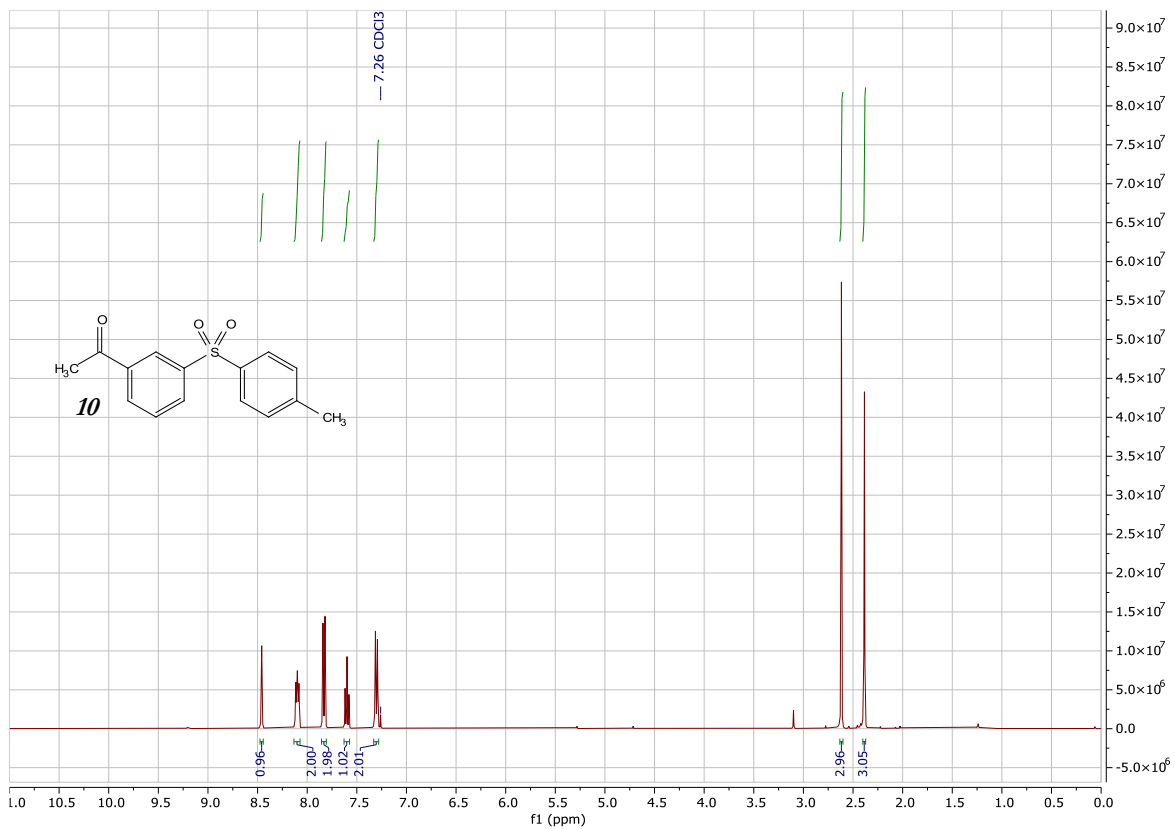
^aReaction conditions: 4-iodobenzotrifluoride (300 μmol), sodium *p*-toluenesulfonate (600 μmol), $\text{NiCl}_2 \cdot \text{glyme}$ (7.5-15 μmol), poly-czbpby (7.3 mg, 15 μmol calculated using monomer's molecular weight), DMAc (anhydrous, 6 mL), 440 nm LED (2 lamps at full power). ^bNMR yields determined by ¹H-NMR using 1,3,5-trimethoxybenzene as internal standard. glyme = 1,2-dimethoxyethane.

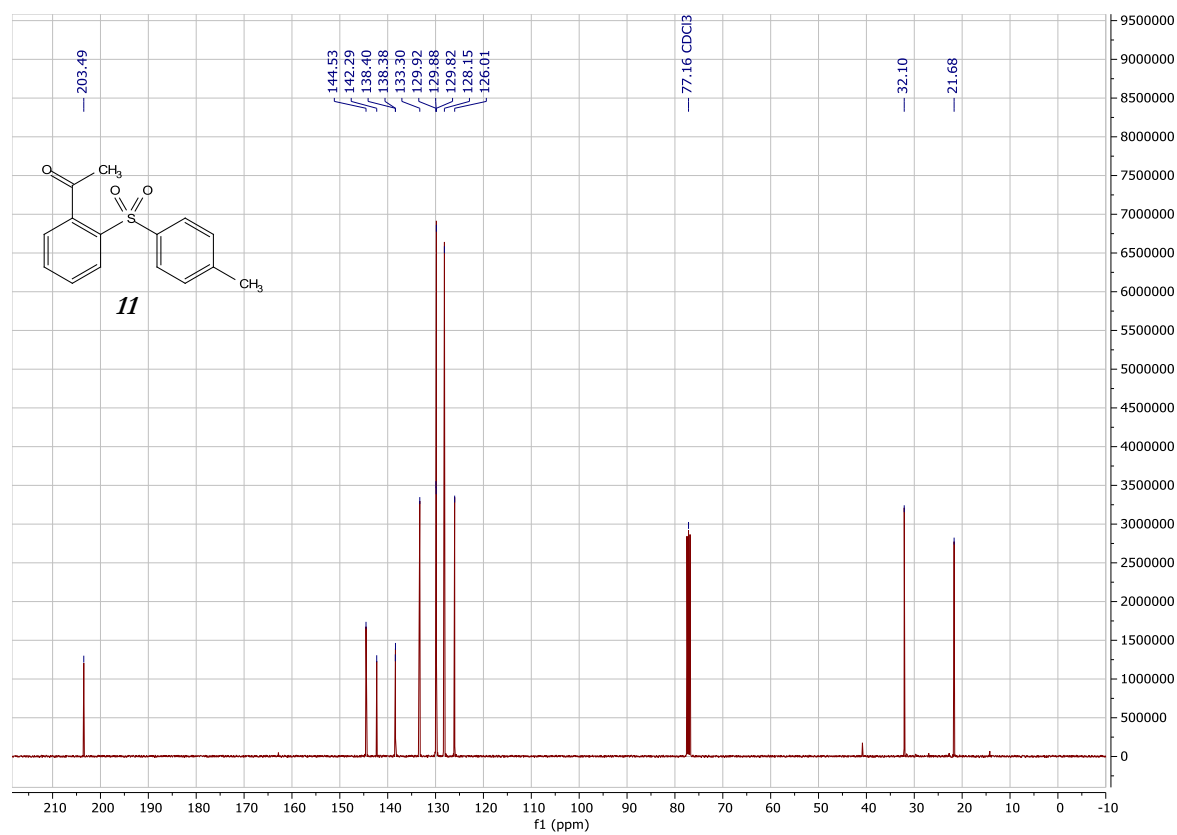
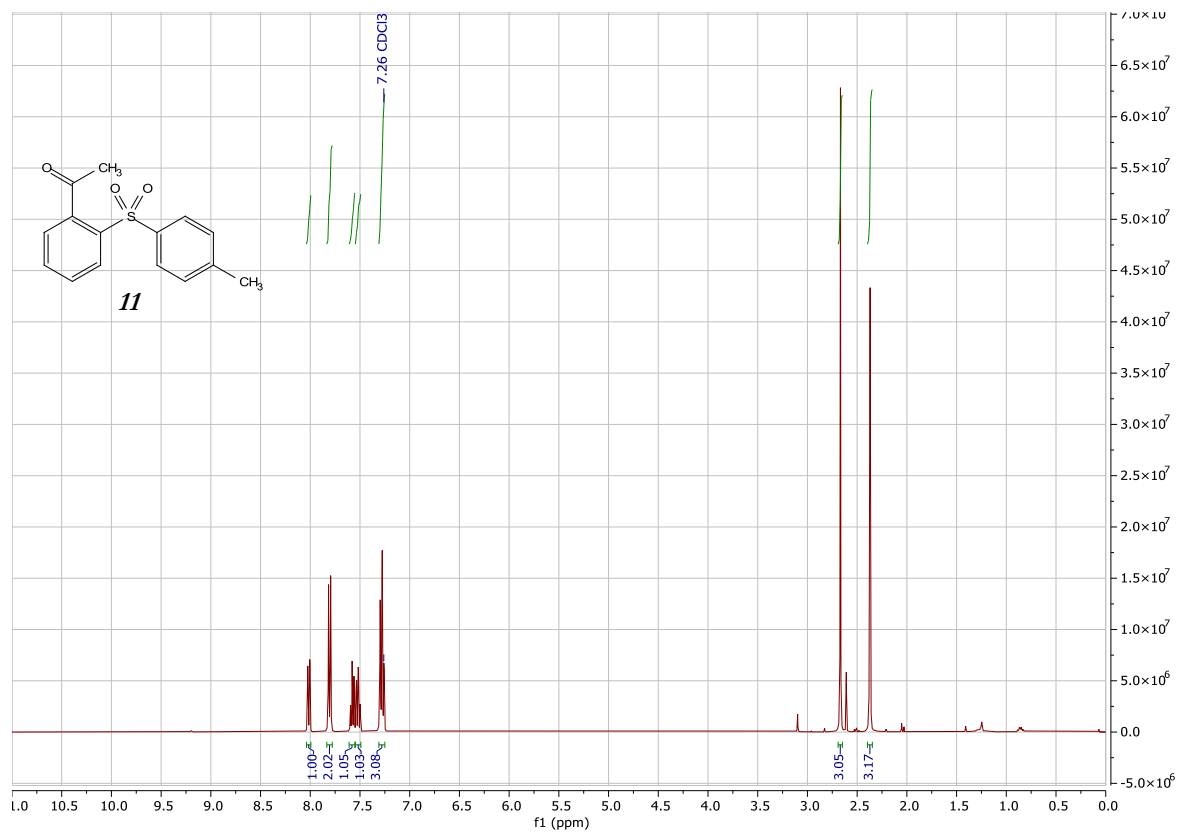
5.6 Copies of NMR spectra of new isolated compounds

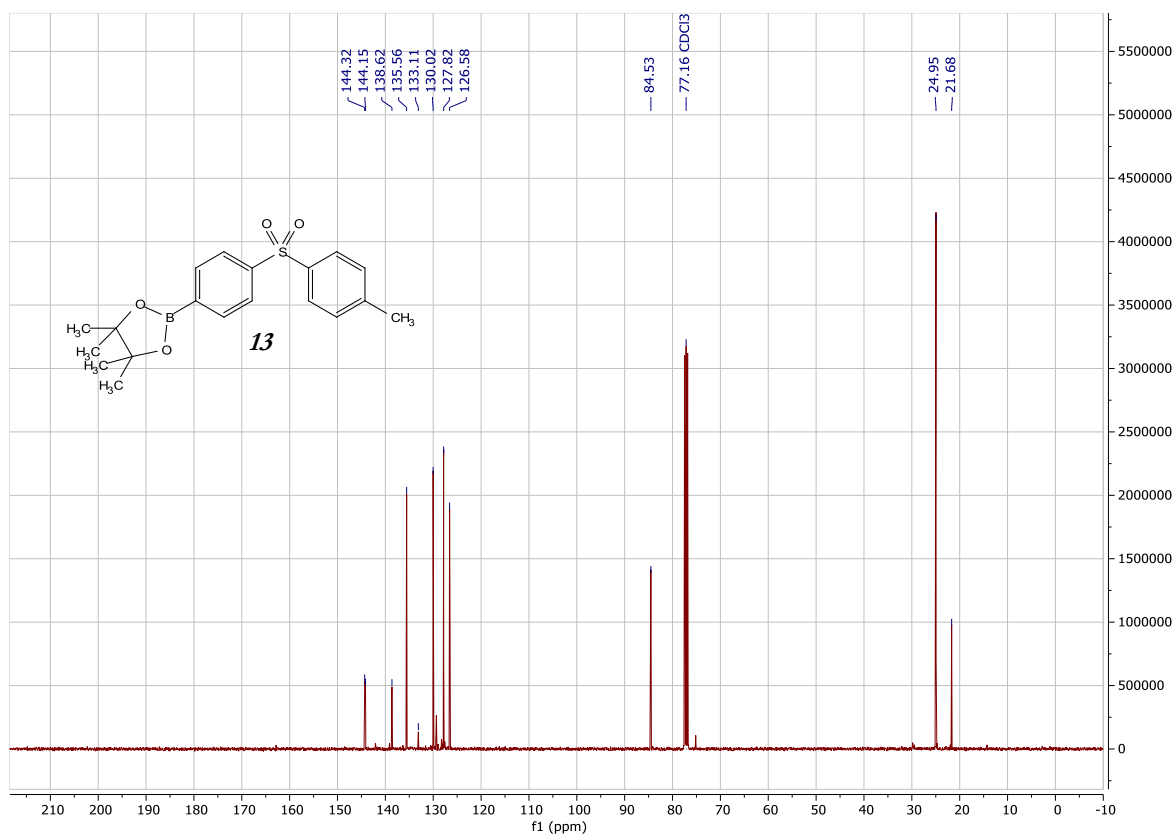
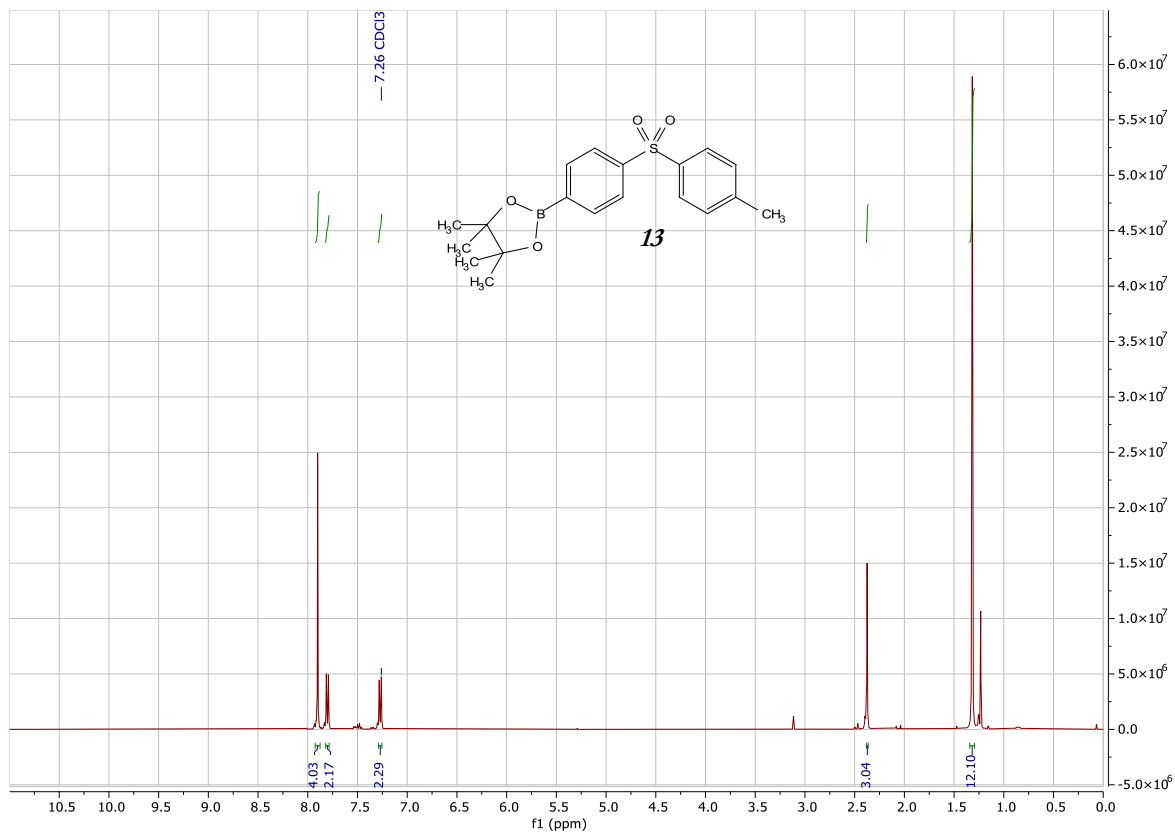




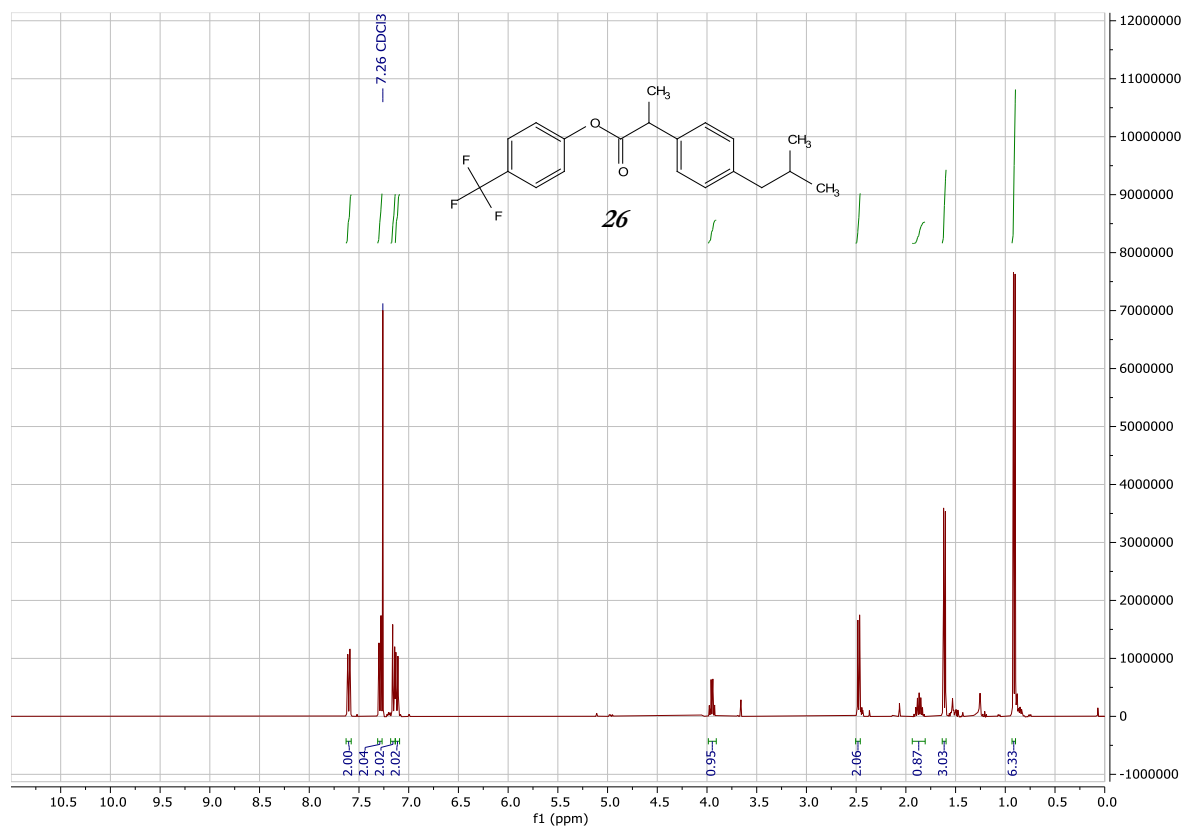
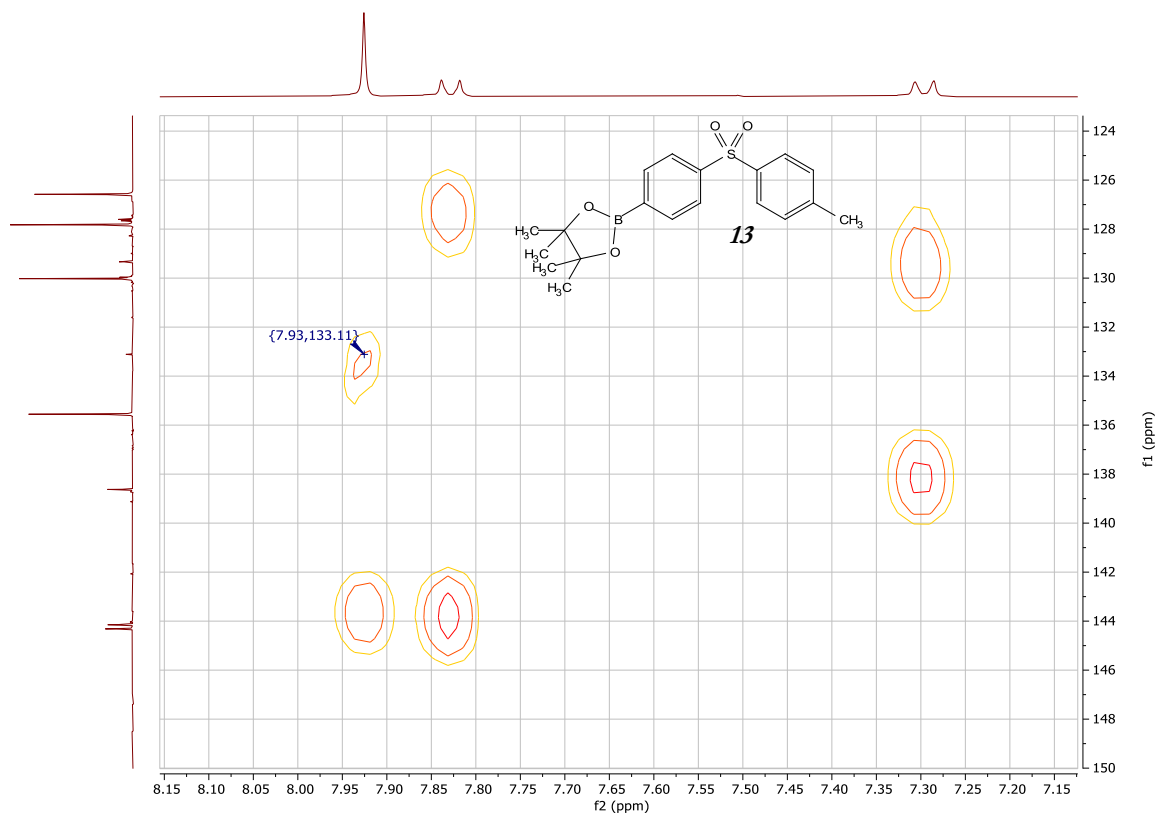


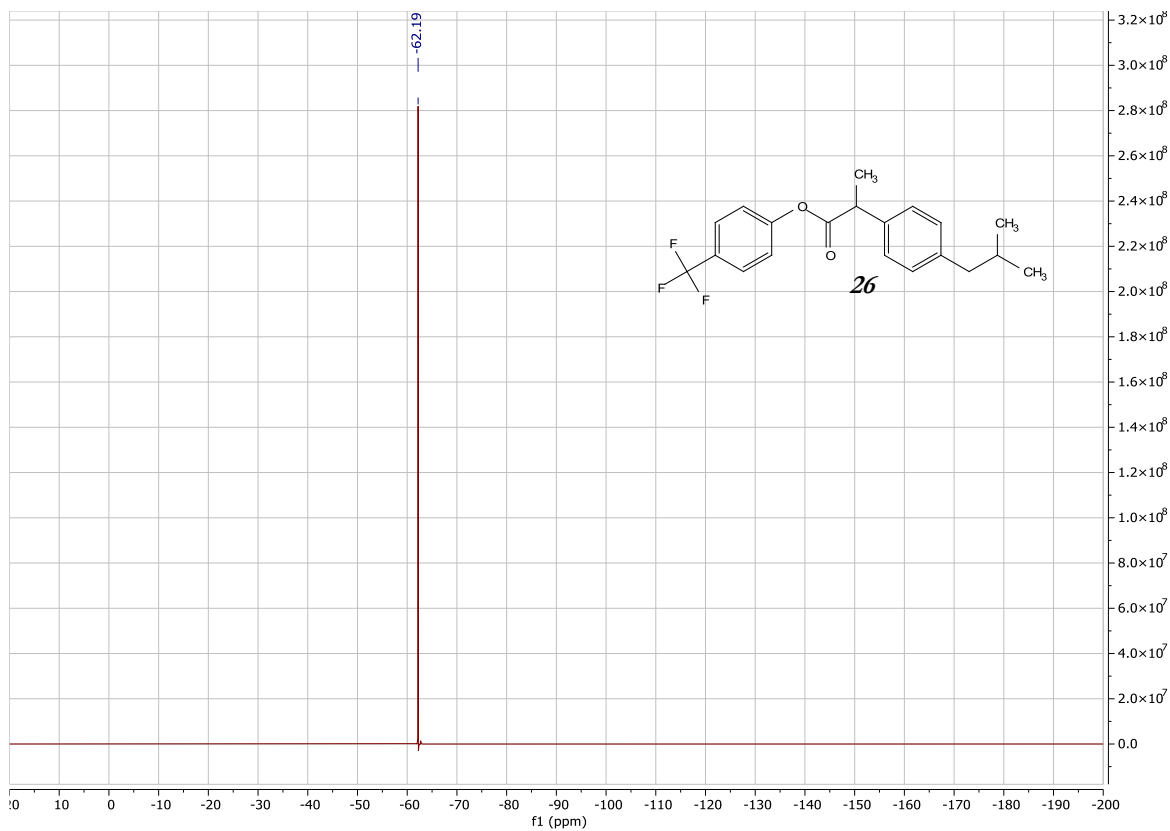
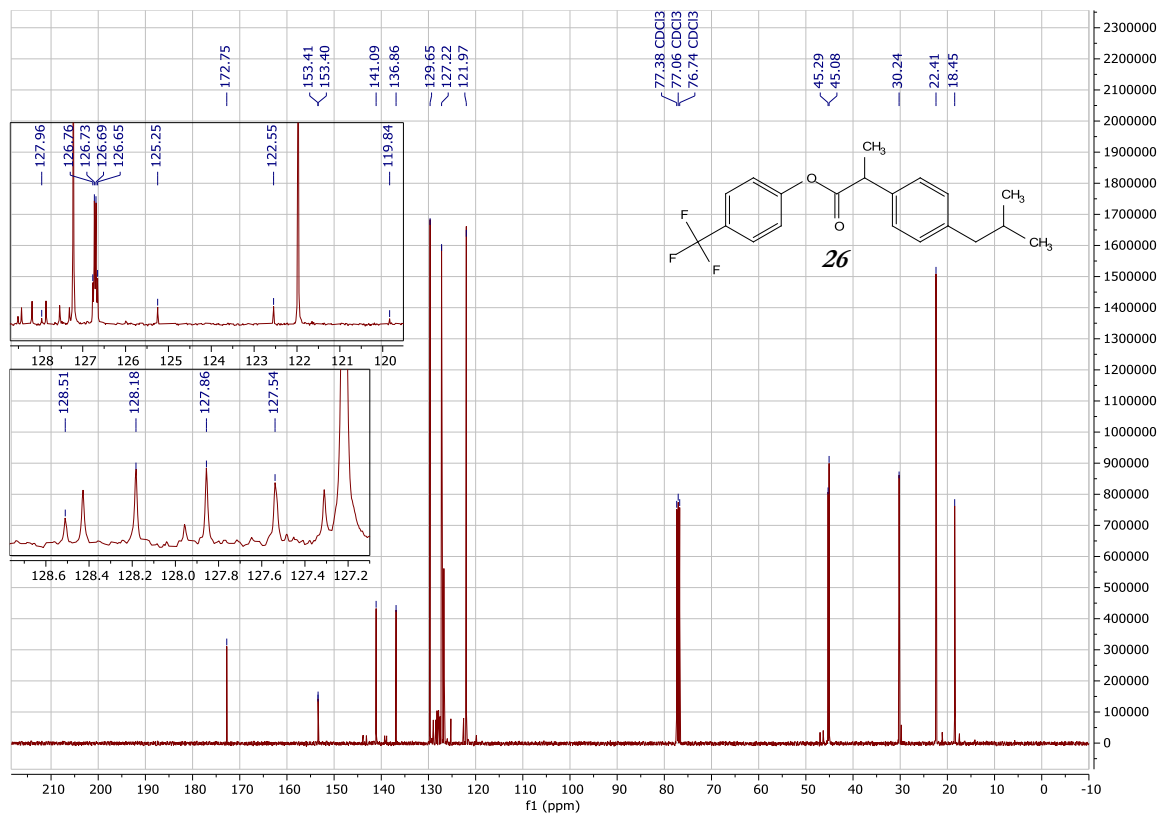


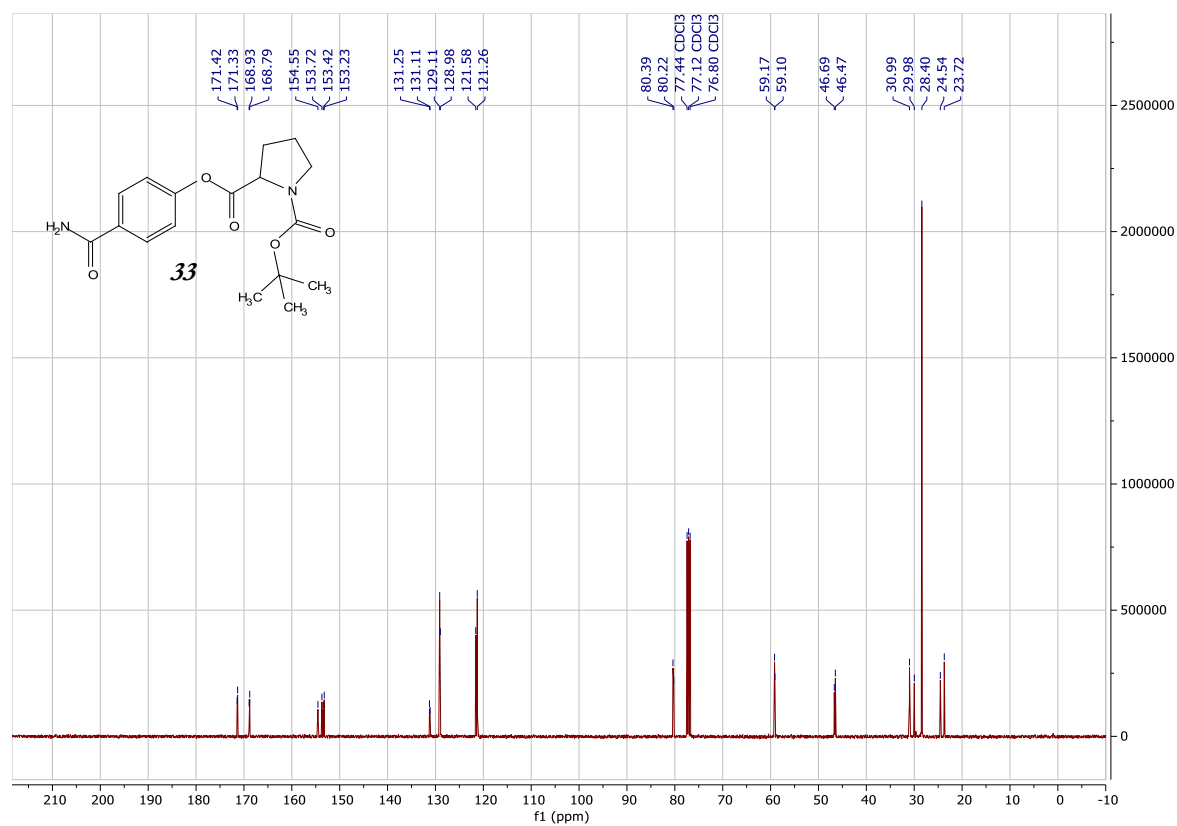
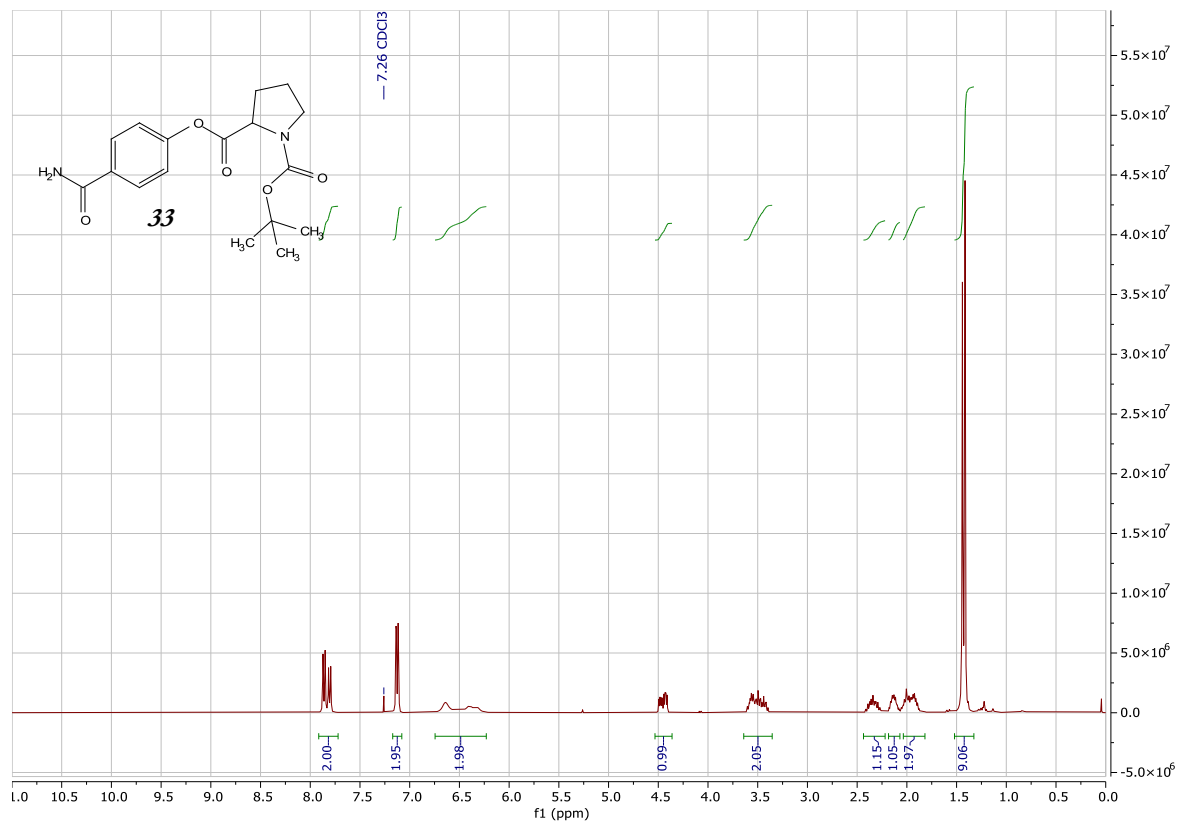


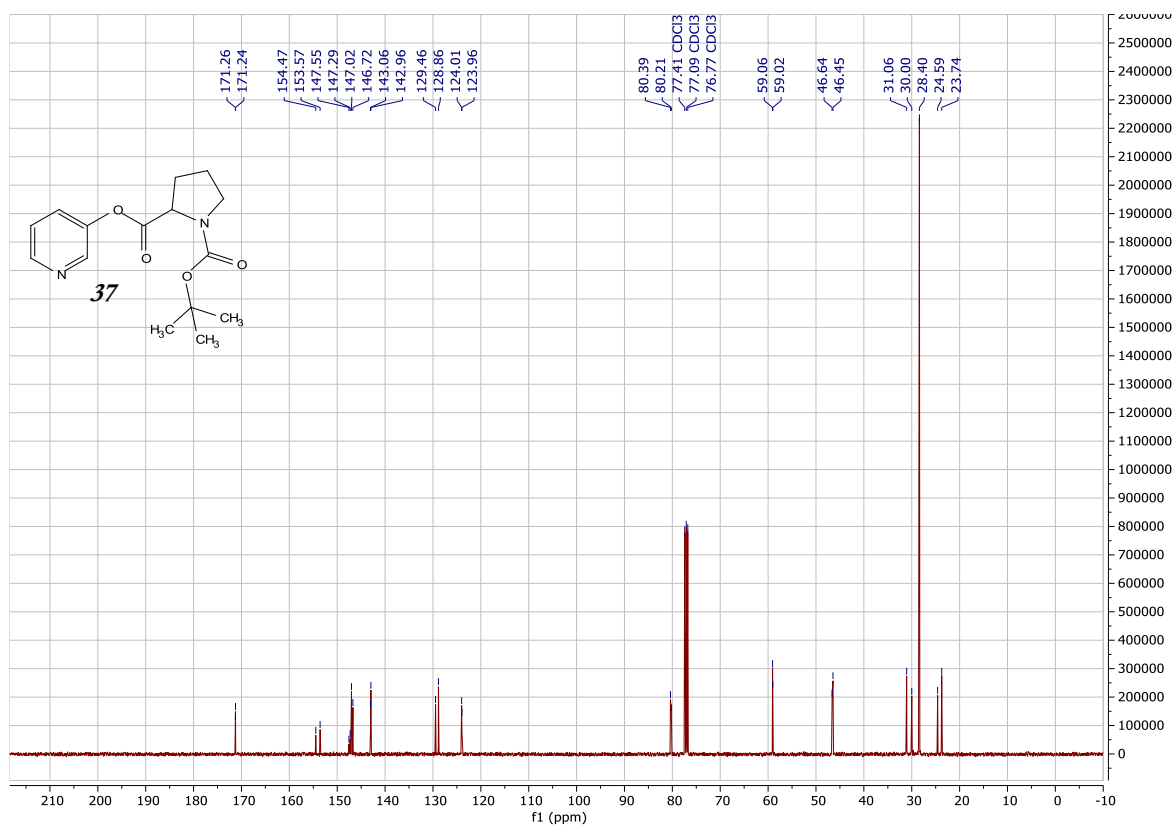
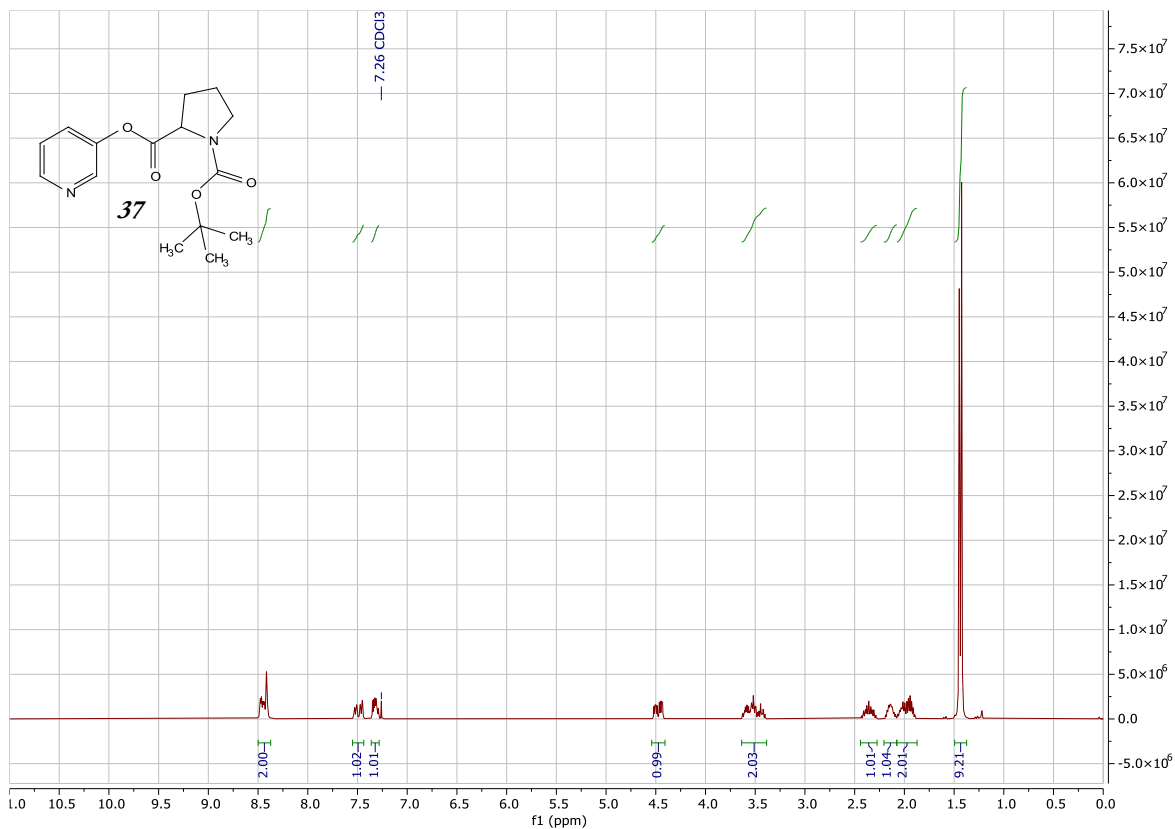


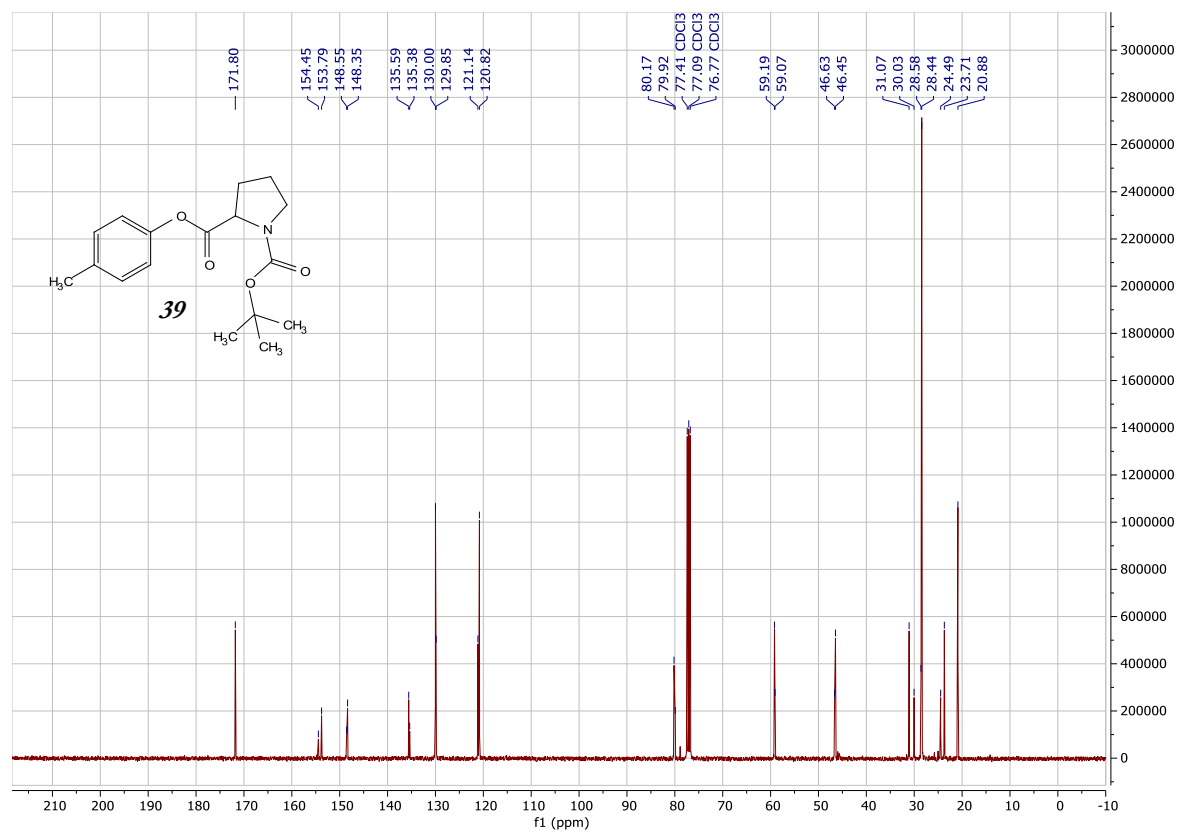
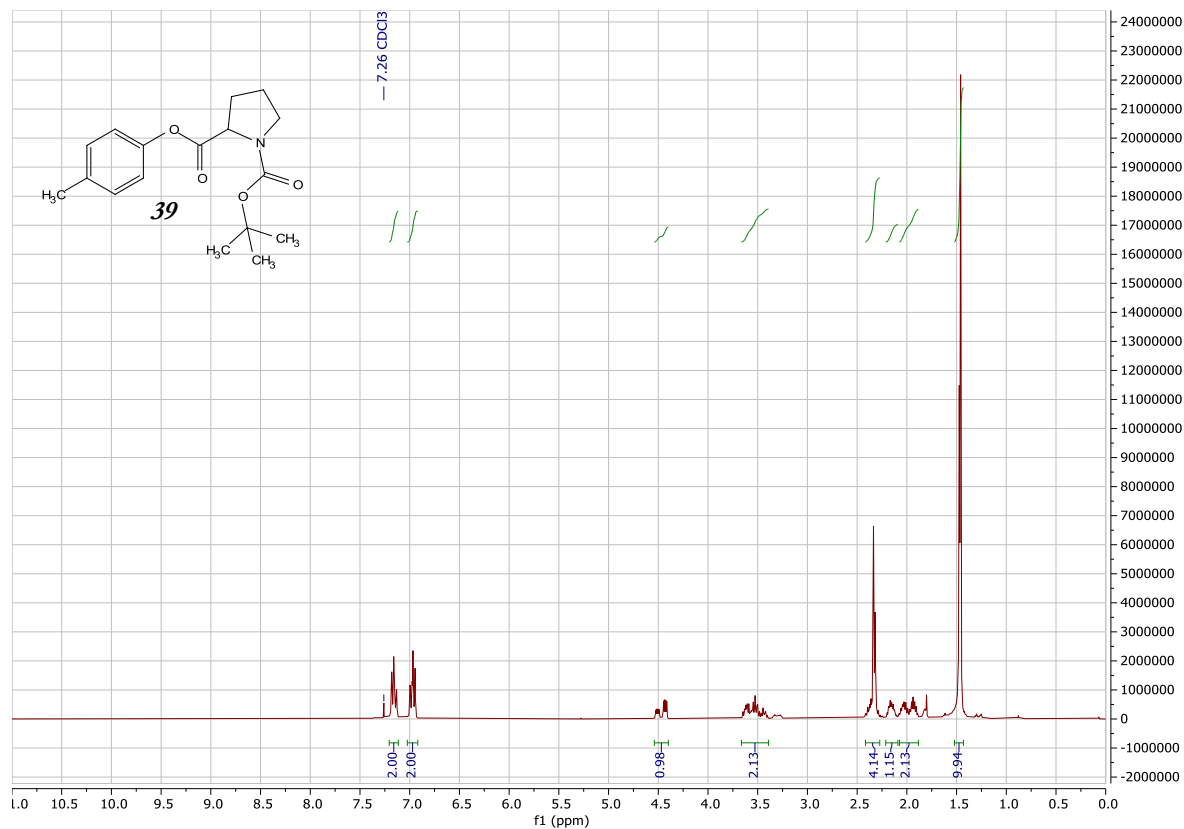
HMBC experiment to assign the C(sp²)-B signal of **13**.

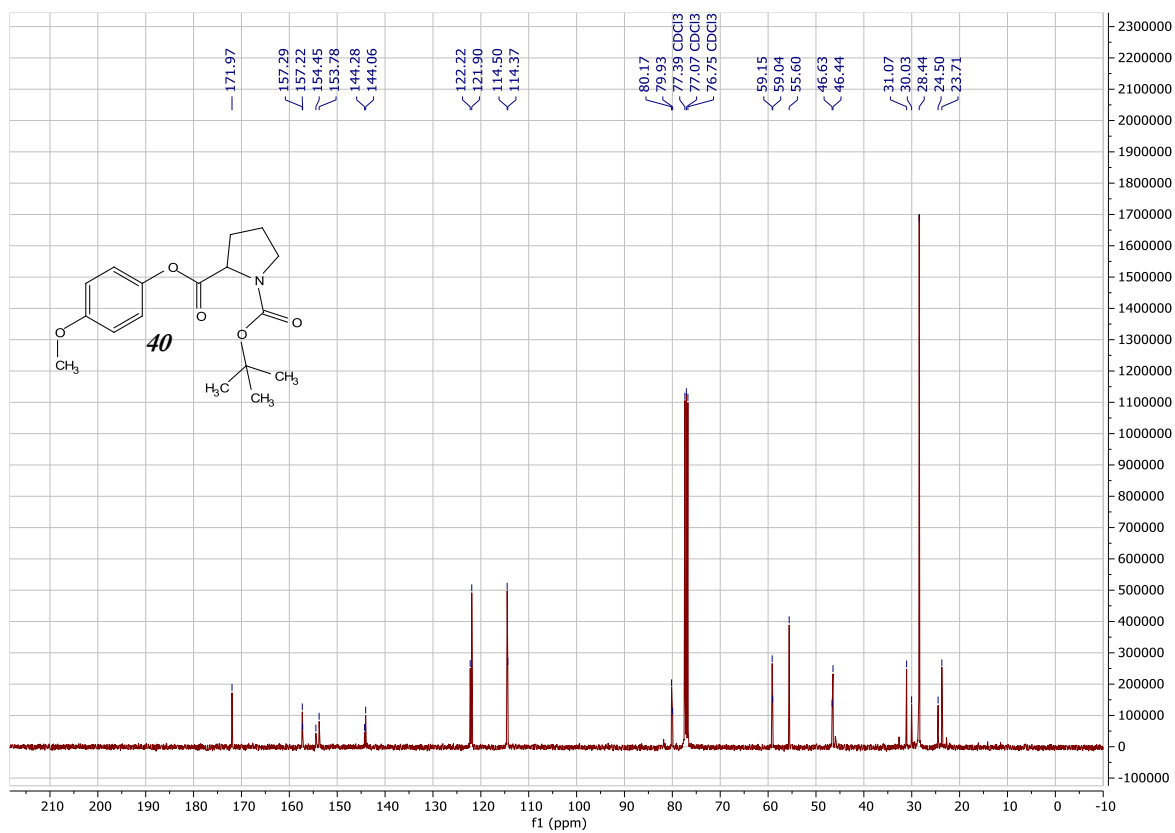
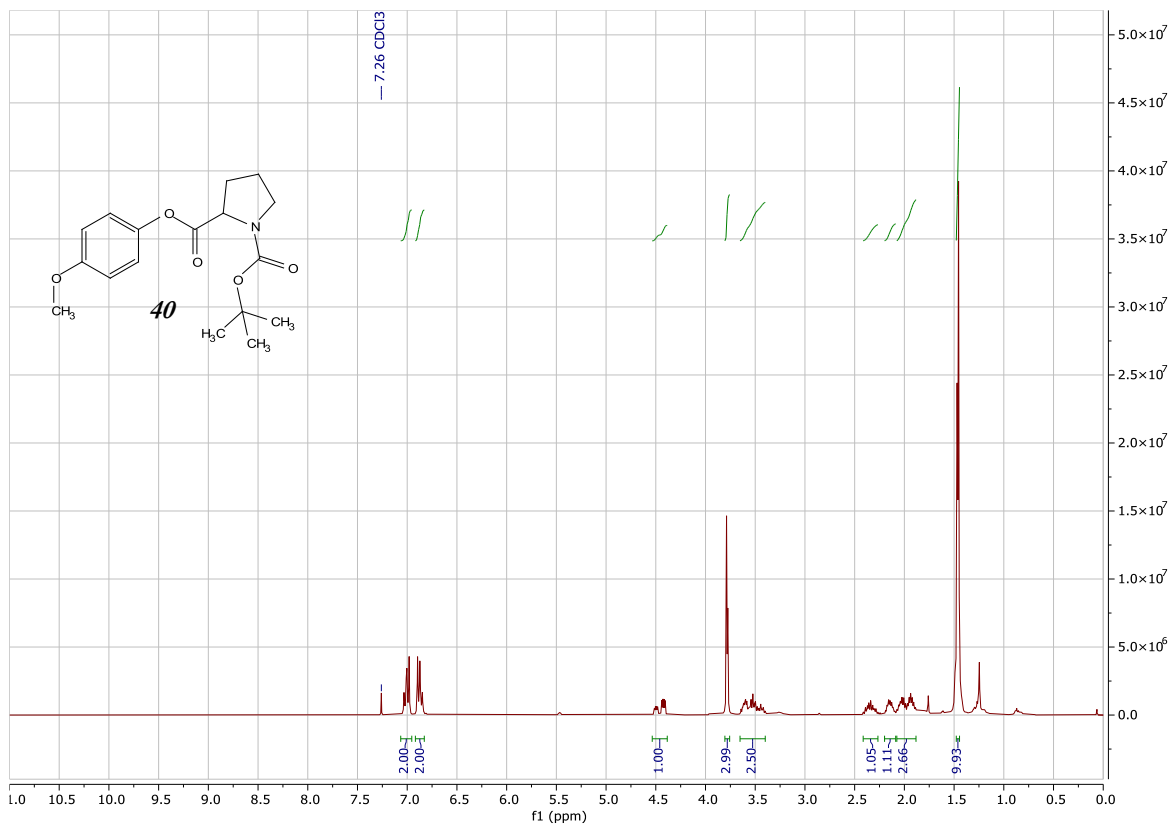


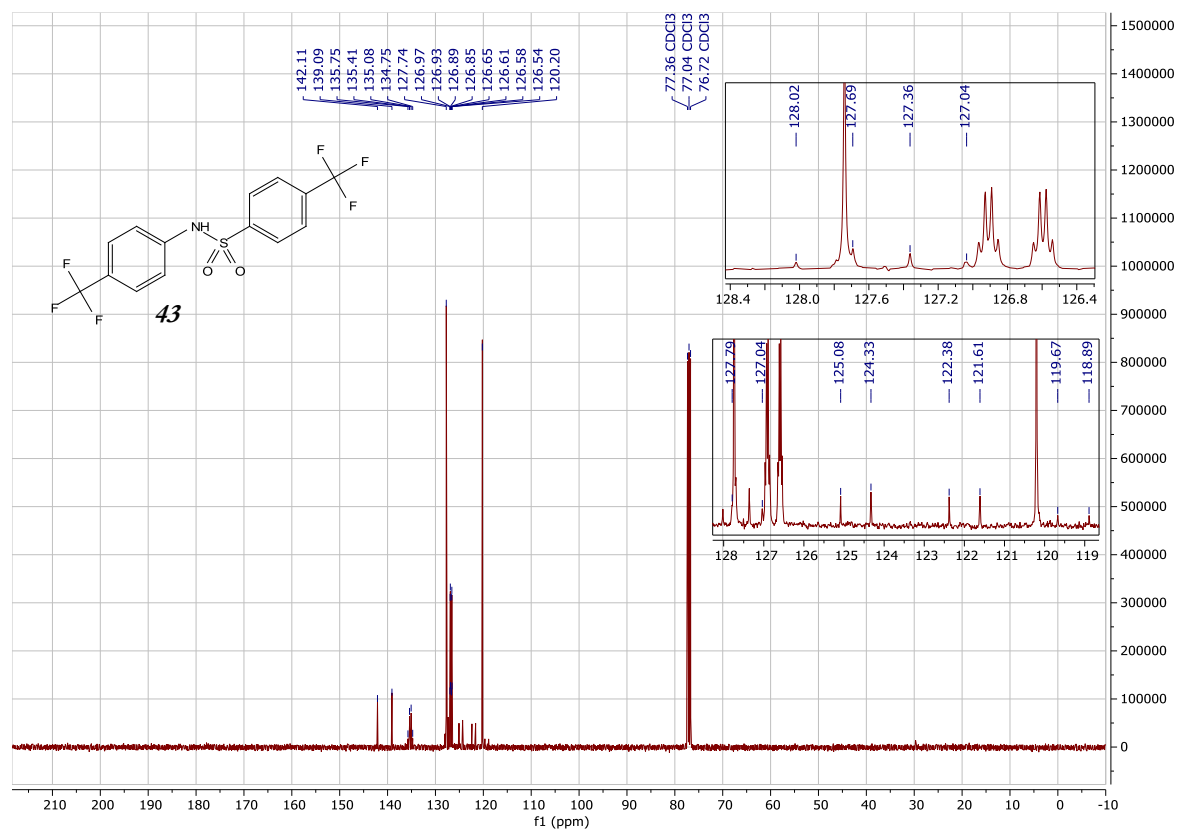
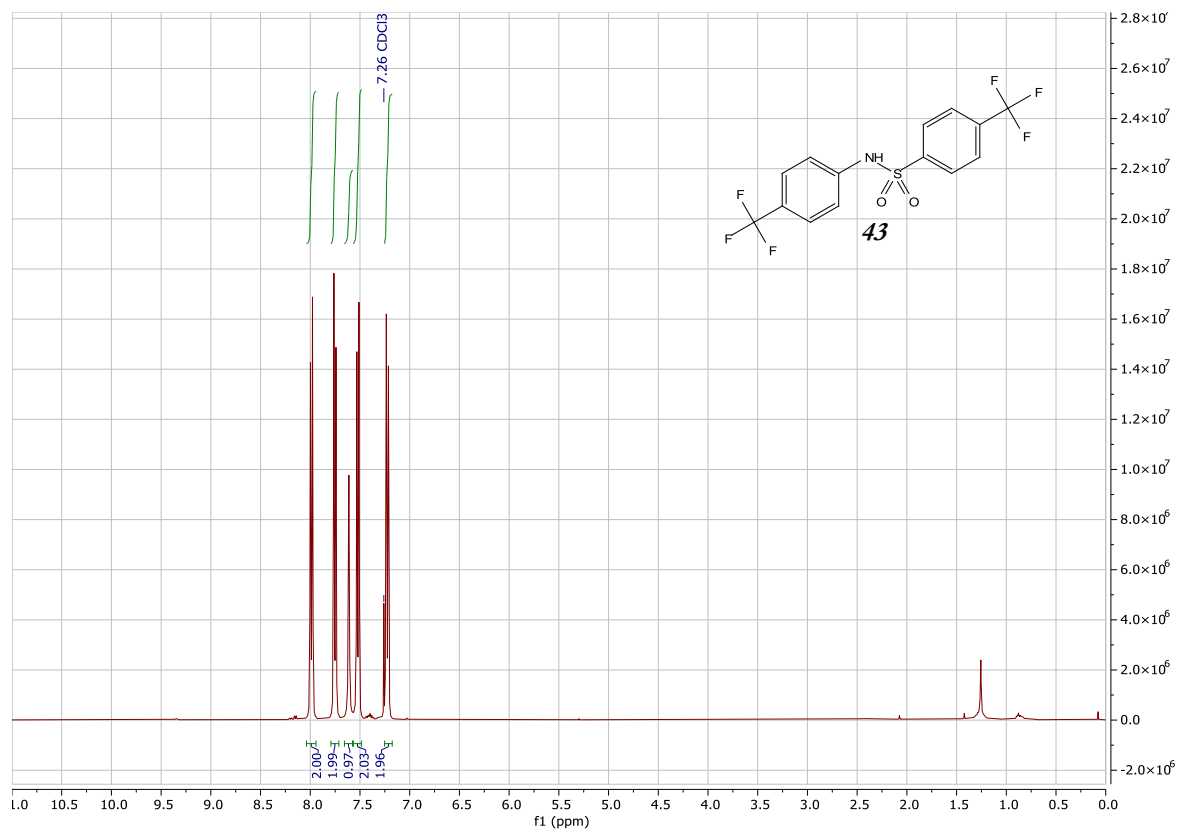


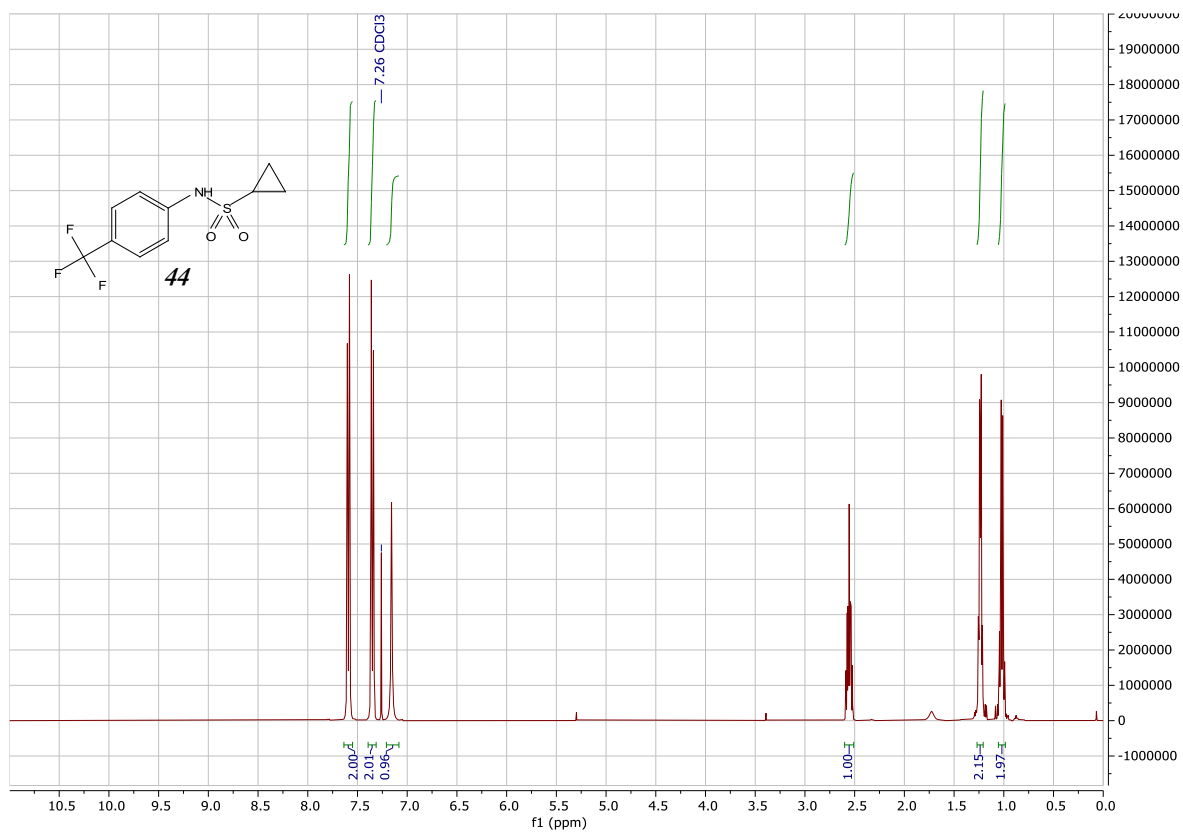
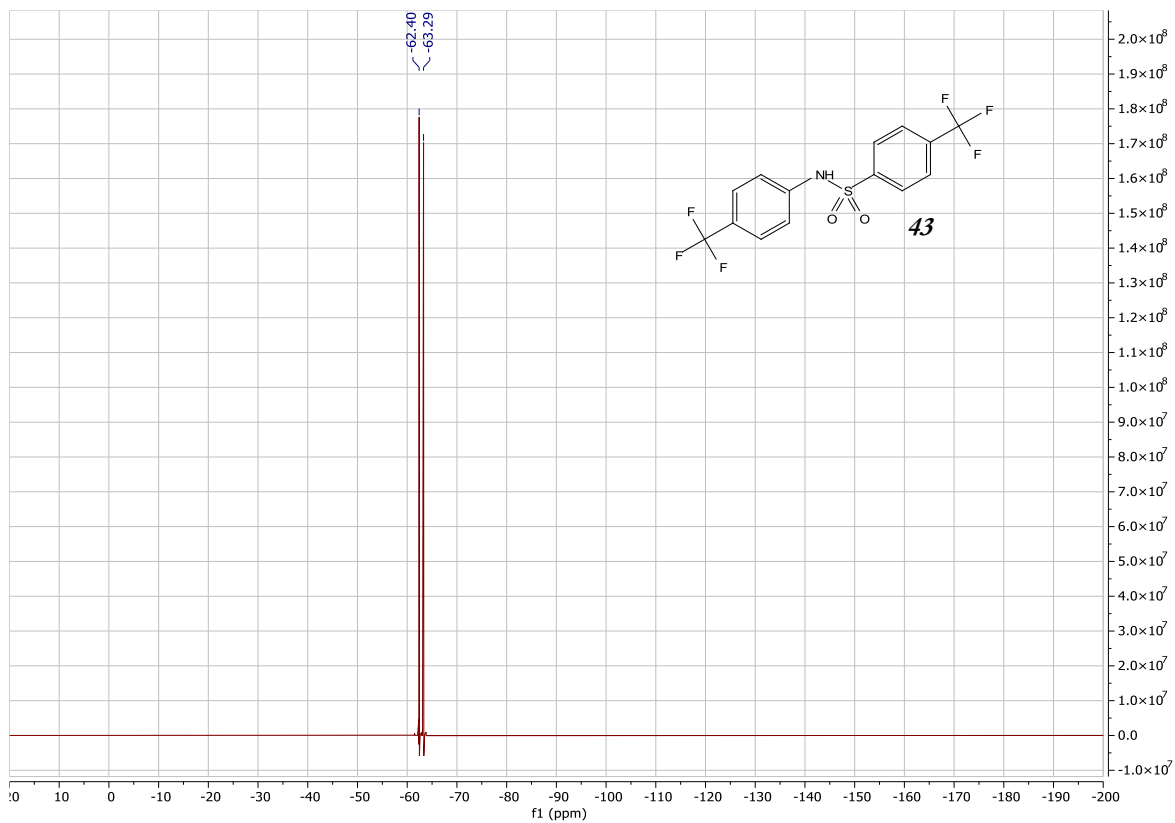


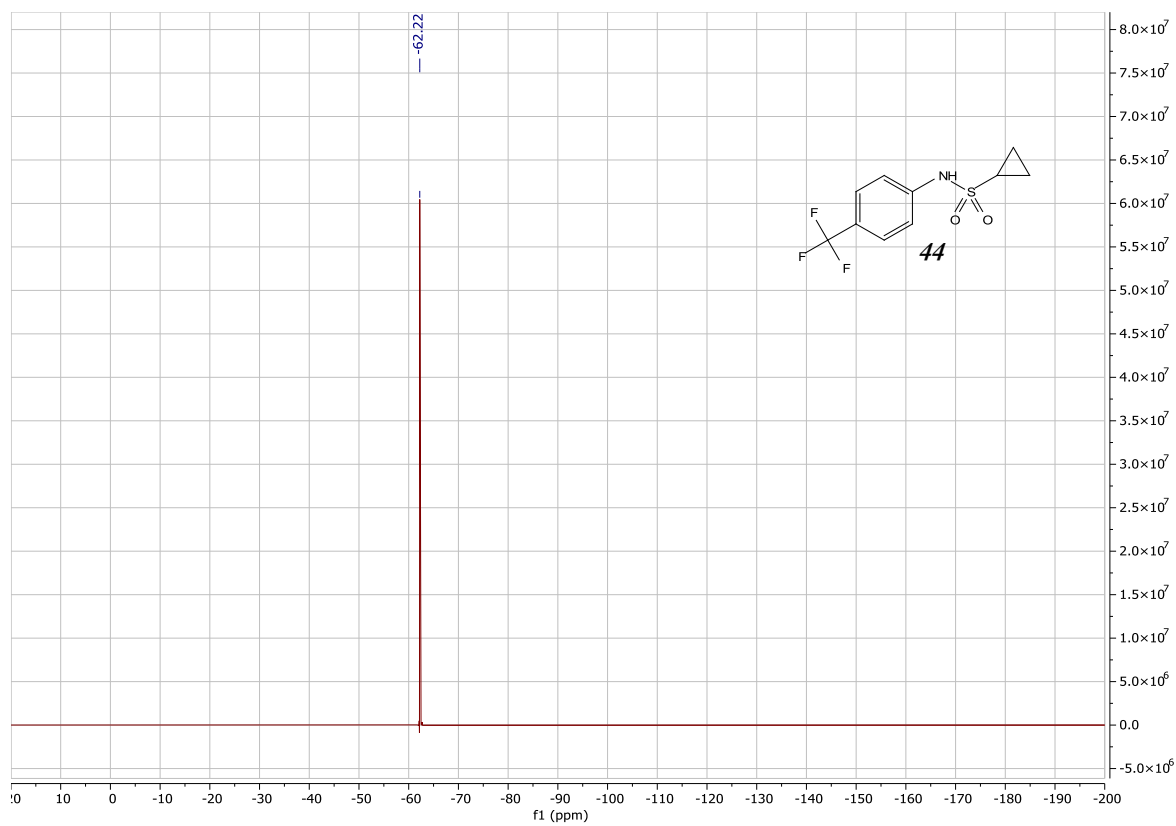
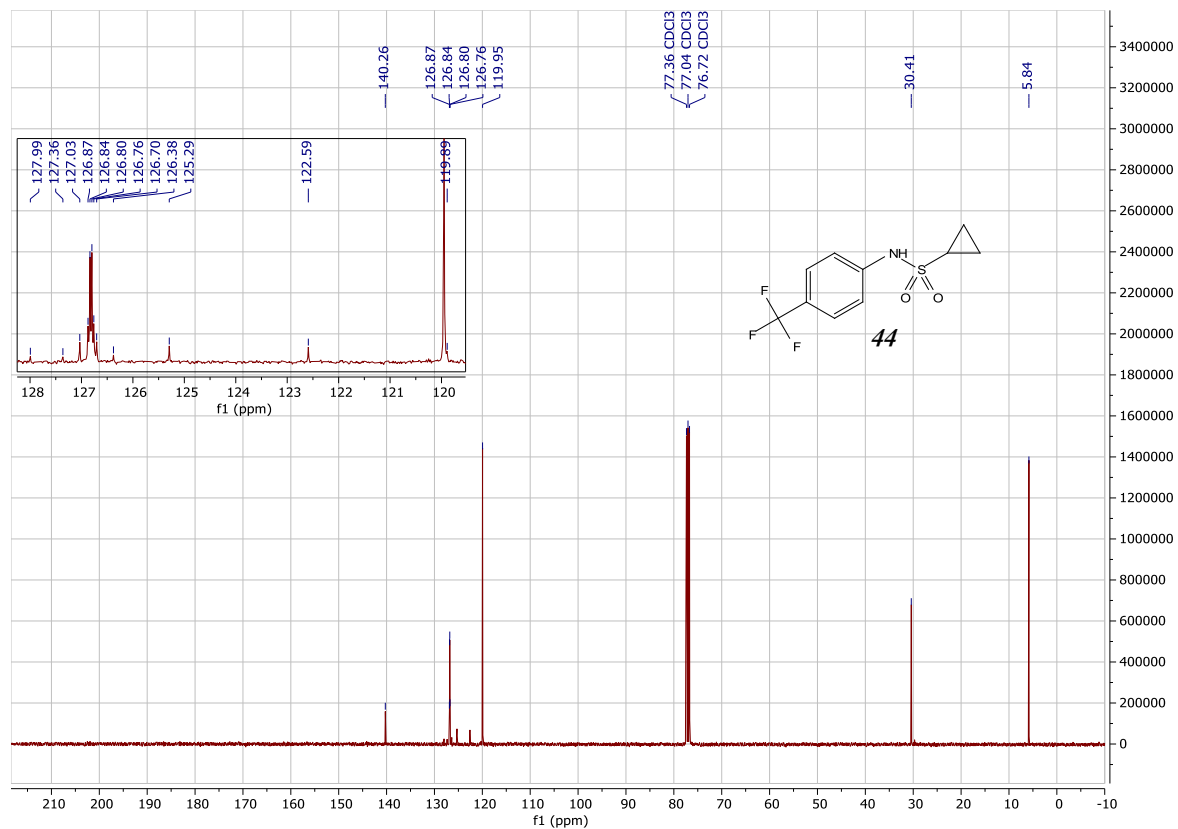


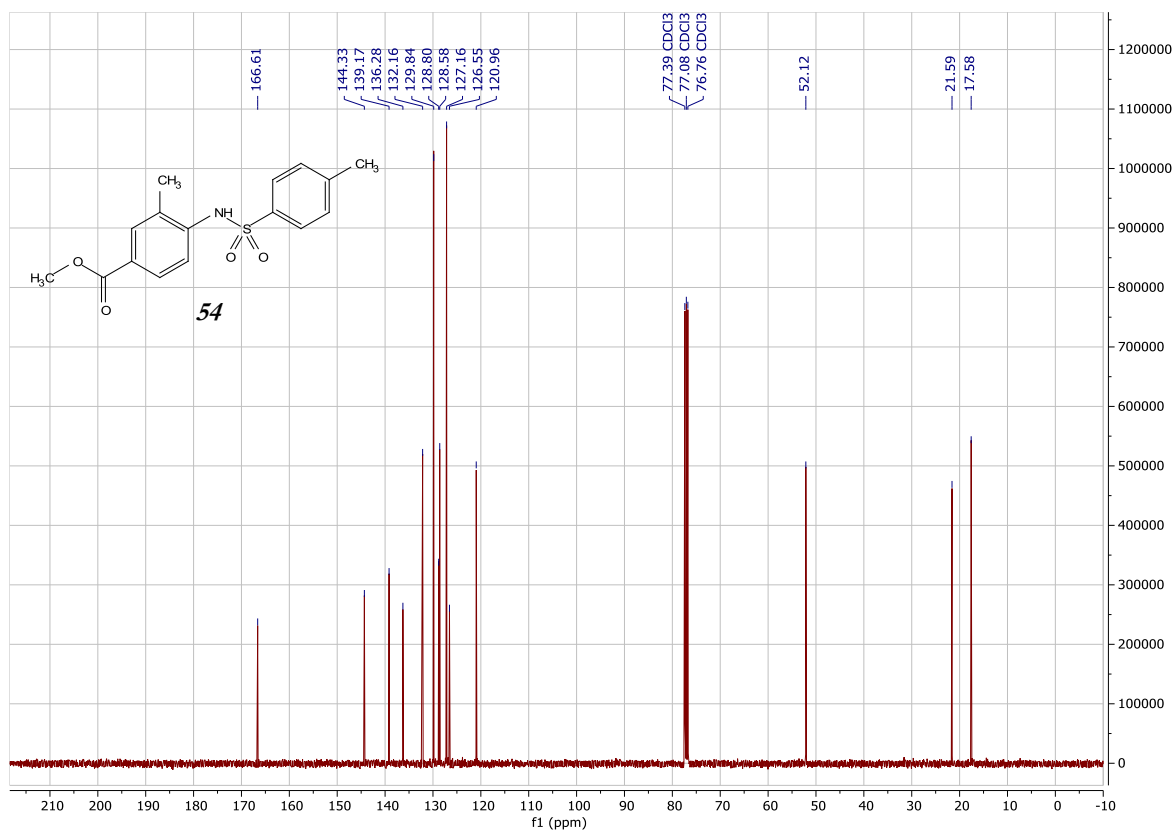
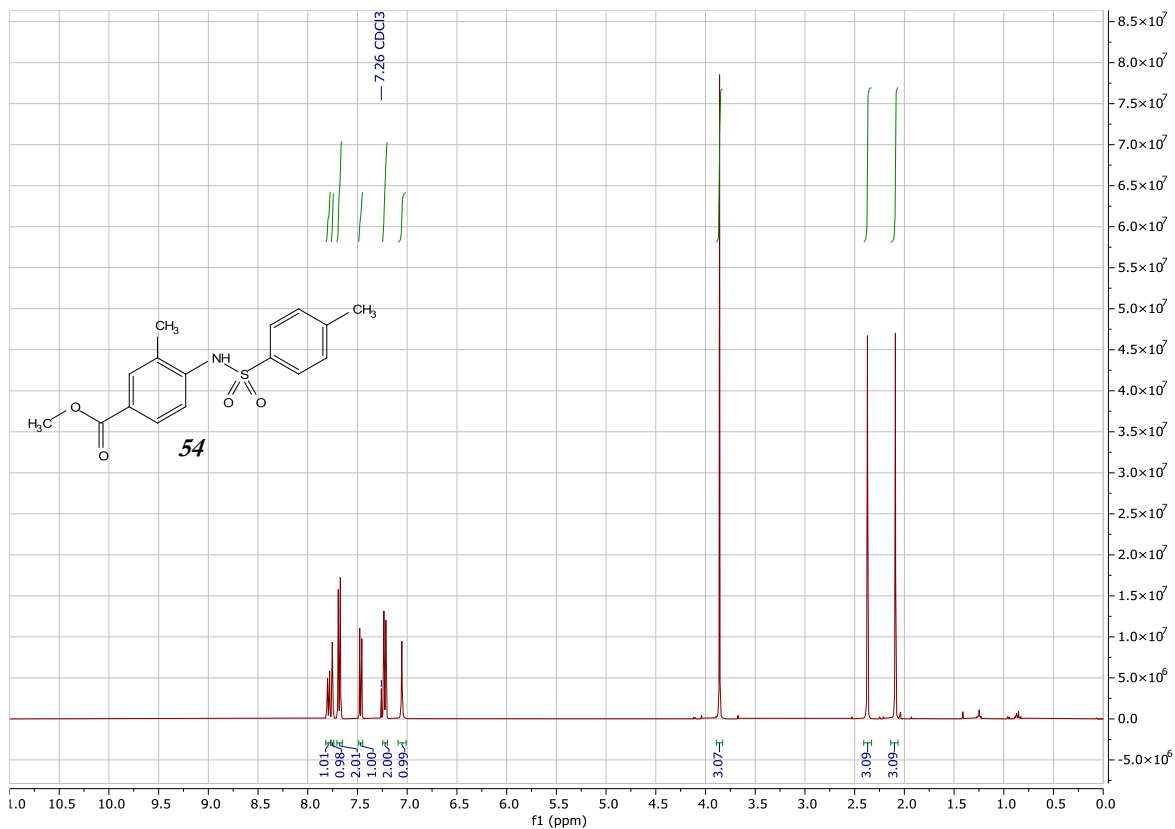












5.7 References

- (1) Kohei, T.; Miyaura, N. Introduction to Cross-Coupling Reactions. In *Cross-Coupling Reactions*, 1st ed.; Miyaura, N., Ed.; Springer: Berlin, 2002; pp 1-9.
- (2) Biffis, A.; Centomo, P.; Del Zotto, A.; Zecca, M. Pd Metal Catalysts for Cross-Couplings and Related Reactions in the 21st Century: A Critical Review. *Chem. Rev.* **2018**, *118*, 2249-2295.
- (3) Ruiz-Castillo, P.; Buchwald, S. L. Applications of Palladium-Catalyzed C–N Cross-Coupling Reactions. *Chem. Rev.* **2016**, *116*, 12564-12649.
- (4) Tasker, S. Z.; Standley, E. A.; Jamison, T. F. Recent advances in homogeneous nickel catalysis. *Nature* **2014**, *509*, 299-309.
- (5) Ananikov, V. P. Nickel: The “Spirited Horse” of Transition Metal Catalysis. *ACS Catal.* **2015**, *5*, 1964-1971.
- (6) Lavoie, C. M.; Stradiotto, M. Bisphosphines: A Prominent Ancillary Ligand Class for Application in Nickel-Catalyzed C–N Cross-Coupling. *ACS Catal.* **2018**, *8*, 7228-7250.
- (7) MacQueen, P. M.; Tassone, J. P.; Diaz, C.; Stradiotto, M. Exploiting Ancillary Ligation To Enable Nickel-Catalyzed C–O Cross-Couplings of Aryl Electrophiles with Aliphatic Alcohols. *J. Am. Chem. Soc.* **2018**, *140*, 5023-5027.
- (8) Twilton, J.; Le, C.; Zhang, P.; Shaw, M. H.; Evans, R. W.; MacMillan, D. W. C. The merger of transition metal and photocatalysis. *Nat. Rev. Chem.* **2017**, *1*, 0052.
- (9) Cavedon, C.; Seeberger, P. H.; Pieber, B. Photochemical Strategies for Carbon–Heteroatom Bond Formation. *Eur. J. Org. Chem.* **2020**, *2020*, 1379-1392.
- (10) Zhu, C.; Yue, H.; Jia, J.; Rueping, M. Nickel-Catalyzed C-Heteroatom Cross-Coupling Reactions under Mild Conditions via Facilitated Reductive Elimination. *Angew. Chem. Int. Ed.* **2020**, doi: 10.1002/anie.202013852,
- (11) Lan, G.; Quan, Y.; Wang, M.; Nash, G. T.; You, E.; Song, Y.; Veroneau, S. S.; Jiang, X.; Lin, W. Metal–Organic Layers as Multifunctional Two-Dimensional Nanomaterials for Enhanced Photoredox Catalysis. *J. Am. Chem. Soc.* **2019**, *141*, 15767-15772.
- (12) Zhu, Y.-Y.; Lan, G.; Fan, Y.; Veroneau, S. S.; Song, Y.; Micheroni, D.; Lin, W. Merging Photoredox and Organometallic Catalysts in a Metal–Organic Framework Significantly Boosts Photocatalytic Activities. *Angew. Chem. Int. Ed.* **2018**, *57*, 14090-14094.
- (13) Pan, Y.; Zhang, N.; Liu, C.-H.; Fan, S.; Guo, S.; Zhang, Z.-M.; Zhu, Y.-Y. Boosting Photocatalytic Activities for Organic Transformations through Merging Photocatalyst and Transition-Metal Catalyst in Flexible Polymers. *ACS Catal.* **2020**, *10*, 11758-11767.

- (14) Reischauer, S.; Strauss, V.; Pieber, B. Modular, Self-Assembling Metallaphotocatalyst for Cross-Couplings Using the Full Visible-Light Spectrum. *ACS Catal.* **2020**, *10*, 13269-13274.
- (15) Vijeta, A.; Casadevall, C.; Roy, S.; Reisner, E. Visible-Light Promoted C–O Bond Formation with an Integrated Carbon Nitride–Nickel Heterogeneous Photocatalyst. *Angew. Chem. Int. Ed.* **2021**, *60*, 8494-8499.
- (16) Zhao, X.; Deng, C.; Meng, D.; Ji, H.; Chen, C.; Song, W.; Zhao, J. Nickel-Coordinated Carbon Nitride as a Metallaphotoredox Platform for the Cross-Coupling of Aryl Halides with Alcohols. *ACS Catal.* **2020**, *10*, 15178-15185.
- (17) Reischauer, S.; Pieber, B. Recyclable, bifunctional metallaphotocatalysts for C-S cross-couplings. *ChemPhotoChem* **2021**, doi: 10.1002/cptc.202100062,
- (18) Qi, Z.-H.; Ma, J. Dual Role of a Photocatalyst: Generation of Ni(0) Catalyst and Promotion of Catalytic C–N Bond Formation. *ACS Catal.* **2018**, *8*, 1456-1463.
- (19) Qin, Y.; Sun, R.; Gianoulis, N. P.; Nocera, D. G. Photoredox Nickel-Catalyzed C–S Cross-Coupling: Mechanism, Kinetics, and Generalization. *J. Am. Chem. Soc.* **2021**, *143*, 2005-2015.
- (20) Till, N. A.; Tian, L.; Dong, Z.; Scholes, G. D.; MacMillan, D. W. C. Mechanistic Analysis of Metallaphotoredox C–N Coupling: Photocatalysis Initiates and Perpetuates Ni(I)/Ni(III) Coupling Activity. *J. Am. Chem. Soc.* **2020**, *142*, 15830-15841.
- (21) Sun, R.; Qin, Y.; Ruccolo, S.; Schnedermann, C.; Costentin, C.; Nocera, D. G. Elucidation of a Redox-Mediated Reaction Cycle for Nickel-Catalyzed Cross Coupling. *J. Am. Chem. Soc.* **2019**, *141*, 89-93.
- (22) Ting, S. I.; Garakyaraghi, S.; Taliaferro, C. M.; Shields, B. J.; Scholes, G. D.; Castellano, F. N.; Doyle, A. G. 3d-d Excited States of Ni(II) Complexes Relevant to Photoredox Catalysis: Spectroscopic Identification and Mechanistic Implications. *J. Am. Chem. Soc.* **2020**, *142*, 5800-5810.
- (23) Shields, B. J.; Kudisch, B.; Scholes, G. D.; Doyle, A. G. Long-Lived Charge-Transfer States of Nickel(II) Aryl Halide Complexes Facilitate Bimolecular Photoinduced Electron Transfer. *J. Am. Chem. Soc.* **2018**, *140*, 3035-3039.
- (24) Li, G.; Yang, L.; Liu, J.-J.; Zhang, W.; Cao, R.; Wang, C.; Zhang, Z.; Xiao, J.; Xue, D. Light-Promoted C–N Coupling of Aryl Halides with Nitroarenes. *Angew. Chem. Int. Ed.* **2021**, *60*, 5230-5234.
- (25) Yang, L.; Lu, H.-H.; Lai, C.-H.; Li, G.; Zhang, W.; Cao, R.; Liu, F.; Wang, C.; Xiao, J.; Xue, D. Light-Promoted Nickel Catalysis: Etherification of Aryl Electrophiles with Alcohols Catalyzed by a NiII-Aryl Complex. *Angew. Chem. Int. Ed.* **2020**, *59*, 12714-12719.

- (26) Sun, R.; Qin, Y.; Nocera, D. G. General Paradigm in Photoredox Nickel-Catalyzed Cross-Coupling Allows for Light-Free Access to Reactivity. *Angew. Chem. Int. Ed.* **2020**, *59*, 9527-9533.
- (27) Liang, H.-P.; Achariya, A.; Anito, D. A.; Vogl, S.; Wang, T.-X.; Thomas, A.; Han, B.-H. Rhenium-Metalated Polypyridine-Based Porous Polycarbazoles for Visible-Light CO₂ Photoreduction. *ACS Catal.* **2019**, *9*, 3959-3968.
- (28) The same strategy was not suitable for the coupling of aryl halides with amines, thiols or alcohols that were reported instead under dual nickel/photocatalytic catalysis in Ref. 45 and Ref. 48.
- (29) Tellis, J. C.; Primer, D. N.; Molander, G. A. Single-electron transmetalation in organoboron cross-coupling by photoredox/nickel dual catalysis. *Science* **2014**, *345*, 433-436.
- (30) Remeur, C.; Kelly, C. B.; Patel, N. R.; Molander, G. A. Aminomethylation of Aryl Halides Using α -Silylamines Enabled by Ni/Photoredox Dual Catalysis. *ACS Catal.* **2017**, *7*, 6065-6069.
- (31) Yue, H.; Zhu, C.; Rueping, M. Cross-Coupling of Sodium Sulfinates with Aryl, Heteroaryl, and Vinyl Halides by Nickel/Photoredox Dual Catalysis. *Angew. Chem. Int. Ed.* **2018**, *57*, 1371-1375.
- (32) Cabrera-Afonso, M. J.; Lu, Z.-P.; Kelly, C. B.; Lang, S. B.; Dykstra, R.; Gutierrez, O.; Molander, G. A. Engaging sulfinate salts via Ni/photoredox dual catalysis enables facile Csp²-SO₂R coupling. *Chem. Sci.* **2018**, *9*, 3186-3191.
- (33) Liu, N.-W.; Hofman, K.; Herbert, A.; Manolikakes, G. Visible-Light Photoredox/Nickel Dual Catalysis for the Cross-Coupling of Sulfinic Acid Salts with Aryl Iodides. *Org. Lett.* **2018**, *20*, 760-763.
- (34) Chen, L.; Liang, J.; Chen, Z.-y.; Chen, J.; Yan, M.; Zhang, X.-j. A Convenient Synthesis of Sulfones via Light Promoted Coupling of Sodium Sulfinates and Aryl Halides. *Adv. Synth. Catal.* **2019**, *361*, 956-960.
- (35) Malik, J. A.; Madani, A.; Pieber, B.; Seeberger, P. H. Evidence for Photocatalyst Involvement in Oxidative Additions of Nickel-Catalyzed Carboxylate O-Arylations. *J. Am. Chem. Soc.* **2020**, *142*, 11042-11049.
- (36) Wong, Y.-S.; Tang, M.-C.; Ng, M.; Yam, V. W.-W. Toward the Design of Phosphorescent Emitters of Cyclometalated Earth-Abundant Nickel(II) and Their Supramolecular Study. *J. Am. Chem. Soc.* **2020**, *142*, 7638-7646.
- (37) Alrefai, R.; Hörner, G.; Schubert, H.; Berkefeld, A. Broadly versus Barely Variable Complex Chromophores of Planar Nickel(II) from κ^3 -N,N',C and κ^3 -N,N',O Donor Platforms. *Organometallics* **2021**, *40*, 1163-1177.

- (38) Pieber, B.; Malik, J. A.; Cavedon, C.; Gisbertz, S.; Savateev, A.; Cruz, D.; Heil, T.; Zhang, G.; Seeberger, P. H. Semi-heterogeneous Dual Nickel/Photocatalysis using Carbon Nitrides: Esterification of Carboxylic Acids with Aryl Halides. *Angew. Chem. Int. Ed.* **2019**, *58*, 9575-9580.
- (39) Welin, E. R.; Le, C.; Arias-Rotondo, D. M.; McCusker, J. K.; MacMillan, D. W. C. Photosensitized, energy transfer-mediated organometallic catalysis through electronically excited nickel(II). *Science* **2017**, *355*, 380-385.
- (40) Kim, T.; McCarver, S. J.; Lee, C.; MacMillan, D. W. C. Sulfonamidation of Aryl and Heteroaryl Halides through Photosensitized Nickel Catalysis. *Angew. Chem. Int. Ed.* **2018**, *57*, 3488-3492.
- (41) Gisbertz, S.; Pieber, B. Heterogeneous Photocatalysis in Organic Synthesis. *ChemPhotoChem* **2020**, *4*, 456-475.
- (42) Kim, W.; Kim, H. Y.; Oh, K. Electrochemical Radical–Radical Cross-Coupling Approach between Sodium Sulfinates and 2H-Indazoles to 3-Sulfonylated 2H-Indazoles. *Org. Lett.* **2020**, *22*, 6319-6323.
- (43) <https://www.kessil.com/photoreaction/PR160L.php> (Germany, May 2021).
- (44) Li, H.-Y.; Wu, J.; Zhou, X.-H.; Kang, L.-C.; Li, D.-P.; Sui, Y.; Zhou, Y.-H.; Zheng, Y.-X.; Zuo, J.-L.; You, X.-Z. Synthesis, structural characterization and photoluminescence properties of rhenium(I) complexes based on bipyridine derivatives with carbazole moieties. *Dalton Tran.* **2009**, 10563-10569.
- (45) Gisbertz, S.; Reischauer, S.; Pieber, B. Overcoming limitations in dual photoredox/nickel-catalysed C–N cross-couplings due to catalyst deactivation. *Nat. Catal.* **2020**, *3*, 611-620.
- (46) Corcoran, E. B.; Pirnot, M. T.; Lin, S.; Dreher, S. D.; DiRocco, D. A.; Davies, I. W.; Buchwald, S. L.; MacMillan, D. W. C. Aryl amination using ligand-free Ni(II) salts and photoredox catalysis. *Science* **2016**, *353*, 279-283.
- (47) Terrett, J. A.; Cuthbertson, J. D.; Shurtleff, V. W.; MacMillan, D. W. C. Switching on elusive organometallic mechanisms with photoredox catalysis. *Nature* **2015**, *524*, 330-334.
- (48) Cavedon, C.; Madani, A.; Seeberger, P. H.; Pieber, B. Semiheterogeneous Dual Nickel/Photocatalytic (Thio)etherification Using Carbon Nitrides. *Org. Lett.* **2019**, *21*, 5331-5334.
- (49) Yang, X.; Shi, L.; Fu, H. Copper-Mediated Cascade Synthesis of Diaryl Sulfones via the Sandmeyer Reaction. *Synlett* **2014**, *25*, 847-852.

- (50) Phanindrudu, M.; Jaya, P.; Likhar, P. R.; Tiwari, D. K. Nano copper catalyzed synthesis of symmetrical/unsymmetrical sulfones from aryl/alkyl halides and p-toluenesulfonylmethylisocyanide: TosMIC as a tosyl source. *Tetrahedron* **2020**, *76*, 131263.
- (51) Nguyen, V. D.; Nguyen, V. T.; Haug, G. C.; Dang, H. T.; Arman, H. D.; Ermler, W. C.; Larionov, O. V. Rapid and Chemodivergent Synthesis of N-Heterocyclic Sulfones and Sulfides: Mechanistic and Computational Details of the Persulfate-Initiated Catalysis. *ACS Catal.* **2019**, *9*, 4015-4024.
- (52) Cacchi, S.; Fabrizi, G.; Goggiamani, A.; Parisi, L. M. Unsymmetrical Diaryl Sulfones through Palladium-Catalyzed Coupling of Aryl Iodides and Arenesulfinates. *Org. Lett.* **2002**, *4*, 4719-4721.
- (53) Lu, J.; Pattengale, B.; Liu, Q.; Yang, S.; Shi, W.; Li, S.; Huang, J.; Zhang, J. Donor–Acceptor Fluorophores for Energy-Transfer-Mediated Photocatalysis. *J. Am. Chem. Soc.* **2018**, *140*, 13719-13725.
- (54) Meng, J.-J.; Gao, M.; Wei, Y.-P.; Zhang, W.-Q. N-Heterocyclic Carbene-Catalyzed Aerobic Oxidative Direct Esterification of Aldehydes with Organoboronic Acids. *Chem. Asian J.* **2012**, *7*, 872-875.
- (55) Ackerman, L. K. G.; Martinez Alvarado, J. I.; Doyle, A. G. Direct C–C Bond Formation from Alkanes Using Ni-Photoredox Catalysis. *J. Am. Chem. Soc.* **2018**, *140*, 14059-14063.
- (56) Ye, F.; Berger, F.; Jia, H.; Ford, J.; Wortman, A.; Börgel, J.; Genicot, C.; Ritter, T. Aryl Sulfonium Salts for Site-Selective Late-Stage Trifluoromethylation. *Angew. Chem. Int. Ed.* **2019**, *58*, 14615-14619.
- (57) Meyer, D.; Jangra, H.; Walther, F.; Zipse, H.; Renaud, P. A third generation of radical fluorinating agents based on N-fluoro-N-arylsulfonamides. *Nat. Commun.* **2018**, *9*, 4888.
- (58) Thiam, A.; Iojoiu, C.; Leprêtre, J. C.; Sanchez, J. Y. Lithium salts based on a series of new aniliny-perfluorosulfonamide salts and their polymer electrolytes. *J. Power Sources* **2017**, *364*, 138-147.
- (59) Zhang, W.; Xie, J.; Rao, B.; Luo, M. Iron-Catalyzed N-Arylsulfonamide Formation through Directly Using Nitroarenes as Nitrogen Sources. *J. Org. Chem.* **2015**, *80*, 3504-3511.
- (60) Zhao, F.; Li, B.; Huang, H.; Deng, G.-J. Palladium-catalyzed N-arylsulfonamide formation from arylsulfonyl hydrazides and nitroarenes. *RSC Adv.* **2016**, *6*, 13010-13013.
- (61) Michaelidou, S. S.; Koutentis, P. A. Detosylation of 3-amino-1-tosylindole-2-carbonitriles using DBU and thiophenol. *Tetrahedron* **2010**, *66*, 3016-3023.

Chapter 5

(62) Zhang, K.; Zhang, Y.; Liu, Q.; He, D.; Tian, J.; Zhou, H. Metal-Free One-Pot Synthesis of Sulfonamides from Nitroarenes and Arylsulfonyl Chlorides in Water. *ChemistrySelect* **2019**, *4*, 7413-7415.

(63) Nitelet, A.; Thevenet, D.; Schiavi, B.; Hardouin, C.; Fournier, J.; Tamion, R.; Pannecoucke, X.; Jubault, P.; Poisson, T. Copper-Photocatalyzed Borylation of Organic Halides under Batch and Continuous-Flow Conditions. *Chem. Eur. J.* **2019**, *25*, 3262-3266.

(64) Bordi, S.; Starr, J. T. Hydroxyarylation of Olefins by Intramolecular Minisci Reaction. *Org. Lett.* **2017**, *19*, 2290-2293.

(65) Fu, Y.; Li, Q.-Z.; Xu, Q.-S.; Hugel, H.; Li, M.-P.; Du, Z. NaI-Catalyzed Oxidative Amination of Aromatic Sodium Sulfinates: Synergetic Effect of Ethylene Dibromide and Air as Oxidants. *Eur. J. Org. Chem.* **2018**, *2018*, 6966-6970.

Chapter 6

Visible light-mediated oxidative debenylation enables the use of benzyl ethers as temporary protecting groups

Cavedon, C.; Sletten, E. T.; Madani, A.; Niemeyer, O.; Seeberger, P. H.; Pieber, B. Visible-Light-Mediated Oxidative Debenzylation Enables the Use of Benzyl Ethers as Temporary Protecting Groups *Org. Lett.* **2021**, *23*, 514-518.

<https://doi.org/10.1021/acs.orglett.0c04026>

Specific contribution

Dr. B. Pieber and I conceived the idea behind the project. I verified its feasibility, optimized the reaction protocols and evaluated their scope and limitations. Dr. E. Sletten and I implemented a continuous flow setup to study the reaction. A. Madani and I studied the reaction using illumination NMR spectroscopy. I wrote the first draft of the manuscript.

Dr. E. Sletten synthesized starting materials that were not commercially available.

O. Niemeyer built the illumination NMR device.

Dr. E. Sletten, Dr. B. Pieber and Prof. P. H. Seeberger revised and corrected the manuscript.

Chapter 7

Discussion of individual works

7.1 Photochemical strategies for carbon–heteroatom bond formation

Chapter 2 consists of the work “Photochemical Strategies for Carbon-Heteroatom Bond Formation” published as a minireview in the European Journal of Organic Chemistry. Selected synthetic methodologies are discussed on the basis of the underlying mechanistic proposal. Organic chemistry has a long-standing interest in photochemistry and in investigating how the reactivity of chromophores in their excited states differs from the ground state.

At the end of the 1990s, the growing interest in sustainability and green chemistry¹ led to a renaissance of photochemistry as a means to enable new reactivities and harness abundant sunlight energy rather than heat to promote reactions. In particular, visible-light photocatalysis became a valuable alternative to stoichiometric reagents and harsh reaction conditions. Different approaches exist to form a bond between carbon and nitrogen, oxygen, sulfur or phosphor. These rely on the use of a photocatalyst (PC), alone or in combination with a nickel catalyst, or in specific cases even in the absence of a PC.

Selecting the best photocatalytic methodology to the synthesis of a specific target usually requires evaluation of parameters such as functional group compatibility, redox potential of the PC and optical properties of the coupling partners. This literature survey guides the reader through those methodologies and evaluates these parameters.

The specific criteria used to select the literature were defined on the following considerations:

i) Light irradiation is responsible for the reaction. Whether the photocatalyst activates reagents or a second catalyst, the reaction must be light-mediated and present improved selectivity, alternative reaction pathways or milder conditions compared to thermally driven reactions. Section 2.4 presents the photoactivation of coupling partners through the formation of EDA complexes or reaction intermediates that absorb light. The use of light to activate stoichiometric amounts of mediators was not discussed as these are less sustainable and less valuable strategies.

ii) Product formation results from cross-coupling of two distinct fragments. Many photocatalytic reactions were developed during the last two decades, in which the formation of radicals enables cyclizations, Giese-type reactions and polymerizations. My literature survey focuses on cross-coupling reactions, because of their high potential in organic chemistry to enable facile synthesis of diverse compound libraries.

iii) Selective formation of carbon-heteroatom bonds. The photocatalytic generation of nitrogen-, oxygen-, sulfur- and phosphorous-centered radicals that subsequently form a carbon-heteroatom bond was surveyed. Many of these transformations have high synthetic potential due to the ubiquity of heteroatoms in pharmaceutical ingredients and biopolymers.

The first section of the review discusses protocols in which the photocatalyst interacts directly with one of the coupling partners via electron or energy transfers to trigger the couplings. During the literature survey I observed that formation of radical species via electron transfer dominates this field, while only one methodology was proposed to work via energy transfer (Scheme 2.14).

Next, methods that combine photocatalysis and transition metal catalysis are reported. A particular attention was dedicated to the combination of nickel- and photocatalysis. This topic, which was also investigated in chapters 3-5, gained significant attention due to the possibility to use nickel complexes as a sustainable alternatives to palladium catalysts in, for example, Buchwald-Hartwig-type reactions.² Two main hypothesis were proposed for dual nickel/photocatalytic cross-couplings when the review was written: energy transfer catalysis and oxidation state modulation of nickel intermediates (see Chapter 1). Recently, however, it was suggested that the PC plays a minor role and only reduces the Ni(II) precatalyst to form an active nickel(I) species.³⁻⁵

Photocatalyst-free cross-coupling reactions are presented last. Here, visible-light activates photolabile starting materials/reagents, electron-donor acceptor complexes or catalytic intermediates, such as nickel and copper complexes. Analysis of the literature inspired the work reported in Chapter 5, in which I developed the direct photoactivation of a nickel complex for cross-coupling reactions.

7.2 Semi-heterogeneous nickel/carbon nitride catalysis for cross-coupling reactions

Palladium catalysis is the benchmark for catalytic cross-coupling reactions, but because of relatively high price and low abundance of this metal, more sustainable alternatives are desirable. Nickel is a promising alternative with electronic properties similar to palladium, but reactivity is lower and carbon-heteroatom cross couplings require often high temperatures and tailored ancillary ligands.⁶ Hillhouse and coworkers showed that Ni(II) intermediates are thermodynamically stable, but reductive elimination can be promoted by oxidation to Ni(III) species.⁷⁻⁸ This led to nickel catalyzed reactions that are enabled by an additional photoredox catalyst and visible light as energy source. The majority of these dual nickel/photocatalytic approaches rely on the use of homogeneous photocatalysts based on noble metals, such as iridium- or ruthenium-polypyridyl complexes. Some organic dyes were reported as alternatives but have limited applicability.

Chapters 3 and 4 report my research efforts towards the use of heterogeneous semiconductors as sustainable alternatives to homogeneous photocatalysts for dual nickel/photocatalytic cross-couplings.

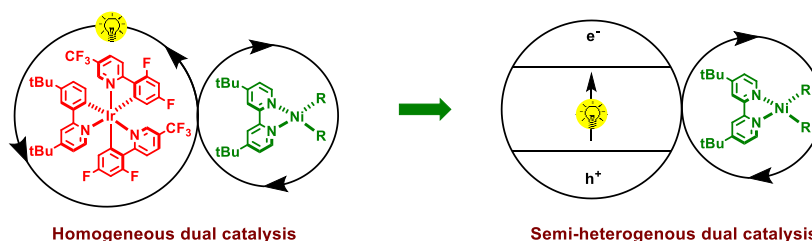
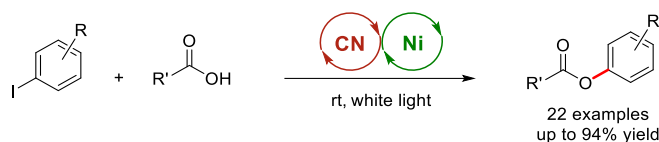


Figure 7.1. Semiconductors as sustainable alternatives in dual nickel/photocatalysis.

Graphitic carbon nitrides are a class of metal-free, polymeric semiconductors that can be prepared from inexpensive, abundant bulk chemicals and absorb visible light. As described in Section 1.2, light irradiation can induce charge separation in semiconductors, generating an excited electron and an electron hole which can participate in single electron transfer events. The carbon nitride CN-OA-m was prepared by calcination of urea and oxamide at 500°C, followed by anaerobic polymerization at 550°C using molten potassium salts as structural templates.⁹ This material absorbs visible-light up to 700 nm.

Chapter 3 consists of the work “Semi-Heterogeneous Dual Nickel/Photocatalysis using Carbon Nitrides: Esterification of Carboxylic Acids with Aryl Halides” published in *Angewandte Chemie International Edition*. The work describes the development of a synthetic protocol for the cross coupling of aryl iodides and carboxylic acids, catalyzed by a nickel-bipyridine complex formed *in situ* and the carbon nitride material CN-OA-m (Scheme 7.1).



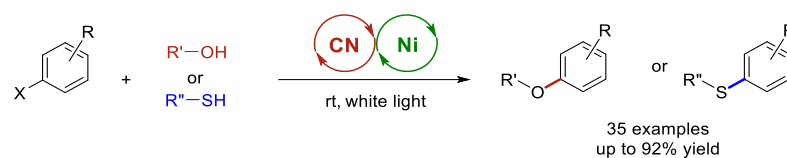
Scheme 7.1. Semi-heterogeneous esterification with carbon nitrides (CN) and nickel catalysis.

Optimized reaction conditions consist of a cocktail of $\text{NiCl}_2 \cdot \text{glyme}$, 4,4'-di-*tert*-butyl-2,2'-bipyridyl (dtbbpy), CN-OA-m and *N-tert*-butylisopropylamine (BIPA) in DMSO, and white light irradiation. The nickel salt can be replaced with the cheaper $\text{Ni}(\text{OAc})_2 \cdot 4\text{H}_2\text{O}$ although lower selectivity results from formation of the acetate ester side-product. Investigation of scope and limitations didn't show significant differences between this semi-heterogeneous approach and a protocol that uses $\text{Ir}(\text{ppy})_3$ as PC.¹⁰ The reaction works well for multiple carboxylic acids but is limited to electron-poor aryl halides.

Aryl bromides were significantly less reactive than aryl iodides, whereas in the original, homogeneous protocol that uses $\text{Ir}(\text{ppy})_3$ bromides were the substrate of choice. This observation led to hypothesize that the photocatalyst might be involved in the initial addition of the aryl halide to the nickel catalyst. A subsequent kinetic analysis by our group suggests that the photocatalyst facilitates oxidative addition to nickel by formation of aryl radicals.¹¹

Use of CN-OA-m as photocatalysts was of particular interest as it enables straightforward recycling of the heterogeneous material. CN-OA-m was recovered by centrifugation after the reaction and reused 5 times without significant loss in reactivity. Characterization of the material after catalysis highlighted deposition of nickel ($1.4\%_{\text{w/w}}$) as nanoparticles that are not catalytically active. Addition of fresh nickel salt and ligand were required at each reaction cycle.

Chapter 4 consists of the work “Semiheterogeneous Dual Nickel/Photocatalytic (Thio)etherification Using Carbon Nitrides” published in *Organic Letters* and extends the semi-heterogeneous, dual-catalytic approach to the cross-coupling of aryl halides with alcohols and thiols.



Scheme 7.2. Semi-heterogeneous (thio)etherification with carbon nitrides and nickel catalysis.

Reaction optimization indicated that a combination of CN-OA-m, $\text{NiBr}_2 \cdot 3\text{H}_2\text{O}$, dtbbpy and BIPA in acetonitrile works best for the coupling of aryl bromides and alcohols. Primary alcohols were coupled to aryl bromides in 24 to 48 hours. Scope investigation highlighted two trends:

i) Electronic properties determine reactivity of aryl bromides: electron-neutral and electron-rich substrates didn't participate in the reaction and substitution with weak electron-withdrawing groups, as well as meta-functionalized aryl halides required long reaction times.

ii) Nucleophilicity determines reactivity of the alcohol: two equivalents of primary alcohols afforded the desired products in good yields with reaction times ranging from 24 to 96 hours. Four equivalents of secondary alcohols were required to maintain reaction times under 120 hours. *tert*-Butanol afforded only traces of product and phenols didn't react at all.

The optimized reaction conditions were also suitable to synthesize dihydrobenzofurane by intramolecular reaction, phenols by using water as instead of alcohols, and thioethers through the cross-coupling of aryl iodides and thiols. Both aliphatic and aromatic thiols take part in the reaction, most likely through formation of radical intermediates that are readily intercepted by the nickel catalyst.¹² Reactivity of aryl iodides was superior to the one of aryl bromides for these transformation, and we assigned this to the formation of aryl radicals as observed in the previous esterification protocol.

CN-OA-m can be recovered from the reaction mixture by centrifugation and was reused 6 times without loss in reactivity. Although 2.2%_{w/w} of nickel accumulated on the catalyst during the recycling study, addition of fresh nickel salt and ligand was necessary at each reaction cycle.

7.3 Photocatalyst-free, visible-light-mediated nickel catalysis for cross coupling reactions

Chapter 5 consists of the work “Photocatalyst-free, visible-light-mediated nickel catalysis for carbon–heteroatom cross-couplings”. This work overcomes the need of an exogenous photocatalyst and reports nickel-catalyzed cross-couplings enabled by a functionalized bipyridyl ligand that absorbs visible light. Polymerizing this ligand further provided a heterogeneous, recyclable catalyst for light-mediated carbon–heteroatom cross-couplings.

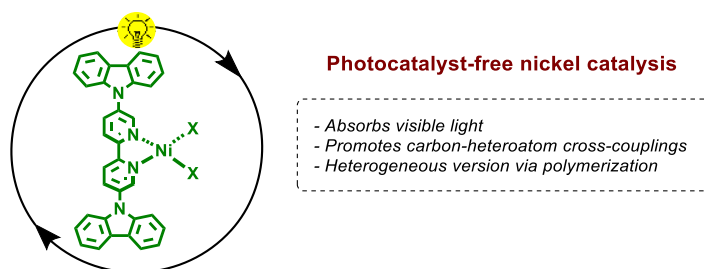
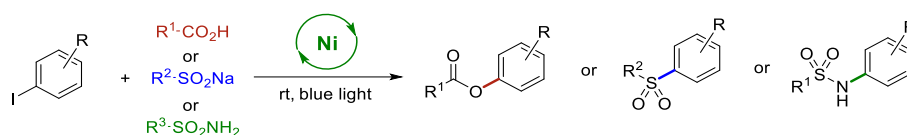


Figure 7.2. Photocatalyst-free nickel catalysis mediated by visible light

Initial reports on dual nickel/photocatalysis proposed mechanistic pathways based on oxidative addition to Ni(0), ligand exchange on the Ni(II) intermediate and reductive elimination after photoexcitation or oxidation to Ni(III). An alternative mechanistic proposal suggests that these reactions can proceed through thermally sustained Ni(I)-Ni(III) cycles. This reactivity was proposed to be active in the background of multiple dual nickel/photocatalytic cross-couplings, in which Ni(I) complexes result from photocatalytic reductions.^{3,5} More evidence was provided by showing that the nickel catalyzed reactions can be also carried out by adding substoichiometric amounts of zinc.¹³ Formation of such nickel(I) complexes was also observed by photoexcitation and disproportionation of Ni(II) complexes,¹⁴ and photocatalyst-free cross-coupling reactions that use direct photoexcitation of nickel catalysts were subsequently developed.¹⁵⁻¹⁷ Nevertheless, excitation of these nickel catalysts requires irradiation with highly energetic UV light, that might trigger side reactions and reduce reaction selectivity.

To overcome the need of photocatalysts, reductants or UV-irradiation, we synthesized the ligand 5,5'-dicarbazolyl-2,2'-bipyridyl¹⁸ (czbpy), which forms a nickel complex that absorbs visible light up to 450 nm. We investigated this ligand for the cross-coupling of aryl halides with several nucleophiles and showed that aryl iodides can be coupled with carboxylic acids, sodium sulfonates and sulfonamides under blue light irradiation without an additional photocatalyst.



Scheme 7.3. Photocatalyst-free, visible-light-mediated nickel catalysis for C–O, C–S and C–N couplings.

A porous organic polymer (poly-czbpy) obtained from polymerization of czbpy serves as a heterogeneous ligand framework that absorbs visible light up to 600 nm after nickel complexation. XPS analysis confirmed that nickel coordinates to nitrogen atoms of bipyridine units. The heterogeneous material was also suitable to catalyze the previously developed, light-mediated C–O, C–S and C–N couplings. Lower nickel-to-polymer ratios, which result in optimal immobilization of nickel on the ligand framework, were beneficial to improve the selectivity. The heterogeneous poly-czbpy containing nickel is recyclable: the material was recovered by centrifugation after the reaction, washed and reused 10 times.

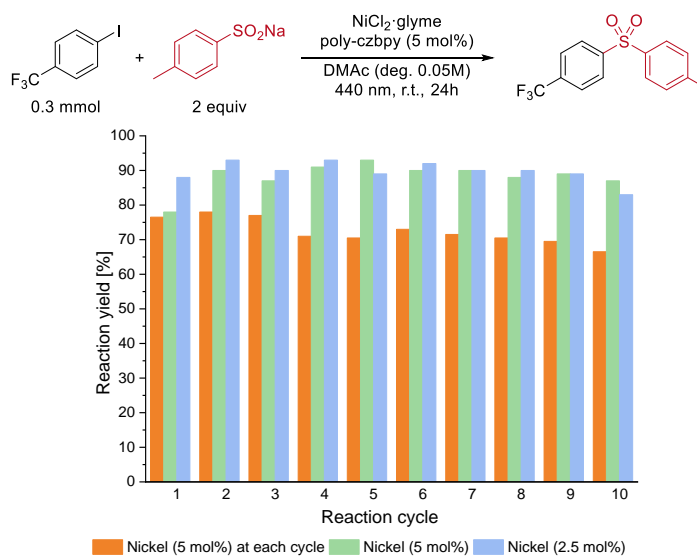


Figure 7.3. Recycling of the heterogeneous catalyst for the C–S coupling.

This work offers a versatile catalytic platform for nickel catalyzed carbon-heteroatom cross-couplings that features: i) use of visible light to promote the reaction, ii) no need for an additional photocatalyst and iii) immobilization and recyclability of the nickel metal.

7.4 Visible-light-mediated cleavage of benzyl ethers for selective deprotection of carbohydrates

Chapter 6 consists of the work “Visible-Light-Mediated Oxidative Debenzylation Enables the Use of Benzyl Ethers as Temporary Protecting Groups” published in *Organic Letters*. The selective cleavage of benzyl ethers in presence of multiple functional groups was achieved through a photocatalytic approach that enables mild reaction conditions and high selectivity.

Due to their high stability, benzyl ethers are among the most stable protecting groups in organic chemistry. Their removal, however, requires harsh reduction or oxidation processes, such as catalytic hydrogenation, Birch reduction or ozonolysis, which suffer from low functional group compatibility. This is a major drawback in synthetic carbohydrate chemistry, and benzyl groups are used as stable and permanent protection, removed only at the very end of the synthesis. Methods for the mild and selective cleavage of benzyl ethers would render them attractive orthogonal protective groups that would conceptually change the strategic approach towards the synthesis of complex glycans.

The cleavage of electron-rich *para*-methoxybenzyl ethers (PMB) was previously reported using visible light photocatalysis.¹⁹⁻²¹ The proposed mechanism involves oxidation of the starting material by the photocatalyst, followed by hydrogen atom transfer (HAT) between the radical intermediate and a suitable oxidant, and final hydrolysis to the product. Considering that benzyl ethers are less electron-rich than PMB ethers, a more oxidizing PC was thought to be necessary. Combinations of an acridinium photocatalyst and multiple oxidants were tested for the debenzilation of a model monobenzylated glucose. Despite initial positive results, the reaction couldn't be improved to achieve full conversion of the starting material. 2,3-Dichloro-5,6-dicyano-1,4-benzoquinone (DDQ) can participate in both SET and HAT events and was found to promote the desired transformation without need for an additional, stoichiometric oxidant.

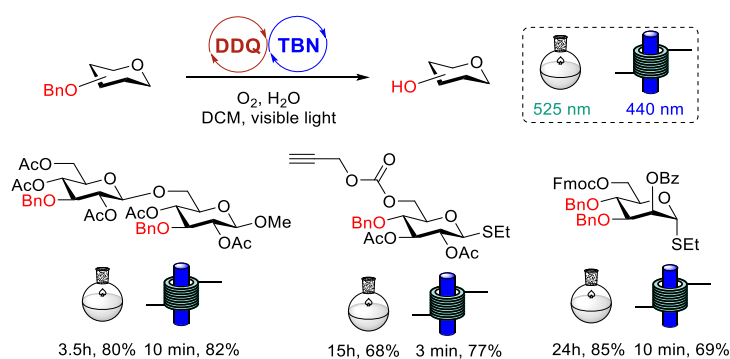


Figure 7.4. Photocatalysis as a selective deprotection strategy for benzyl ethers in carbohydrates.

Visible light irradiation of DDQ generates a strongly oxidizing excited state ($E^{\circ}_{\text{DDQ}^*/\text{DDQ}\cdot} = 3.18 \text{ V vs SCE}$) that selectively induces the cleavage of benzyl ethers in carbohydrate substrates containing several functional groups. To avoid the tedious separation of the stoichiometric

byproduct resulting from reduction of DDQ, I developed a catalytic protocol using DDQ (25 mol%) as photocatalyst, *tert*-butyl nitrite (TBN, 25 mol%) as co-catalyst and air as terminal oxidant. The irradiation source was crucial for achieving high selectivity. While irradiation at 440 nm resulted in the formation of significant amounts of a benzoyl ester side product, higher wavelength (525 nm) allowed to slow down the reaction and achieve optimal selectivity.

To gain further insights in the reaction, *in situ* NMR spectroscopy, using a home-built LED-NMR setup, was used to track the homogeneous reaction and confirm the role of DDQ and TBN. The scope and limitations of the reaction was demonstrated on carbohydrate structures that are equipped with a range of other protecting groups, such as esters, carbonates, as well as thioethers. Moreover, functional groups like azide, allyl and propargyl, that would be cleaved using the traditional catalytic hydrogenation, were tolerated in the oxidative debenzoylation approach. Finally, reaction times could be drastically decreased with a continuous flow system to control the irradiation and maximize the selectivity under blue light irradiation.



Scheme 7.4. Comparison between batch and flow debenzoylation for selected substrates.

7.5 References

- (1) Anastas, P.; Eghbali, N. Green Chemistry: Principles and Practice. *Chem. Soc. Rev.* **2010**, *39*, 301-312.
- (2) Zhu, C.; Yue, H.; Jia, J.; Rueping, M. Nickel-Catalyzed C-Heteroatom Cross-Coupling Reactions under Mild Conditions via Facilitated Reductive Elimination. *Angew. Chem. Int. Ed.* **2020**, doi: 10.1002/anie.202013852,
- (3) Qin, Y.; Sun, R.; Gianoulis, N. P.; Nocera, D. G. Photoredox Nickel-Catalyzed C–S Cross-Coupling: Mechanism, Kinetics, and Generalization. *J. Am. Chem. Soc.* **2021**, *143*, 2005-2015.
- (4) Till, N. A.; Tian, L.; Dong, Z.; Scholes, G. D.; MacMillan, D. W. C. Mechanistic Analysis of Metallaphotoredox C–N Coupling: Photocatalysis Initiates and Perpetuates Ni(I)/Ni(III) Coupling Activity. *J. Am. Chem. Soc.* **2020**, *142*, 15830-15841.
- (5) Sun, R.; Qin, Y.; Rucolo, S.; Schnedermann, C.; Costentin, C.; Daniel, G. N. Elucidation of a Redox-Mediated Reaction Cycle for Nickel-Catalyzed Cross Coupling. *J. Am. Chem. Soc.* **2019**, *141*, 89-93.
- (6) Lavoie, C. M.; Stradiotto, M. Bisphosphines: A Prominent Ancillary Ligand Class for Application in Nickel-Catalyzed C–N Cross-Coupling. *ACS Catal.* **2018**, *8*, 7228-7250.
- (7) Matsunaga, P. T.; Hillhouse, G. L.; Rheingold, A. L. Oxygen-atom transfer from nitrous oxide to a nickel metallacycle. Synthesis, structure, and reactions of [cyclic] (2,2'-bipyridine)Ni(OCH₂CH₂CH₂CH₂). *J. Am. Chem. Soc.* **1993**, *115*, 2075-2077.
- (8) Han, R.; Hillhouse, G. L. Carbon–Oxygen Reductive-Elimination from Nickel(II) Oxametallacycles and Factors That Control Formation of Ether, Aldehyde, Alcohol, or Ester Products. *J. Am. Chem. Soc.* **1997**, *119*, 8135-8136.
- (9) Zhang, G.; Li, G.; Lan, Z.-A.; Lin, L.; Savateev, A.; Heil, T.; Zafeiratos, S.; Wang, X.; Antonietti, M. Optimizing Optical Absorption, Exciton Dissociation, and Charge Transfer of a Polymeric Carbon Nitride with Ultrahigh Solar Hydrogen Production Activity. *Angew. Chem. Int. Ed.* **2017**, *56*, 13445-13449.
- (10) Welin, E. R.; Le, C.; Arias-Rotondo, D. M.; McCusker, J. K.; MacMillan, D. W. C. Photosensitized, energy transfer-mediated organometallic catalysis through electronically excited nickel(II). *Science* **2017**, *355*, 380-385.
- (11) Malik, J. A.; Madani, A.; Pieber, B.; Seeberger, P. H. Evidence for Photocatalyst Involvement in Oxidative Additions of Nickel-Catalyzed Carboxylate O-Arylations. *J. Am. Chem. Soc.* **2020**, *142*, 11042-11049.

- (12) Oderinde, M. S.; Frenette, M.; Robbins, D. W.; Aquila, B.; Johannes, J. W. Photoredox Mediated Nickel Catalyzed Cross-Coupling of Thiols With Aryl and Heteroaryl Iodides via Thiyl Radicals. *J. Am. Chem. Soc.* **2016**, *138*, 1760-1763.
- (13) Sun, R.; Qin, Y.; Nocera, D. G. General Paradigm in Photoredox Nickel-Catalyzed Cross-Coupling Allows for Light-Free Access to Reactivity. *Angew. Chem. Int. Ed.* **2020**, *59*, 9527-9533.
- (14) Shields, B. J.; Kudisch, B.; Scholes, G. D.; Doyle, A. G. Long-Lived Charge-Transfer States of Nickel(II) Aryl Halide Complexes Facilitate Bimolecular Photoinduced Electron Transfer. *J. Am. Chem. Soc.* **2018**, *140*, 3035-3039.
- (15) Yang, L.; Lu, H.-H.; Lai, C.-H.; Li, G.; Zhang, W.; Cao, R.; Liu, F.; Wang, C.; Xiao, J.; Xue, D. Light-Promoted Nickel Catalysis: Etherification of Aryl Electrophiles with Alcohols Catalyzed by a Ni(II)-Aryl Complex. *Angew. Chem. Int. Ed.* **2020**, *59*, 12714-12719.
- (16) Li, G.; Yang, L.; Liu, J.-J.; Zhang, W.; Cao, R.; Wang, C.; Zhang, Z.; Xiao, J.; Xue, D. Light-Promoted C–N Coupling of Aryl Halides with Nitroarenes. *Angew. Chem. Int. Ed.* **2021**, *60*, 5230-5234.
- (17) Lim, C.-H.; Kudisch, M.; Liu, B.; Miyake, G. M. C–N Cross-Coupling via Photoexcitation of Nickel–Amine Complexes. *J. Am. Chem. Soc.* **2018**, *140*, 7667-7673.
- (18) Liang, H.-P.; Acharjya, A.; Anito, D. A.; Vogl, S.; Wang, T.-X.; Thomas, A.; Han, B.-H. Rhenium-Metalated Polypyridine-Based Porous Polycarbazoles for Visible-Light CO₂ Photoreduction. *ACS Catal.* **2019**, *9*, 3959-3968.
- (19) Tucker, J. W.; Narayanam, J. M. R.; Shah, P. S.; Stephenson, C. R. J. Oxidative photoredox catalysis: mild and selective deprotection of PMB ethers mediated by visible light. *Chem. Commun.* **2011**, *47*, 5040-5042.
- (20) Ahn, D. K.; Kang, Y. W.; Woo, S. K. Oxidative Deprotection of p-Methoxybenzyl Ethers via Metal-Free Photoredox Catalysis. *J. Org. Chem.* **2019**, *84*, 3612-3623.
- (21) Liu, Z.; Zhang, Y.; Cai, Z.; Sun, H.; Cheng, X. Photoredox Removal of p-Methoxybenzyl Ether Protecting Group with Hydrogen Peroxide as Terminal Oxidant. *Adv. Synth. Catal.* **2015**, *357*, 589-593.

Abbreviations List

$^1\text{O}_2$	Singlet oxygen
$^3\text{DDQ}^*$	Triplet excited state of DDQ
$^3\text{MLCT}$	Triplet excited state resulting from a metal-to-ligand charge transfer transition
4-CzIPN	1,2,3,5-Tetrakis(carbazol-9-yl)-4,6-dicyanobenzene
A	Electron acceptor
acac	Acetylacetonate
API	Active pharmaceutical ingredient
BET	Brunauer-Emmett-Teller (surface area)
BIPA	<i>N</i> - <i>tert</i> -Butylisopropylamine
Bn	Benzyl
Boc-Pro-OH	<i>N</i> -(<i>tert</i> -Butoxycarbonyl)proline
Bpin	Boronic acid pinacolate ester
bpy	2,2'-Bipyridine
bpz	2,2'-Bipyrazine
BTMG	2- <i>tert</i> -Butyl-1,1,3,3-tetramethylguanidine
Bz	Benzoyl
CB	Conduction band
cbz	Benzyloxycarbonyl
CDC	Cross-dehydrogenative coupling
CN	Carbon nitride
COD	1,5-Cyclooctadiene
czbpy	5,5'-Dicarbazolyl-2,2'-bipyridyl
D	Electron donor

d	Doublet
DABCO	1,4-Diazabicyclo[2.2.2]octane
DBU	1,8-Diazabicyclo[5.4.0]undec-7-ene
DCE	Dichloroethane
DCM	Dichloromethane
DDQ	2,3-Dichloro-5,6-dicyano-1,4-benzoquinone
DDQH ₂	2,3-Dichloro-5,6-dicyano-1,4-hydroquinone
dF(CF ₃)ppy	2-(2,4-Difluorophenyl)-5-(trifluoromethyl)pyridine
diglyme	Diethylene glycol dimethyl ether
DIPEA	<i>N,N</i> -diisopropylethylamine
DMA or DMAc	<i>N,N</i> -Dimethylacetamide
DMAP	<i>N,N</i> -Dimethylaminopyridine
dme	Dimethyl ether
DMF	<i>N,N</i> -Dimethylformamide
dmg	Dimethylglyoxime
DMPU	<i>N,N'</i> -Dimethylpropyleneurea
DMSO	Dimethylsulfoxide
donor*	Excited state participating in energy transfers
DQ	Duroquinone
dtbbpy	4,4'-Di-tert-butyl-2,2'-bipyridine
EDA	Electron-donor acceptor (complex)
EdX	Energy-dispersive X-ray
EI	Electronic ionization
EnT	Energy transfer
EPR	Electron paramagnetic resonance spectroscopy
ESI	Electrospray ionization

ET	Electron transfer
EY	Eosin Y
EY*	Excited state of Eosin Y
EY ^{ox}	Eosin Y after oxidative quenching
FEP	Fluorinated ethylene-propylene
Fmoc	9-Fluorenylmethoxycarbonyl
FTIR	Fourier-transform infrared spectroscopy
g-CN	Graphitic carbon nitride
glyme	1,2-Dimethoxyethane
HAADF	High-angle annular dark-field
HAT	Hydrogen atom transfer
HOMO	Highest occupied molecular orbital
HR-MS	High resolution mass spectrometry
ICP-OES	Inductively coupled plasma - optical emission spectroscopy
ISC	Intersystem crossing
Lev	4-Oxopentanoyl
LUMO	Lowest unoccupied molecular orbital
m	Multiplet
Me ₂ -Mes-Acr ⁺	9-Mesityl-2,7-dimethyl-10-phenylacridinium
MeCN	Acetonitrile
MeOH	Methanol
Mes-Acr ⁺ or Me-Mes-Acr	9-Mesityl-10-methylacridinium
MLCT	Metal-to-ligand charge transfer
MTBD	7-Methyl-1,5,7-triazabicyclo[4.4.0]dec-5-en
n.d.	Not detected

n.d.o.	Not determined due to overlapping peaks
NAP	2-Naphtylmethyl
NCS	<i>N</i> -Chlorosuccinimide
NIS	<i>N</i> -Iodosuccinimide
NMR	Nuclear magnetic resonance spectroscopy
Nu-H	Nucleophile in its protonated form
ODNS	Dinitrophenylsulfonyloxy
OMs	Methanesulfonate
OTf	Trifluoromethanesulfonate
OTs	<i>para</i> -Toluensulfonate
PC	Photocatalyst
PC*	Excited state of the photocatalyst
PC ^{ox}	Photocatalyst after oxidative quenching
PC ^{red}	Photocatalyst after reductive quenching
PET	Photoinduced electron transfer
PG	Protecting group
PMB	<i>para</i> -Methoxybenzyl (ether)
ppy	2-Phenylpyridine
PRC	Photoredox catalysis
PTFE	Polytetrafluoroethylene
p-TSA	<i>para</i> -Toluensulfonic acid
q	Quartet
quinuclidine	1-Azabicyclo[2.2.2]octane
s	Singlet
S ₀	Singlet state
S ₁	Singlet excited state

SCE	Saturated calomel electrode
SEM	Scanning electron microscopy
SET	Single electron transfer
STEM	Scanning transmission electron microscopy
t	Triplet
T ₁	Triplet excited state
TBAI	Tetrabutylammonium iodide
TBD	1,5,7-Triazabicyclodec-5-ene.
TBN	<i>tert</i> -Butyl nitrite
TBS	<i>tert</i> -Butyldimethylsilyl
<i>t</i> -Bu ₂ -Mes-Acr ⁺	9-Mesityl-3,6-di- <i>tert</i> -butyl-10-phenylacridinium
TEM	Transmission electron microscopy
TEMPO	2,2,6,6-Tetramethylpiperidine-1-oxyl
TFE	Trifluoroethane
TfOH	Trifluoromethanesulfonic acid
THF	Tetrahydrofuran
TLC	Thin layer chromatography
TMG	1,1,3,3-Tetramethylguanidine
TMSOTf	Trimethylsilyl trifluoromethanesulfonate
Tol	Toluene
TriPhPyrilium	2,4,6-Triphenyl-pyrylium
Ts	<i>para</i> -Toluensulfonyl
VB	Valence band
XPS	X-ray photoelectron spectroscopy
XRD	X-ray powder diffraction